NASA/CR–2011-217080

A Compilation of Space Shuttle Sonic Boom Measurements

Domenic J. Maglieri and Herbert R. Henderson
Eagle Aeronautics, Inc., Hampton, Virginia

Steven J. Massey
NASA Langley Research Center, Hampton, Virginia

Eugene G. Stansbery
NASA Johnson Space Center, Houston, Texas

April 2011

NASA STI Program . . . in Profile

Since its founding, NASA has been dedicated to the advancement of aeronautics and space science. The NASA scientific and technical information (STI) program plays a key part in helping NASA maintain this important role.

The NASA STI program operates under the auspices of the Agency Chief Information Officer. It collects, organizes, provides for archiving, and disseminates NASA's STI. The NASA STI program provides access to the NASA Aeronautics and Space Database and its public interface, the NASA Technical Report Server, thus providing one of the largest collections of aeronautical and space science STI in the world. Results are published in both non-NASA channels and by NASA in the NASA STI Report Series, which includes the following report types:

- TECHNICAL PUBLICATION. Reports of completed research or a major significant phase of research that present the results of NASA programs and include extensive data or theoretical analysis. Includes compilations of significant scientific and technical data and information deemed to be of continuing reference value. NASA counterpart of peer-reviewed formal professional papers, but having less stringent limitations on manuscript length and extent of graphic presentations.

- TECHNICAL MEMORANDUM. Scientific and technical findings that are preliminary or of specialized interest, e.g., quick release reports, working papers, and bibliographies that contain minimal annotation. Does not contain extensive analysis.

- CONTRACTOR REPORT. Scientific and technical findings by NASA-sponsored contractors and grantees.

- CONFERENCE PUBLICATION. Collected papers from scientific and technical conferences, symposia, seminars, or other meetings sponsored or co-sponsored by NASA.

- SPECIAL PUBLICATION. Scientific, technical, or historical information from NASA programs, projects, and missions, often concerned with subjects having substantial public interest.

- TECHNICAL TRANSLATION. English-language translations of foreign scientific and technical material pertinent to NASA's mission.

Specialized services also include creating custom thesauri, building customized databases, and organizing and publishing research results.

For more information about the NASA STI program, see the following:

- Access the NASA STI program home page at *http://www.sti.nasa.gov*

- E-mail your question via the Internet to help@sti.nasa.gov

- Fax your question to the NASA STI Help Desk at 443-757-5803

- Phone the NASA STI Help Desk at 443-757-5802

- Write to:
  NASA STI Help Desk
  NASA Center for AeroSpace Information
  7115 Standard Drive
  Hanover, MD 21076-1320

NASA/CR–2011-217080

A Compilation of Space Shuttle Sonic Boom Measurements

Domenic J. Maglieri and Herbert R. Henderson
Eagle Aeronautics, Inc., Hampton, Virginia

Steven J. Massey
NASA Langley Research Center, Hampton, Virginia

Eugene G. Stansbery
NASA Johnson Space Center, Houston, Texas

National Aeronautics and
Space Administration

Langley Research Center
Hampton, Virginia 23681-2199

Prepared for Langley Research Center
under Contract NNL05AB74T

April 2011

Available from:

NASA Center for AeroSpace Information
7115 Standard Drive
Hanover, MD 21076-1320
443-757-5802

TABLE OF CONTENTS

LIST OF TABLES

Tables:

List of Symbols

C	Centigrade
DG	degrees
GMT	Greenwich mean time
H	altitude, ft.
I_o	boom signature positive impulse, lb/ft^2-sec
JSC	Johnson Space Center
KSC	Kennedy Space Center
M	Mach number
meas.	measured
MSL	mean sea level
MSN	mission number
NOAA	National Oceanographic and Atmospheric Administration
Δp	sonic boom overpressure, lb/ft^2
Δp_o	maximum positive boom overpressure, lb/ft^2
pred.	predicted
STS	Space Transportation System
ΔT	total period of boom signature, sec.
Δt_o	time duration of positive phase of boom signature, sec
$\tau_{1/2}$	rise time of bow shock to one-half amplitude, msec
$\tau_{3/4}$	rise time of bow shock to three-fourths amplitude, msec
$\tau_{10\text{-}90}$	rise time of bow shock from 10 to 90 percent amplitude, msec
τ_{max}	rise time of bow shock to maximum amplitude, msec

LIST OF ILLUSTRATIONS

A COMPILATION OF SPACE SHUTTLE SONIC BOOM MEASUREMENTS

SUMMARY

Sonic boom measurements have been obtained on 26 flights of the Space Shuttle beginning with the first launch of STS-1 on April 12, 1981, to the reentry-descent of STS-41 into EAFB on October 10, 1990. A total of 136 boom measurements were acquired; 23 during three STS launch-ascents and 113 during the 23 STS reentry-descents to landing. A total of 123 boom signatures were acquired, 20 on ascent and 103 on reentry. These sonic boom measurements were made under and to the side of the vehicle ground track and cover the Mach and altitude range of about 1.3 to 23 and 58,000 feet to 243,000 feet, respectively.

For the launch-ascent phase of flight, measurements were concentrated off the Florida coast in an area of the Atlantic Ocean, about 40 n.mi east of the launch site in order to define the magnitude of the focus boom. Single shock pressure signatures, similar to blast explosion waveforms, with periods of about 2.0 seconds to 8 seconds, were observed with overpressure levels ranging from about 0.4 psf in the pre- and post-focus region to 6.81 psf along the focus line. The nature of the focus region and signature characteristics are quite similar to those obtained during launch-ascent of the Apollo-Saturn vehicle. In each case the predictive tools were suitable to define the location and extent of the focus region.

For the reentry-descent phase of flight, the measurements were made on land with the majority acquired in the state of California and about 25 percent in the state of Florida. The measured boom signatures were generally N-wave in character, similar to those observed from supersonic aircraft, with amplitudes ranging from about 0.10 psf from the vehicle at about 243,000 feet altitude to a maximum of 2.32 psf just prior to landing. Signature periods, however, were much greater than those observed on aircraft being on the order of about 0.40 second to about 2.5 seconds. Predictions of the magnitude of sonic booms and ground footprints for Mach numbers to about 6.0 compared favorably with measurements.

Even though the Orbiter performs maneuvers during the reentry-descent phase of flight, which result in roll angle and heading changes, they were not predicted to result in focus booms at the ground and none were observed. Atmospheric turbulence, especially in the lower layers of the atmosphere. result in peaking or rounding of the N-wave signatures similar to what has been observed from aircraft in supersonic flight where the changes to the bow-shock are repeated on the tail shock. It is observed, however, that when the Orbiter is at very high altitudes where the signature periods are large and overpressures relatively low that the bow and tail shock distortions resulting from the atmosphere sometimes differ.

INTRODUCTION

Over the past half century, sonic boom technology development has been focused on high-performance supersonic aircraft and an extensive database has been developed for these aircraft. Since the geometric and operational characteristics of the Space Shuttle differ significantly from supersonic aircraft, estimation of its sonic boom characteristics requires a new technology base. As a result, considerable effort was directed towards developing an extensive sonic boom database for the Space Shuttle for both the launch-ascent and reentry-descent phases of operation. The sonic boom measurements acquired during the launch and ascent of the Saturn-Apollo Program (refs. 1-3) during the early 1970's, along with the associated wind-tunnel and prediction activities (refs. 4-8), would have direct application to Shuttle. Likewise, the 20-year sonic boom database acquired on supersonic aircraft (ref. 9-13) is also applicable to the Shuttle Orbiter reentry-descent phase of flight. However, this latter database did not cover the high Mach-altitude operating range of the more blunt low fineness ratio Orbiter. These existing databases aided immensely in defining the needs regarding the prediction of sonic booms for shuttle.

During the mid- and late-1970's, a number of wind tunnel tests of both launch vehicle and Orbiter reentry vehicle were conducted (refs. 14-17) and empirical schemes were developed to apply to the prediction of sonic booms at high Mach-altitude conditions (refs. 18-22). Sufficient information was developed to provide for a fairly complete description of the booms expected of the Shuttle (ref. 23), and to produce an environmental impact statement (ref. 24). In addition, the information helped define the type of sonic boom measurements that should be acquired on the planned STS flights (refs.25-29).

Sonic boom measurements have been obtained on 26 flights of the Space Shuttle system beginning with the first launch of STS-1 on April 12, 1981, to the reentry-descent of STS-41 into EAFB on October 10, 1990. A total of 23 boom measurements were acquired within the focus region off the Florida coast during 3 STS launch-ascents and boom measurements were acquired during 23 STS reentry-descent to landing into Florida and California. These sonic boom measurements were made under, and lateral to, the vehicle ground track and cover the Mach-altitude range of about 1.3 to 23 and 58,000 feet to 243,000 feet, respectively. In addition to the measured sonic boom signatures, vehicle operational data, flight profiles, and weather data were also gathered during the flights. This STS boom measurement database is contained in 26 documents, a few of which are formal and referenceable (refs. 30-38), but most are internal documents and are not referenceable and also not readily available. Another 38 documents, also non-referenceable, contain predicted sonic boom footprints for reentry-descent flights on which no measurements were made.

The purpose of this report is to provide an overview of the STS sonic boom database and summarize the main findings. An electronic database of the STS boom signatures, spectra, and characteristics along with operational conditions and weather data is contained in a supplemental electronic file that also includes all of the existing STS sonic boom documents that formed the database.

VEHICLE DESCRIPTION

A photograph of the Space Shuttle vehicle at lift-off from Cape Kennedy is presented in figure 1. In figure 2 is shown a schematic of the Space Shuttle launch vehicle in the ascent configuration.

The launch vehicle consists of an Orbiter, an external tank and a booster made up of two solid rocket motors as shown in figure 2. The solid rocket motors burn in parallel with the Orbiter main propulsion engines and are separated from the Orbiter/external tank at burnout of about 150,000 feet altitude. Thereafter the Orbiter main propulsion engines continue to burn until the Orbiter is injected into the required ascent trajectory. The launch vehicle has an overall length of 184.2 feet and had a gross lift-off weight of about 4-1/2 million pounds.

Figure 3 is a photograph of the Space Shuttle Orbiter Columbia nearing touchdown. The Orbiter is a lifting vehicle capable of maneuvering and landing much like an airplane by using its control surfaces which are augmented by a reaction control system. During its atmospheric flight, it is capable of flying at angles of attack as high as 40 degrees and rolling about the velocity vector to $\pm$ 70 degrees. A three-view illustration and dimensions of the Orbiter along with details of the fuselage and wing sections are shown in figure 4. The Orbiter is comparable in size and weight to modern transport aircraft. It weighs about 200,000 pounds at landing, is 122.25 feet in length and has a wing-span of 78.06 feet and a fineness ratio of about 4, considerably less than 10 to 12 of supersonic transport (SST) designs. From reentry to landing, the Orbiter is a gliding vehicle since it does not have any propulsion system. The orbiter vehicle is trimmed to provide a hypersonic lift-to-drag ratio of approximately 1.3 during entry. At subsonic speeds, the maximum trimmed lift-to-drag ratio, with the speed brake closed, is about 4.9.

LAUNCH-ASCENT AND REENTRY-DESCENT MEASUREMENT LOCATIONS

All Shuttle launches are performed at the Kennedy Space Center launch site in Florida. As shown in figure 5, the launch trajectories are in an easterly direction out over the Atlantic Ocean. The sonic boom measurement region of interest is an area some 40-50 miles east of the launch site where boom focussing occurs at the ocean surface as the vehicle accelerates from subsonic to supersonic speeds. Boom measurements aimed at describing the focus boom region were acquired on three Shuttle launches. As noted earlier and also in Table I, a total of 23 boom measurements were made during Shuttle ascents including a single boom measurement on STS-5 (ref. 33), seven on STS-7 (ref. 34) and fifteen on STS-41-D (ref. 36).

STS landing sites and sonic boom measurement regions are shown in figure 6. Recovery for all but one STS missions occurred at either Edwards Air Force Base (EAFB), California or Kennedy Space Center (KSC), Florida; STS-3 was recovered at White Sands, New Mexico. As shown in Table I, of the twenty-three STS reentry flights on which sonic boom measurements were obtained, eighteen landed at EAFB, and five at KSC. As can be seen from figure 6, reentry to landing at EAFB was from the west, southwest, and north. Sonic boom measurements were acquired at numerous locations in California and also in Oregon. Reentry into KSC was from the west, and north. Sonic boom measurements were acquired at a number of locations in Florida and one in Texas. On STS reentry flights, the number of measurements varied from two to fourteen; the total number of measurements made was 113 (see Table 1).

In addition to the 26 STS missions (ascent and descent) on which 136 sonic boom measurements were acquired, there were another 38 STS missions on which descent sonic boom ground foot-prints were predicted but no measurements were obtained. Those are listed in Table 2 along with the launch and landing dates, appropriate ground track and land areas involved and landing site. It can be seen that of these 38 STS missions, 21 landed at EAFB, 16 at KSC, and one at White Sands.

FLIGHT TRAJECTORIES

Representative launch-ascent and reentry-descent-to-landing trajectories are given in figures 7, 8, and 9 for STS-5, STS-26 and STS-51-D, respectively.

The Mach-altitude time history for STS-5 is presented in figure 7 and is typical of all launch-ascent trajectories. This initial phase of the launch-ascent of the Shuttle results in the down-range focused booms. Note from figure 7 that the origin of the focus booms region occurs slightly less than 2 minutes after launch when the vehicle is at about Mach 3.6 and 110,000 feet altitude. The boom arrives at the measurement site some three minutes later. Table 3 presents selected parameters from a preflight launch-ascent trajectory for Shuttle (STS-41D) as a function of time from lift-off. Listed are down range distance, Mach number, altitude, latitude, longitude, heading and flight path angle.

Presented in figure 8 are typical time histories of six flight parameters of the STS-26 Orbiter reentry-descent that were used in sonic-boom predictions (refs. 38-39). Included are vehicle altitude, Mach number, flight path angle, angle of attack, heading and roll angle. These plots, which begin at about Mach 10 at an altitude of 160,000 feet, are plotted against time to touchdown. Note that with the exception of heading and roll angle, most of the time histories are relatively smooth without any large excursions. In fact, the maximum roll-angle rate, associated with heading changes, is only about 8 degrees per second as compared to military aircraft maneuvers, whose roll-angle rates may be an order of magnitude greater. Any significant and rapid change in any of these parameters would be of concern relative to possible sonic-boom focussing. Such is not the case for the Orbiter reentry (ref. 40).

The Mach-altitude time history for STS-51D during descent to landing is presented in figure 9. Note that the Orbiter becomes subsonic below about 50,000 feet. It is of interest to note that for level flight in a standard atmosphere, no booms will reach the ground with the vehicle flying above the tropopause (36,000 feet altitude) at a Mach number less than about 1.15. However, with the Orbiter at a flight path angle of about -16 degrees (i.e., dive angle), the cutoff Mach number (Mach below which booms will not propagate to the ground) is about 1.02 (ref. 41). As can be seen from figure 9, the Orbiter descent profile is designed to avoid booms reaching the ground from flights below 50,000 feet altitude. Table 4 presents selected parameters for the last 7 minutes of the Orbiter descent trajectory to landing for STS-51D as a function of time to Mach 1.0. Listed are Mach number, altitude, flight path angle, latitude, longitude, heading, roll angle and angle of attack.

Trajectories for all 26 STS missions on which sonic boom signatures were obtained (see Table 1) are contained in the supplemental electronic database.

ATMOSPHERIC OBSERVATIONS

Prior to an STS mission detailed weather observations were made at the Cape Kennedy launch site which included climatological data (surface temperature, relative humidity, surface winds and direction and cloud cover) windsonde observations, rawinsonde soundings from near the surface to about 80,000 feet and rocketsonde measurements to about 200,000 feet altitude. These latter

two soundings provided measures of atmospheric pressure, temperature, relative humidity, wind speed and direction. An example of these observations associated with the launch of STS-41D is presented in Table 5 and the pressure, temperature and wind speed and direction, graphically illustrated in figure 10. Similar observations were made at the recovery site prior to the Orbiter reentry and descent-to-landing.

For the majority of the STS missions on which booms were acquired, weather observations were not performed at the measurement locations. However, rawinsonde soundings from the nearest NOAA weather station and at the closest time to sonic boom arrival (NOAA standard rawinsonde launch times are at OO GMT and 1200 GMT) were acquired and these are contained in the supplemental electronic database for 25 of the 26 STS missions on which booms were measured. Data for STS-2 is no longer available in NOAA files.

SONIC BOOM MEASUREMENTS SYSTEMS

Two different sonic boom measurement systems were utilized to acquire the signatures associated with the Shuttle ascent and Orbiter descent to landing; the analog Sonic Boom Data Acquisition System (SBDAS) and the digital Portable Automatic Triggering System (PATS). The SBDAS, which was the measurement standard for a majority of the sonic boom measurements from supersonic aircraft (refs. 9 and 42) and Apollo was the only system available during the early STS missions. These systems, which are no longer available, were subsequently complemented with the digital PATS (ref. 38) which also are no longer available and have been excessed. These PATS, of the time,eventually dominated the boom measurement activity on Shuttle. Photographs and schematics of the analog SBDAS and digital PATS sonic boom measurements systems is shown in figure 11. A brief description of each follows.

Sonic Boom Data Acquisition System

The SBDAS and its block diagram is shown in figure 11(a). The system components included condenser microphones, Dynagages, signal conditioning amplifiers, FM magnetic tape recorders and satellite time code receivers.

The microphones employed were Photocon Model 404 condenser units designed for use in conjunction with Photocon Model DG-605 Dynagages that had a high frequency response essentially flat to 10K Hz with a low frequency response averaging approximately -5 dB at 0.01 Hz. The microphone had a small capillary hole through the housing which allowed some airflow so that the static pressure within the capsule was always equal on both sides of the diaphragm even at frequencies well below 20 Hz. This technique allowed for system balancing and tuning in response to changes in temperature and atmospheric pressure during field operation. The diaphragm of the microphone, in conjunction with an insulated electrode, formed an electrical capacitor. The Dynagages consisted of a radio frequency oscillator coupled to a diode detector circuit such that small changes in the microphone produced relatively large changes in the diode detector. The output from the Dynagage was then input to Burr-Brown Model 3640-1 DC amplifiers with 60 dB gain (in 2 dB steps) to meet the input voltage requirements of the FM magnetic tape recorder. Typically, four microphones were used with amplifiers to provide six different gain settings. These six

pressure signals were recorded along with a voice track and IRIG-B time code provided by True Time Model 468-time code receivers designed to receive the NOAA “GOES” satellite.

Portable Automatic Triggering System

The PATS and its block diagram shown in figure 11b was a small portable, sound recording device capable of unmanned operation. It consisted of a solid state piezoresistive pressure transducer, signal conditioning amplifier, analog-to-digital converter, clock, and eight solid state Random Access memory (RAM) banks all powered by a rechargeable battery. Generally, pressure data from the transducer was amplified and conditioned by a low noise amplifier/high pass filter with a cut-off of about 0.3 Hz. This signal was digitized with 8-bit resolution at a switch selectable sampling rate of either 8.0 or 1.5 kHz. Digitized pressure was recorded in a continuous loop in one of the eight memory banks until an overpressure of greater than a predetermined trigger level and duration of at least 10 msec was detected. The data loop was then stopped with the captured data remaining in memory, time was annotated and the next memory bank was selected.

The pressure transducer employed was the Motorola MPX-50D. Although this was a differential pressure transducer, it was employed here in a gauge mode of operation. The back side of the transducer was evacuated to 1/2 atmospheric pressure, while an epoxy cement was allowed to set, sealing the vent. This allowed the transducer to operate in the middle of its static range, thereby increasing the linearity and reducing the signal noise when compared to an absolute pressure transducer referenced to a vacuum. The frequency response of the MPX-50D in this mode of operation was essentially a function of the slew rate, but was generally greater than 10 kHz for this application.

The output of the MPX-50D was input into a three-stage amplifier/high-pass filter with offset capabilities. The first stage used a Burr-Brown OPA-27 ultra low noise operational amplifier. The high pass filter had a cutoff of approximately 0.3 Hz. A total amplifier gain on the order of 10,000 produced a system capable of recording a full-scale reading of approximately 600 Pa (about 12 psf). The pressure transducer and amplifier/high pass filter were housed in a grounded metal enclosure and connected to the main unit by a shielded extension cable.

The signal from the amplifier was sent to a sample and hold device and then digitized at a switch selectable rate by an Analog Device (ADC-0802) eight bit analog-to-digital converter. The digitized data are recorded in a continuous loop by a 16,000 byte Random Access Memory bank. A trigger detecting circuit also receives the input signal from the amplifier. This circuit produced a trigger pulse when a positive impulse was received. The impulse must have a time to preset threshold of less then 100 msec and it must remain at or above the threshold longer than 10 msec. When a triggering signal was received, further triggering was inhibited, the RAM memory bank continues recording pressure data for 15,000 counts at which point time was annotated, and the next memory bank was selected.

Field calibration of these units was accomplished by recording the sine wave of a Photocon PC-125 fixed frequency sound pressure level calibrator into one of the unit’s memory banks.

SONIC BOOM MEASUREMENT STATION SET-UP

Two different boom measurement arrangements were used for the ascent and reentry phases of the STS flights and these are shown in figure 12. In order to acquire the ascent focus boom signatures,

the measurement systems were placed aboard ships, as shown in figure 12(a) which were positioned within a region defined by a preflight STS sonic boom analysis. Range safety considerations did not allow ships to be deployed any closer than 6.5 nautical miles to the Shuttle ground track. All boats were equipped with LORAN C navigation aids with some having Global Positioning Systems and LORAC (Long Range Accuracy). The analog SBDAS was used on all three ascent measurements (STS-5, STS-7, and STS-41D). The PATS, which were then called the Remote Sonic Boom Monitoring Systems (RSBMS) were also used on STS-7 and STS-41D and deployed on the ocean in specially designed buoys. An accompanying radar reflector allowed tracking of the buoy, thus, it was possible for one boat to deploy several of the units and allow them to drift in the current. This greatly increased the cost effectiveness of the boat. The obvious problem with this method was the inability to place the buoy in a precisely determined position. However, considering the narrowness (width) of the focus line and the difficulties, due to atmospheric variations, in predicting its precise position, even one buoy nearby increased the chances of bracketing the focus.

Measurements for all 23 of the STS reentry flights were made on land and deployed as illustrated in figure 12(b). Both the analog SBDAS and digital PATS boom measurement systems were deployed on a number of flights, the SBDAS systems on the early missions and the PATS dominating the measurements as the program progressed.

SONIC BOOM MEASUREMENTS

The measured sonic boom ground signatures associated with the STS launch-ascent and Orbiter reentry-descent are quite different in character as illustrated in figure 13. Note, from figure 13(a) that the boom signature measured in the post-focus region (i.e., downtrack of the focus line) during the STS-41D ascent phase consists of an initial bow shock followed by a long expansion, similar to signatures associated with the Saturn-Apollo ascents (refs. 1-3) and explosive charges. Thus, only a single boom was observed. Note that the boom signature period was almost 4.0 seconds. Although the Shuttle, in the launch configuration represents quite a large vehicle, the initial shock results from the very large STS exhaust plume. In comparison the reentry-descent signatures from the Orbiter on STS-41B, shown in figure 13(b), was typical of those observed from supersonic aircraft in that it was N-wave in shape, consisting of a bow and tail shock. Two booms would be observed from such a signature. The signature period, however, was about twice those observed from aircraft.

The relatively large period associated with the ascent signature results in a noise spectrum that has its peak energy at a much lower frequency (about 0.15 Hz) than the descent signature (about 1.0 Hz) as can be seen in figure 14. Both, however, occur at frequencies lower than those for aircraft sonic booms. The signature spectrum plays a significant role in the outdoor and indoor response of people to sonic booms and the building response (ref. 43).

Sonic Boom Signature Characteristics

Each STS measured boom signature, was characterized by the parameters shown in figure 15 and include its overpressure (Δp_o), total period (ΔT), time period of the positive phase (Δt_o), the impulse of the positive phase (I_o) and readings of the initial bow shock rise time (τ). Although only the rise time to the maximum overpressure (τ_{max}) was shown on the figure, the rise time to

the half amplitude ($\tau_{1/2}$), three-fourths amplitude ($\tau_{3/4}$) and rise times from the ten percent to ninety percent amplitude ($\tau_{10\text{-}90}$) were also electronically read for each measured signature and are listed in Table 6 along with the other parameters and also on the supplemental electronic file.

Launch Ascent Focus Boom Region Signatures

A description of the launch-ascent focus boom region can be illustrated with figure 16. The origin of the launch-ascent focus boom region is shown schematically in figure 16(a) When the Space Shuttle first achieves supersonic velocities, it is in nearly vertical flight and the propagation of the disturbance is upward, away from the ground. As the vehicle continues to accelerate and pitches over, the flight path angle decreases sufficiently so that the disturbance propagation path intersects the ground surface. The combination of angular and linear acceleration rates results in a region some 40 n.mi or so from the launch site in which the acoustical energy is focused, as indicated by the loci of focal areas shown in the profile view on figure 16(a). These loci define a focus "line" which is parabolic in shape as depicted in figure 16(b) and extends laterally approximately 40 n.mi or so to each side of the vehicle ground track out to the lateral cutoffs. Beyond the lateral cutoff the pressure wave is refracted up by the atmosphere and does not intersect the ground. Behind (downrange from) the focus line, overpressure peaks originating from different points on the flight path reach the ground at different times producing signatures with multiple peaks. The area where these peaks begin to add together can be called the focus "zone." In front of the focus line, no sonic boom reaches the ground. The highest peak overpressure is obtained at the focus line beneath the flight path and falls off both laterally from the ground track and downrange from the focus line.

Sonic boom signatures, representative of those measured within the STS launch-ascent focus region are shown in figure 17 along with an indication of the change in overpressure levels from the pre- to post-focus boom regions. The uppermost signature was measured at a location in the pre-focus region slightly uptrack (before) the focus line. The signature exhibits an initial shock from the direct boom immediately followed by a second shock from the refracted shock a very short time later. The signature shown at the center of figure 17 was measured within the focus line and is seen to consist of sharp signal shock of large amplitude which may not represent the maximum value. A considerable database on focus booms associated with supersonic aircraft suggest that the downrange "thickness" of the focus line is on the order of a few hundred feet. Downtrack, behind the focus line, and in the post-focus region the measured signature shown at the bottom of figure 17 also displays a two-shock trace, the initial shock being attributed to the direct boom and the second the reflected shock arriving at a slightly later time and from a slightly different location along the ascent trajectory.

The pre-focus, focus, and post-focus signatures are very similar to those observed from measurements acquired during Apollo 17 (ref. 3) mission and shown in figure 18. Six U. S. Naval vessels were located in the Atlantic Ocean directly under the flight path of the launch vehicle and positioned to cover the extent of the focus region. Note that although two of the measurements were near the focus line, the chart suggests that the values measured do not represent the maximum overpressures within the focus line.

Reentry-Descent Signatures

The upper two signatures shown in figure 19 (from ref. 37) were measured near the ground track of STS-1 Orbiter during the reentry-descent phase of flight to landing at EAFB, California. Boom origin occurred at about Mach 3.41 and 99,715 feet altitude for the Station 2 measurement and at about Mach 1.4 and 62,658 feet altitude for the Station 9 measurement site. It can be observed that both signatures are N-wave in character but with signs of atmospheric influences. Also shown on each signature are predicted levels for the positive phase of the signature based upon Orbiter wind-tunnel model data (ref. 20) extrapolated to full-scale and inserted into the Thomas propagation code (ref. 39). The comparison between measured and predicted signatures is quite good considering that the analytical tools developed for predicting boom signatures from supersonic aircraft are limited in nature and apply quite well to the higher fineness ratios associated with aircraft capable of supersonic flight. The STS Orbiter is a blunt low fineness ratio vehicle that operates over a much higher Mach-altitude range than supersonic aircraft.

It is well known that signature rise time plays a significant role relative to the loudness of sonic booms and thus people response (refs. 13, 43 and 44). In the original reporting of the signatures from STS-1 (ref. 37), the boom signature was examined in more detail by greatly expanding the time scale in the vicinity of the initial bow shock. These portions of the signatures are shown in the lower portion of figure 19. Maximum rise times (τ_{max}) of from about 3 and 5 msec are observed and these are typical of those measured from supersonic aircraft (ref. 13).

Atmospheric effects. - It is known that turbulence, especially in the lower layers of the atmosphere can bring about significant variations to the normally observed N-wave boom signatures from supersonic aircraft resulting in signatures that are “peaked” or “rounded.” Flight measurements (ref. 45) have also suggested that the variability decreases as vehicle Mach number increases since the shock spends much less time and travels shorter distances in the turbulent lower-layer of the earth’s boundary layer. As such, it was believed that boom signatures from the STS Orbiter would be less influenced by the atmosphere, particularly at the higher Mach number conditions. However, at Mach numbers less than about 3.0, similar signature distortions were anticipated. This is what occurred.

In figure 20, three boom signatures measured during the descent of STS Orbiter at about Mach 3.6 and 100,000 feet altitude are shown. The signatures are basically N-wave in shape as depicted by the middle trace and vary from a “peaked” to slightly “rounded” as shown by the top and bottom traces. It is significant that, as in the case of aircraft boom signatures, that the shock-front distortions experienced by the bow shock are also duplicated on the tail shock. This has been found to hold for aircraft boom signatures with periods (ΔT) of from about 70 msec to 300 msec (ref. 10). This suggests that the assumption that the turbulent portion of the atmosphere that brings about these variations is “frozen,” is valid. It will be shown later in this section that for the STS Orbiter signatures associated with very high altitudes this repeatable pattern did not occur.

The three signatures presented in figure 20 have been designated peaked “P”, normal-peaked “NP” and normal rounded “NR” by using the waveform categories established for boom signatures observed from aircraft (refs. 46, 47 and 48) and illustrated in figure 21.

Waveform categories**.** A set of waveform categories has been established for aircraft sonic boom flight test programs to reflect the character of the boom signature observed. These same ten waveform categories, illustrated in figure 21, are used to catalogue the signatures STS Orbiter reentry-descent phase of flight. In addition to the ten waveshapes, word descriptions are also given to each of the categories by means of a single, two or three letter designation, for instance, a type "NP" was judged to be intermediate between a type "N" normal N-waveform and a type "P" peaked waveform. An "SPR" is a "spiked-peaked-rounded" signature. Such designators are included on both the hard copy listings contained in Table 6 of this report and on the supplemental electronic files. Thus, the three STS Orbiter signatures shown on figure 20 are given the waveform categories of peaked (P), normal-peaked (NP) and normal-rounded (NR).

Although the atmosphere influences the bow-shock associated with the STS launch-ascent signatures measured in the focus boom region, the basic signatures are not N-wave shape and thus they are not assigned a "waveform category." Rather they are designated as being located in the pre-focus, focus, or post-focus region in Table 6.

Influence of altitude. - Measured results from 10 of the 11 sonic boom sites in the California area that were located along and laterally from the ground track on STS-26 reentry, are illustrated in figure 22 (ref. 38). Boom measuring Site 5 was located at the predicted lateral cutoff and, as such, did not receive a boom. Also shown on the figure is the Mach number and altitude at which the boom was generated. Note that the ten signatures cover the range of Mach numbers from 4.57 to 3.18 and altitudes from about 115,000 feet to 95,000 feet.

It can be seen that all signatures are fairly well organized, being N-wave in shape with fairly rapid rise times on most and the signature periods vary from about 0.45 second to 0.68 second and overpressures from 0.61 psf to 1.28 psf. The signatures also show no signs of focussing due to the Orbiter maneuvers. There are indications of atmospheric effects on the signatures, in particular, Site 6 and Site 12, but all 10 signatures remain pretty much N-wave in character.

It should be noted, however, that at the high Mach-altitude conditions where the signature periods are large, the nature of the bow and tail shocks differ (i.e., whatever peaking or rounding of the bow shock resulting from atmospheric turbulence in the lower layers of the atmosphere, is usually repeated at the tail shock). A similar observation is evident for the first two high Mach-altitude on-track measured signatures on STS-1 reentry (ref. 37). This fact suggests that the previously mentioned assumption of a "frozen" atmosphere does not apply in all cases.

Sonic boom footprint. - In order to provide a more complete picture of the significance of these mainland measured boom signatures, shown in figure 22, their overpressure levels will be compared with the predicted sonic boom overpressure ground footprint for this reentry flight using the actual reentry track, operating conditions, and atmosphere. In figure 23 (ref. 38) is presented calculated sonic-boom contours of equal overpressure for the actual STS-26 reentry trajectory and atmosphere. Also shown is the predicted lateral cutoff boundary beyond which no booms are observed and the location of the 12-boom measurement sites and corresponding measured sonic-boom levels.

Note first of all that the contours of sonic-boom overpressure are not symmetrical about the ground-track line as one would expect for a vehicle flying in steady-level flight. The distortions of the contours result from the fact that orbiter is not flying at steady-level conditions along its ground track. Rather, it enters the area at a roll angle of -40^o makes a heading change involving a roll to $+40^o$ along with flight-path and angle-of-attack changes (see fig. 8). The sonic-boom prediction program takes all these variations, that result in changes in loading on the vehicle, into account as both "lift" and "volume" changes in the process of calculating sonic-boom overpressure.

Comparison of the measured bow-wave overpressure values to the predicted overpressure contours are in good agreement for all 11 sites. No boom focussing is evident and the lateral cutoff was as predicted.

COMPARISON OF AIRCRAFT AND SPACECRAFT BOOMS

At this point in the discussion of reentry sonic boom signatures associated with the 122 foot-long, 200,000 pounds Orbiter, it would be of value to compare a few of them with measured boom signatures from aircraft such as the 200-foot long, 300,000 pound Concorde supersonic transport (Ref. 49) and the 105-foot long, 100,000 pounds SR-71 (Ref. 46). These signatures, all drawn to the same pressure and time scale are shown in figure 24. Note that all signatures are N-wave in character and the Orbiter waveforms are not distinguished in any particular manner with the exception of the longer wavelength (period). Overpressures vary from about 0.69 psf for the Orbiter at Mach 6.0 at 129,000 feet to about 2.32 at Mach 1.76 and 70,690 feet and seem to fit in with those associated with the other aircraft. It can be seen that as altitude increases, the signature lengths, ΔT (periods) increase.

Figure 24 has shown that the sonic-boom signatures, measured for Orbiter reentry at Mach numbers from about 1.8 and 6.0 are very similar to those observed from aircraft in that they are N-wave in shape. An indication of how the Orbiter boom levels, taken from maximum values listed in Table 7, vary with flight altitude and where they fit in with boom measurements from small and large military aircraft, the Concorde supersonic transport, and previous Apollo capsule reentry booms is given in figure 25. The data represent on-track measurements, those within $\pm$ 3 n.mi of the ground track.

It can be seen that the predicted trend of decreasing sonic boom overpressure with increasing altitude is reflected in the aircraft data up to 80,000 feet, in the Apollo capsule measurements up to 174,000 feet, and in the Orbiter results up to altitudes of about 250,000 feet. (Note that the two Orbiter data points at about 195,000 feet and 250,000 feet altitude were at offset distances of about 33 n.mi and 75 n.mi, respectively.) In addition, the larger the vehicle the greater the overpressure, varying from about 3.5 lbs/ft^2 for the large XB-70 to about 1.0 lbs/ft^2 for the smaller F104 fighter at the same altitude, then again to 0.2 lbs/ft^2 for the even smaller Apollo capsule. Orbiter overpressures vary from about 2.3 lbs/ft^2 at 70,000 feet to about 0.7 lbs/ft^2 at 129,000 feet. In all cases, the data, and in particular Orbiter, all fit pretty much the same mold that has been observed from aircraft over the past four decades.

Also shown in figure 25 are sonic boom overpressures measured during the launch-ascent of the Saturn-Apollo vehicle (refs. 1-3) and Space Shuttle (refs. 33, 34 and 36). These measured results do not include overpressures very near or on the focus line. In addition, these ascent boom data are plotted at the approximate altitude at which the booms originated. Previous plots, similar to figure 25 (refs, 2,3, 38 and 50) are plotted at altitudes corresponding to the vehicle overhead position.

In general, the measured overpressures for the launch and ascent portion of spacecraft flights indicate the same trend of decreasing pressure with increasing altitude. However, the magnitudes of the overpressure values are much greater than those of the reentry case. Since the launch vehicle is considerably larger than the reentry vehicle, higher boom levels can be expected. The largest portion of the increased overpressure from launch vehicle results from the “effective body” produced by the rocket exhaust plume. It is of interest to note that disturbances from Apollo rockets in space were measured at ground level for the vehicle operating at altitudes up to about 600,000 feet (ref. 51). Simplified methods for prediction of spacecraft launch and reentry sonic booms are discussed in references 19, 20 and 22.

CONCLUDING REMARKS

A significant sonic boom database relating to the launch-ascent and reentry-descent phases of the Space Shuttle has been established, cataloged, and documented. The measured sonic boom signatures were obtained on 26 flights of the Space Shuttle beginning with the first launch of STS-1 on April 12, 1981, to the reentry-descent of STS-41 into EAFB on October 10, 1990. A total of 23 boom measurements were acquired within the focus region off the Florida coast during 3 STS launch-ascents and 113 boom measurements were acquired during 23 STS reentry-descents-to-landing into Florida and California. A total of 123 boom signatures were acquired, 20 on ascent and 103 on reentry. These sonic boom measurements were made under and lateral to the vehicle ground track and cover the Mach-altitude range of about 1.3 to 23 and 58,000 feet to 243,000 feet, respectively. In addition to the measured sonic boom signatures, vehicle operational data, flight profiles, and weather data were also gathered during the flights. This STS boom measurement database is contained in 26 documents, a few of which are formal and referenceable, but most are internal documents and not referenceable and also not readily available. Another 38 documents, also non-referenceable, contain predicted sonic boom footprints for reentry-descent flights on which no measurements were made.

The boom database consists of the measured signatures, signature characteristics which include the maximum positive overpressures (Δp_o), total period (ΔT), period of positive phase (Δt_o), positive impulse (I_o), and bow shock rise time readings to the half-amplitude ($\tau_{1/2}$), three-fourths amplitude ($\tau_{3/4}$), maximum amplitude (τ_{max}) and from the ten to ninety percent amplitude ($\tau_{10\text{-}90}$). In addition, a waveform category is assigned each signature. The signature spectrum is also available. Complementing the boom measurements are the flight trajectories and atmosphere measurements.

The sonic boom database cited above, along with trajectory and weather information is contained in a supplemental electronic file. Copies of the reports on each of the STS flights on which booms

were measured were electronically scanned and are included on the supplemental CD along with the reports containing predicted boom footprints for 38 STS reentry missions on which no boom measurements were made.

For the launch ascent phase of flight, measurements were concentrated off the Florida Coast in an area of the Atlantic Ocean, about 40 n.mi east of the launch site in order to define the magnitude of the focus boom. Single shock pressure signatures, similar to blast explosion waveforms, with periods of about 2.0 seconds to 8.0 seconds, were observed with overpressure levels ranging from about 0.4psf in the pre- and post-focus region to 6.81 psf along the focus line. The nature of the focus region and signature characteristics is quite similar to those obtained during launch-ascent of the Apollo-Saturn vehicle. In each case, the predictive tools were suitable to define the location and extent of the focus region.

For the reentry-descent phase of flight, the measurements were made on land with the majority acquired in the state of California and about 25 percent in the state of Florida. The measured boom signatures were generally N-wave in character, similar to those observed from supersonic aircraft with amplitudes ranging from about 0.10 psf from the vehicle at about 243,000 feet altitude to a maximum of 2.32 psf just prior to landing. Signature periods, however, were much greater than those observed on aircraft being on the order of about 0.40 second to about 2.5 seconds. Predictions of the magnitude of sonic booms and ground footprints for Mach numbers to about 6.0 compared favorably with measurements.

Even though the Orbiter performs maneuvers during the reentry descent phase of flight, particularly roll angle and heading, they were not predicted to result in focus booms at the ground and none were observed. Atmospheric turbulence, especially in the lower layers of the atmosphere, result in peaking or rounding of the N-wave signatures similar to what has been observed from aircraft in supersonic flight where the changes to the bow-shock are repeated on the tail shock. It is observed, however, that when the Orbiter is at very high altitudes where the signature periods are large and overpressures relatively low that the bow and tail shock distortions resulting from the atmosphere sometimes differ.

REFERENCES:

1. Hilton, David A.; Henderson, Herbert R.: Sonic Boom Ground-Pressure Measurements From Apollo 15. NASA TN D-6950, 1972.
2. Henderson, Herbert R.: and Hilton, David A.: Sonic Boom Ground Pressure Measurements from the Launch and Reentry of Apollo 16. NASA TN D-7606, 1974.
3. Henderson, Herbert R.; and Hilton, David A.: Sonic Boom Measurements in the Focus Region During the Ascent of Apollo 17. NASA TN D-7806, 1974.
4. Hicks, Raymond M.; Mendoza, Joel P.; and Garcia, Frank: A Wind Tunnel Flight Correlation of Apollo 15 Sonic Boom. NASA TM X-62,111, Jan. 28, 1972.
5. Hicks, R. M.; Mendoza, J. P.; and Thomas, C. L.: Pressure Signatures for the Apollo Command Module and the Saturn V Launch Vehicle with a Discussion of Strong Shock Extrapolation Procedures,: NASA TM X-62,117, April 1972.
6. Garcia, Frank; Hicks, Raymond M.; and Mendoza, Joel P.: A Wind Tunnel Fight Correlation of Apollo 16 Sonic Boom. NASA TM X-62,073, Feb. 5, 1973.
7. Hicks, R. M.; and Mendoza, J. P.: Pressure Signatures for a 0.0053 Scale Model of the Saturn V-Apollo Launch Vehicle With Simulated Exhaust Plumes: NASA TM X-62,129, July 23, 1973.
8. Hicks, R. M.; and Mendoza, J. P.: An Investigation of the Feasibility of Simulating Gaseous Exhaust Plumes With Solid Bodies in Sonic boom Studies, NASA TM X-62,131, August 17, 1973.
9. Proceedings of the Sonic Boom Symposium. J. Acous. Soc. America, Vol. 39, No. 5, Pt. 2, May 1966, pp. S1-S80.
10. Seebass, A. R., ed.: Sonic Boom Research. NASA SP-147, 1967.
11. Schwartz, Ira, R., ed.: Second Conference on Sonic Boom Research. NASA SP-180, 1968.
12. Schwartz, Ira R., ed.: Third Conference on Sonic Boom Research. NASA SP-255, 1971.1 .
13. Sonic Boom Symposium. J. Acous. Soc. America, Vol. 51, No. 2, Pt. 3, Feb. 1972, pp. 671-798.
14. Hicks, Raymond M.; and Mendoza, Joel P.: A Brief Study of the Space Shuttle Sonic Boom During Ascent. NASA TM X-62-050, July 23, 1971.
15. Mendoza, Joel P.: Sonic Boom Pressure Signatures for the Space Shuttle Launch Vehicle. NASA TM X-62441, May 1975.
16. Mendoza, Joel P.: Wind Tunnel Pressure Signatures for a 0.0041-Scale Model of the Space Shuttle Orbiter. NASA TM X-62432, 1975.
17. Mendoza, J. P.: Further Wind-Tunnel Measurements of Pressure Signatures for an 0.0041 Scale Model of the Space Shuttle Orbiter. NASA TM X-73120, May 1976.
18. Carlson, Harry W.; and Mack, Robert J.: A Study of the Sonic boom Characteristics of a Blunt Body at a Mach Number of 4.14. NASA TP-1015, Sept. 1977.
19. Carlson, Harry W.: Simplified Sonic Boom Predictions. NASA TP-1122, 1978.
20. Ashby, George C.: Near-Field Sonic Pressure Signatures for the Space Shuttle Launch and Orbiter Vehicles at Mach 6. NASA Tech. Rept. 1405, April 1977.
21. Ashby, George C.: A Study of Sonic Boom Characteristics of a Blunt Body at a Mach Number of 6. NASA TP-1787, 1980.
22. Carlson, Harry W.; and Mack, Robert J.: A Wind-tunnel Study of the Applicability of Far-Field Sonic Boom Theory to the Space Shuttle Orbiter. NASA TP-1186, June 1978.

23. Holloway, Paul F.; Wilhold, Gilbert A.; Jones, Jess H.; Garcia, Frank, Jr.; and Hicks, Raymond M.: Shuttle Sonic Boom - Technology and Predictions. AIAA Paper 73-1039, Oct. 1973.
24. Malkin, Myron S.: Environmental Impact Statement for the Space Shuttle Program. Final Report. NASA TM-82278, 1978.
25. Henderson, Herbert R.: Sonic Boom Measurement Test Plan for Space Shuttle STS-1 Reentry. NASA-TM-85222, Apr. 1981.
26. Henderson, Herbert R.: Sonic Boom Measurement Test Plan for Space Shuttle STS-2 Reentry. NASA-TM 84858, Nov. 1981.
27/ Henderson, Herbert R.: Sonic Boom Measurement Test Plan for Space Shuttle STS-3 Reentry. NASA TM-85223, March 1982.
28. Henderson, Herbert R. Sonic Boom Measurement Test Plan for Space Shuttle STS-4 Reentry. NASA TM-85224, June 1982.
29. Henderson, Herbert R.: Sonic Boom Measurement Test Plan for Space Shuttle STS-5 Reentry. NASA-TM 85225, Nov. 1982.
30. Garcia, Frank, Jr.; Jones, Jess H.; and Henderson, Herbert R.: A Comparison of Measured and Theoretical Predictions for STS Ascent and Entry Sonic Booms. Shuttle Performance: Lessons Learned. NASA CP 2283, Part 2, pp. 1277-1300, October 1983.
31. Potter, Andrew, E.: Space Shuttle Environmental Effects: The First Five Flights. NASA JSC-19091, July 1983, (now NASA CR-171812, July 1983).
32. Garcia, Frank, Jr., Morrison, Karen M.; Jones, Jess H.; and Henderson, Herbert R.: Preliminary Sonic Boom Correlation of Predicted and Measured Levels for STS-1 Entry. NASA TM-58242, Feb. 1982.
33. Garcia, Frank, Jr.,; Jones, Jess H.; and Henderson, Herbert R.: Preliminary Sonic Boom Correlations of Predicted and Measured Levels for STS-5 launch. NASA TM-58253, April 1983.
34. Stansbery, E. G.; Stanley, J. F.; and Potter, A. E.: Sonic Boom Levels Measured for STS-7 Launch. NASA JSC-19237, August 1983.
35. Stansbery, E. G.; and Stanley, J. F.: Sonic Boom Levels Measured for STS-41B Landing. NASA JSC-20091, Sept. 1984.
36. Stansbery, E. G.; and Stanley, J. F.: Sonic Boom Levels Measured for STS-41-D Launch. NASA JSC-20218, Dec. 1984.
37. Garcia, Frank, Jr.; Jones, Jess H.; and Henderson, Herbert H.: Correlation of Predicted and measured Sonic Boom Characteristics From the Reentry of STS-1 Orbiter. NASA TP-2475, 1985.
38. Stansbery, E. G.; and Stanley, J. F.: Descent Sonic Boom Measurements for STS-26 Including a Mach 23 Measurement. NASA JSC-23579, April 1989.
39. Thomas, C. L.: Extrapolation of Sonic Boom Pressure Signatures by the Waveform Parameter Method. NASA TN D-6832, June 1972.
40. Plotkin, Kenneth J.: Potential Sonic Boom Focal Zones From Space Shuttle Reentry. Wyle Research Report, WR 89-11, July 1989.
41. Patterson, Donald W.: Sonic Boom Limitations on Supersonic Aircraft Operations. Aero/Space Engineering, pp. 22-24 and 40-45, July 1960.
42. Hubbard, Harvey H.' Maglieri, Domenic J.; Huckel, Vera; and Hilton, David A.: Ground Measurements of Sonic-Boom Pressures for the Altitude Range of 10,000 to 75,000 Feet. NASA TR-R-198, 1964.

43. McCurdy, David A.; Subjective Response to Sonic Booms having Difference Shapes, Rise Times, and Durations. NASA TM 109090, March 1994.
44. Shepherd, K. P.; and Sullivan, B. M.: A Loudness Calculation Procedure Applied to Shaped Sonic Booms. NASA TP-3134, 1991.
45. Maglieri, Domenic J; Huckel, Vera; Henderson, Herbert R.; and McLeod, Norman, J.: Variability in Sonic Boom Signatures Measured Along an 8000-Foot Linear Array. NASA TN D-5040, 1969.
46. Maglieri, Domenic J.; Huckel, Vera; and Henderson, Herbert R.: Sonic Boom Measurements for SR-71 Aircraft Operating at Mach Numbers to 3.0 and Altitudes to 24,384 Meters. NASA TN D-6823, 1972.
47. Maglieri, Domenic J. and Sothcott, Victor E.: Summary of Sonic Boom Rise Times Observed During FAA Community Response Studies Over a 6-Month Period in the Oklahoma City Area. NASA CR 4277, 1980.
48. Maglieri, Domenic J.; Sothcott, Victor E.; and Keefer, Thomas N.: A Summary of XB-70 Sonic Boom Signature Data. NASA CR-189630, April 1992.
49. Holbeche, T.: Measurements of Sonic Bangs from the Prototype Concorde 002 During Supersonic Development of Flying in the United Kingdom. Royal Aircraft Establishment Tech. Memo, Aero. 1405, 1972.
50. Maglieri, Domenic J.; and Plotkin, Kenneth: Sonic Boom, Chapter 10, pp. 519-561. Aeroacoustics of Flight Vehicles: theory and Practice, NASA RP-1258, Vol. I and WRDC TR 90-3052, August 1991.
51. Cotten, Donald; and Donn, William L.: Sound From Apollo Rockets in Space. Science, Vol. 171, No. 3971, Feb. 12, 1971, pp. 565-567.

APPENDIX

DESCRIPTON OF SUPPLEMENTAL STS SONIC BOOM ELECTRONIC FILES

A complete listing of all STS sonic boom material addressed in this hard copy report has been electronically cataloged on a single supplemental CD. Figure A-1 presents a description of STS sonic boom electronic files which includes this hard copy report, the 26 STS missions on which boom measurements were obtained and the 39 STS descent missions on which boom footprints were predicted but no measurements were made. For the STS missions on which sonic boom ground footprints were calculated, but no measurements were made, the files contain the one to two page report containing the text and predicted ground footprint for each of the 38 reentry flights.

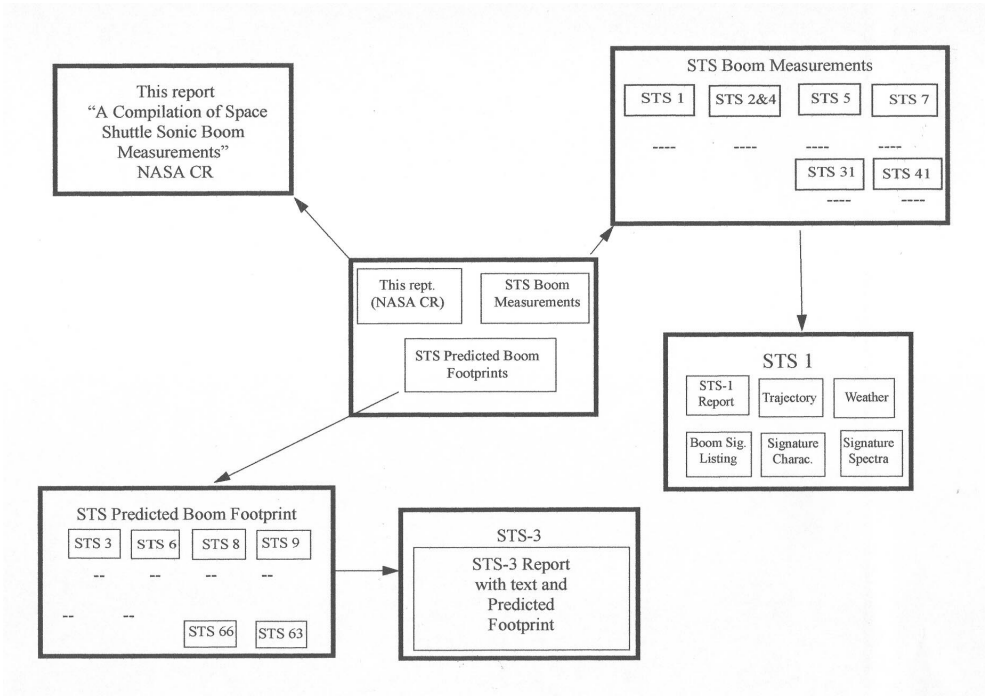

Figure A-1. - Description of STS Sonic Boom Electronic File.

With each STS mission on which boom measurements were made, the files include the STS report, corresponding ascent or reentry trajectory, available weather data, sonic boom signature pressure time history of each measurement station for that specific mission, the boom signature characteristics (Δp_o, ΔT, Δt_o, I_o, $\tau_{1/2}$, $\tau_{3/4}$, τ_{max} and $\tau_{10\text{-}90}$ and waveform category) and the sonic boom signature spectrum. A description of the algorithm used to provide the information on electronic file follows:

Description of Algorithm

The waveform characteristics were calculated by computer algorithm except for waveform category, which was done manually. Digital data, either from the raw PATS files or from the electronically scanned signatures, were stored in an array of time and pressure. The array was searched to find the maximum (Δp_o) and minimum pressures and their corresponding times. Intermediate pressure values were calculated included 10%, 50%, 75% and 90% of the maximum value. The

array was then searched backwards in time from the maximum pressure value. As each point in the pressure signature was examined, it was compared with the 10%, 50%, 75% and 90% values. If the pressure was greater than these thresholds, the time was saved for corresponding threshold. This has the effect of saving the earliest time that each threshold is exceeded. The most difficult point to reliably determine was the onset of the shock. This was not defined as the point at which the pressure signature reaches zero, since ambient noise may keep the pressure above zero for an arbitrary time. Instead, for the purposes of the automated algorithm, the onset of the shock was defined as when the rate of pressure increase between two successive points fall to approximately 0.0075 psf/0.000125 seconds and the pressure level was below 10% of the maximum level.

τ_{max} is then the difference in time between the onset of the shock and the time that the maximum pressure was recorded. Similarly, $\tau_{1/2}$ and $\tau_{3/4}$ are the differences between onset and the first joint where the signature exceeds 50% or 75% of the maximum pressure, respectively. $\tau_{10\text{-}90}$ is the difference in time between the first point at which 10% of the maximum pressure is reached and the first point at which 90% of the maximum pressure is reached. The total period (ΔT) also requires the time of the trailing or return shock. Since the return shock often does not return immediately to zero pressure, the time of the return shock was chosen to be the point where pressures rise above 50% of the minimum pressure. ΔT is then the time between the onset of the initial shock and the defined time of the return shock.

To calculate the positive impulse (I_o) of the N-wave, the time/pressure array was searched from the onset of the initial shock to the time of the minimum pressure. Any data point in the array, with a pressure greater than zero, was multiplied by the time between successive points and the sum of these positive pressure/delta time values is the total positive impulse. The period of the positive phase (Δt_o) is the time between the onset of the initial shock and the first point in time when the pressure level fell back to a negative value.

The spectrum files were produced using a standard Fast Fourier Transform (FFT0 algorithm) adapted from a program published in "*Byte Magazine," December 1978 by W. D. Stanley and S. J. Peterson.*

Each measured boom signature was examined and assigned one of the ten waveform categories depicted in figure 21 of this report. Since the signatures acquired during the three launch-ascent flights were not N-wave in character, they are not assigned a "waveform category." Rather, they are designated as being measurements at locations before the focus (pre-focus), near the focus, at focus and after the focus (post focus) region.

Comparison of Signature Characteristics

Both the analog SBDA and digital PATS measurement systems had frequency response characteristics that permitted definition of the sonic boom signature rise time to about 100 μsec. Of the 123 measured signatures, 38 were from the SBDA analog systems and 85 from the PATS digital systems. Sixty-two of the digital signatures were processed directly to acquire boom characteristics. Hard copies of the remaining 61 signatures (38 analog and 23 digital) were electronically scanned. Although the hard copy signatures, which varied in length from about 2 to 4 inches, were scanned at the rate of 800 points per inch. the actual signature resolution is dictated by the quality of the hard copy signature, its "noisiness" and especially the thickness of the line tracing. This is illustrated with the aid of figure A2 in which is presented the two N-wave measured signatures during STS-33 reentry.

At Site 1, a “normal peaked (NP)” waveform is experienced and at Site 2 a “peaked (P)” waveform. In each case, the solid line represents the signature resulting from the original digital

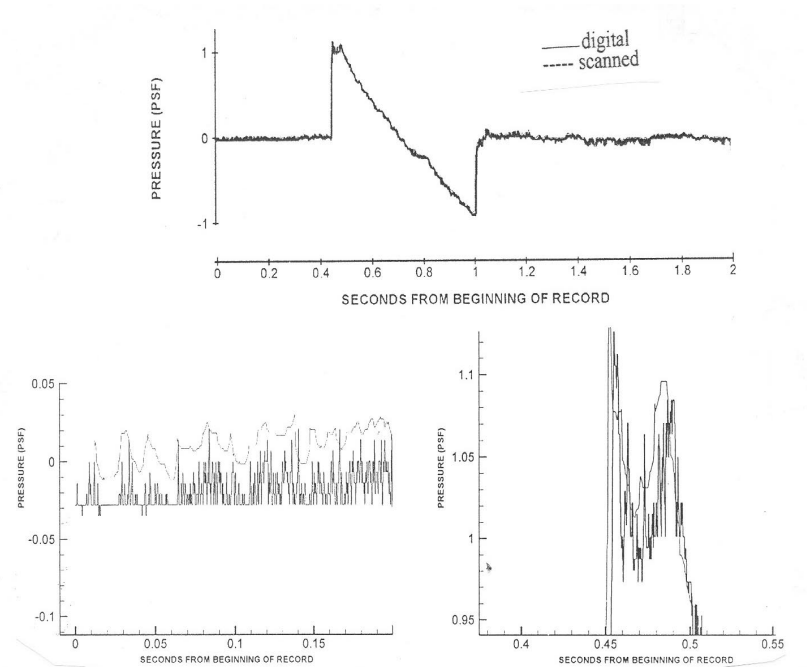

(a) Site 1, U5MBO, Santa Barbara, California.

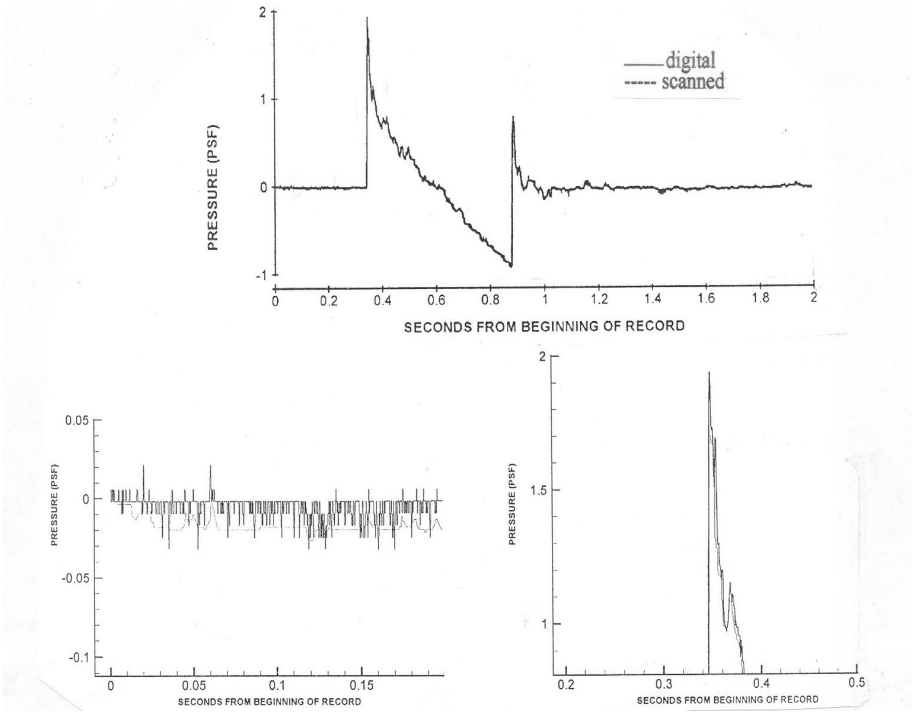

(b) Site 2, U1MBO Ojai, Califronia.

Figure A2 - Comparison of scanned to digital signature for STS-33 reentry.

recording and the dashed line is the results of scanning. It is obvious that the digital and scanned traces are essentially coincident. However, when portions of each of the two signatures are examined in greater detail, differences are noted to exist. The traces presented in the lower portion of figures A-2 (a) and (b) represent two portions of the complete signatures with a greatly expanded pressure and time scale, the trace on the lower left at a time prior to the arrival of the initial shock and the trace to the right at a time that captures the initial shock.

Note that the presence of "system noise" in the original digital trace is not matched in the scanned signature. Rather, scanning tends to seek out the peak values. As such, the initial starting point (Δp) to reading the initial shock overpressure and shock rise times are somewhat altered from that obtained from a manual reading by as much as 0.03 psf in the two examples shown.

Comparison of the original and scanned traces for the expanded traces containing the initial shock shows that for the "normal-peaked" signature of Site 1, although the two traces appear comparable, there is a noticeable time shift of the scanned trace to the left. However, the maximum overpressure readings are the same. For the peaked signature of Site 2 the two traces are almost coincident and the scanned signature is shifted slightly to the left. However, there is an observable difference in the maximum overpressure readings. Since the scanner will read only to the amplitude where "daylight" no longer exists ($\Delta p = 1.75$ psf) it will not acquire the maximum overpressure defined by the "spike" at the top of the bow shock ($\Delta p = 1.94$ psf).

An indication of effects of the differences noted between the original digital and scanned data on the sonic boom signature characteristics for the two measurements from STS-33 are illustrated in Table A-1.

Table A1. - Comparison of Sonic Boom Signature Characteristics for STS-33 Reentry.

Site	Method	Δp_o (psf)	ΔT (sec)	Δt_o (sec)	I_o ($lb/ft^2 sec$	$\tau_{1/2}$ (msec)	$\tau_{3/4}$ (msec)	τ_{max} (msec)	τ_{10-90} (msec)
Santa Barbara	Scanned Original recording	1.13 1.13	0.562 0.564	0.264 0.264	0.150 0.145	1.60 2.02	2.40 3.41	4.80 6.05	3.80 4.16
Ojai	Scanned Original recording	1.75 1.94	0.537 0.539	0.251 0.251	0.120 0.126	2.00 3.89	3.30 4.64	4.10 5.77	3.30 4.01

Good agreement is noted to exist between the digital and scanned signatures relative to the maximum positive overpressure (Δp_o), signature period (ΔT), signature positive duration (Δt_o) and positive impulse (I_o). The differences in rise for the half, three-fourths and maximum readings, however, ranged from about 20 percent to 50 percent. A lesser variation exists in the τ_{10-90} readings (about 10 to 20 percent).

In the documentation of the boom signatures acquired on STS-1 (ref. 37) and STS-26 (ref. 38), in addition to presenting the measured signatures and tabulations of the maximum overpressure and, in some cases, the signature durations, the initial portion of the signature was presented on a time

scale that was expanded by a factor of about 16 in order to provide significantly more detail of the signature shock rise times. Thus, it is possible to also examine the difference in rise time readings obtained from these hard copy traces and those resulting from the electronic readout of the scanned-digitized signatures. The results are shown on Table A-2 and Table A-3.

Table A-2. - Comparison Sonic Boom Signature Characteristics From STS-1 reentry.

Meas. Station	Δp_o, psf		ΔT, sec		Δt_o, sec		$\tau_{1/2}$, msec		$\tau_{3/4}$, msec		τ_{max}, msec		$\tau_{10\text{-}90}$, msec	
	manual	elec-tronic	manual	elec-tronic	manual	elec-tronic	manual	elec-tronic	manual	elec-tronic	manual	elec-tronic	manual	elec-tronic
Call. (0)	0.69	0.70	0.680	0.680	0.349	0.347	1.40	1.60	2.50	2.90	9.60	21.30	3.50	3.60
(1)	1.22	1.23	0.565	0.562	0.260	0.264	0.90	0.50	2.30	2.10	5.20	26.90	3.40	3.00
(2)	0.93	0.92	0.516	0.508	0.280	0.284	1.20	1.30	2.60	3.00	5.90	4.70	3.20	3.30
(3)	1.14	1.15	0.460	0.463	0.260	0.267	1.70	2.00	4.00	9.40	22.50	44.90	16.00	20.00
(4)	1.60	1.56	0.443	0.443	0.230	0.232	1.60	1.70	2.60	2.60	7.20	6.10	4.20	3.20
(5)	1.63	1.60	0.400	0.397	0.220	0.215	0.40	0.80	0.70	1.10	7.50	7.40	3.00	3.70
(6)	2.40	2.32	0.390	0.388	0.210	0.212	0.50	1.30	0.60	1.60	4.00	3.70	2.80	2.20
(7)	1.96	1.94	0.370	0.379	0.192	0.201	0.40	0.80	0.60	1.10	14.00	14.10	3.00	2.60
(8)	1.81	1.78	0.380	0.382	0.201	0.207	0.40	1.50	0.60	1.80	4.90	5.00	3.60	3.70
(9)	2.26	2.16	0.370	0.372	0.199	0.201	1.60	1.60	2.50	2.00	3.00	2.60	2.00	1.70
(10)	1.86	1.86	0.375	0.372	0.202	0.208	0.50	0.80	0.80	1.10	3.40	3.30	1.00	0.90

Table A-3. - Comparison Sonic Boom Signature Characteristics From STS-26 reentry.

Kauai, Hawaii	0.10	0.10	2.630	2.454	1.340	1.305	15.00	12.00	100.00	95.50	135.00	124.50	105.00	102.00
Santa Barbara, Ca.	1.06	1.07	0.620	0.619	0.320	0.314	2.00	2.25	3.10	3.12	7.00	7.87	3.50	4.62
Ventura, Ca.	0.65	0.65	0.660	0.661	0.360	0.352	1.20	2.20	2.50	3.00	12.00	25.20	4.50	10.60
Oxnard, Ca.	0.70	0.68	0.675	0.676	0.355	0.365	1.30	2.40	3.10	4.00	23.00	24.60	12.00	14.90
Lake Sherwood, Ca.	Beyond lateral-cutoff													
Santa Paula, Ca.	1.05	1.04	0.652	0.641	0.325	0.313	6.00	4.80	23.00	28.10	40.00	41.40	27.00	30.10
Oak Flat , Ca.	0.61	0.61	0.540	0.535	0.265	0.260	2.00	1.40	3.30	2.70	5.30	6.00	3.00	3.30
Lions Canyon, Ca.	1.04	1.04	0.580	0.572	0.278	0.272	1.00	1.00	2.00	1.90	5.20	20.70	2.50	3.90
Gold Hill, Ca.	1.14	1.19	0.455	0.453	0.235	0.231	1.00	1.12	1.80	1.68	4.00	4.14	2.70	2.57
Pine Mountain, Ca.	1.15	1.16	0.540	0.543	0.252	0.261	1.90	2.09	2.90	3.03	3.60	3.87	2.30	2.82
Wheeler Ridge, Ca.	1.28	1.28	0.520	0.519	0.260	0.224	1.00	0.86	1.40	1.40	2.60	2.59	1.50	1.40
Conner, Ca.	0.82	0.82	0.593	0.593	0.285	0.284	1.10	1.14	1.80	1.48	3.0	2.63	1.70	1.60

Listed in each table are the maximum positive overpressure (ΔP_o), signature period (ΔT), signature positive duration (Δt_o) and signature rise times in milliseconds to the half overpressure amplitude ($\tau_{1/2}$), three quarters amplitude ($\tau_{3/4}$), maximum amplitude (τ_{max}) and from the 10 percent to 90 percent amplitude ($\tau_{10\text{-}90}$) for the 11 signatures on STS-1 and 11 signatures on STS-26.

Once again, good agreement is noted to exist between the manual and electronic read signatures relative to the maximum overpressure (Δp_o), signature period (ΔT) and signature positive duration (Δt_o). The differences in rise times are in reasonable agreement for signatures that are least distorted by the atmosphere, or are almost void of system noise, thus making the selection of the 1/2, 3/4, maximum and 10 percent to 90 percent amplitudes more accurate. It is again noted that the signature characteristic listings in Table 6 are those resulting from the electronic readout of the original digitized data from the PATS digital measurements systems and the electronically scanned hard copy signatures of the SBDAS analog measurement systems (in addition to those hard copy PATS signatures that were also scanned since the original digital data was not available).

Table 1. - Listing of STS Missions on Which Sonic Boom Measurements Were Acquired

STS MSN	Launch			Sonic Booms Measured during:		No. Sonic Boom Meas. Obtained		Measurement array		Approximate Flight Conditions at which booms were generated				STS Landing			
										Mach Number		Altitude, kft.					
	Site	Date	Time, Z	Ascent	Reentry	Ascent	Reentry	Ascent	Reentry	Ascent	Reentry	Ascent	Reentry	Site	Date	Time Z	Wt., lbs
1	KSC	4-12-81	12:00:03		x		11		Grd.Trk		6.0/1.3		129/58	EAFB	4-14-81	18:20:55	195,472
2	KSC	11-12-81	15:09:59		x		4		Grd.Trk		2.4/1.5		80/65	EAFB	11-14-81	21:23:14	204.263
4	KSC	6-27-82	14:59:59		x		4		Lateral		3.3		97	EAFB	7-04-82	16:09:45	208,947
5	KSC	11-11-82	12:19:00	x		1		Foc. Reg.		3.5		112		EAFB	11-16-82	14:33:26	202,480
7	KSC	6-18-83	11;33:00	x		7		Foc.Reg.		3.5/4.0		140/150		EAFB	6-24-83	13:57:08	204,043
41-B	KSC	2-03-84	13:00:00		x		14		Lat.&Grd.Trk		4.2/3.3		108/95	KSC	2-11-84	12:15:55	201,239
41-D	KSC	8-30-84	12:41:50	x		15		Foc.Reg.		3.5/4.0		150/170		EAFB	9-05-84	13:37:55	201,675
41-G	KSC	10-05-84	11:03:00		x		8		Lat.&Grd.Trk		2.7/1.6		86/66	KSC	10-13-84	16:26:39	202,266
51-A	KSC	11-08-84	12:15:00		x		7		Lat.&Grd.Trk		15/1.3		191/59	KSC	11-16-84	12:00:01	---
51-C	KSC	1-24-85	19-50:00		x		5		Lat.&Grd.Trk		2.2/1.4		77/60	KSC	1-27-85	21:23:29	198,014
51-D	KSC	4-12-85	13:59:05		x		5		Lat.&Grd.Trk.		4.8/1.5		118/59	KSC	4-19-85	13:54:33	198,014
51-G	KSC	6-17-85	11:33:00		x		3		Lateral		4.0		106	EAFB	6-24-85	13:12:00	204,169
51-F	KSC	7-29-85	21:00:00		x		3		Lateral		3.6		99	EAFB	8-06-85	19:45:27	216,735
51-I	KSC	8-27-85	10:58:01		x		2		Lateral		4.0		108	EAFB	9-03-85	13:15:46	196,674
61-A	KSC	10-30-85	17:00:00		x		3		Lateral		3.1		93	EAFB	11-06-85	17:44:53	214,171
26	KSC	9-29-88	15:37:00		x		12		Lateral		23/3.1		243/95	EAFB	10:03:88	16:37:12	----
27	KSC	12-02-88	14:30:33		x		3		Lateral		13/5.0		186/124	EAFB	12-06-88	23:36:11	---
29	KSC	3-13-89	14:57:00		x		2		Lat.&Grd.Trk.		4.2		108	EAFB	3-18-89	14:35:49	192,457
30	KSC	5-04-89	18:46:59		x		2		Lateral		4.5		113	EAFB	5-08-89	19:43:25	192,460
28	KSC	8-08-89	12:37:00		x		12		Lat.&Grd.Trk		3.9/3.0		103/91	EAFB	8-13-89	13:37:08	----
34	KSC	10-18-89	16:53:40		x		2		Lat.&Grd.Trk		3.6		100	EAFB	10-23-89	16:32:01	195,954
33	KSC	11-22-89	00:23:30		x		2		Lat.&Grd.Trk		4.3/3.8		111/95	EAFB	11-28-89	00:30:18	----
32	KSC	1-09-90	12:35:00		x		2		Lat.&Grd.Trk		4.1		104	EAFB	1-20-90	09:35:36	228,335
36	KSC	2-28-90	07:50:22		x		2		Lateral		3.1		95	EAFB	3-04-90	18:08:44	----
31	KSC	4-24-90	12:33:51		x		3		Lat.&Grd.Trk		3.9		105	EAFB	4-29-90	13:49:57	189,118
41	KSC	10-06-90	11:47:14		x		2		Lat.&Grd.Trk		4.5		114	EAFB	10-10-90	13:57:19	----

Notes: 1. Total STS MSN on which sonic booms measured = 26 (3 ascent, 23 reentry)
2. Total boom signature measurements = 136 (23 ascent, 113 reentry)

Table 2. LISTING OF STS MISSIONS ON WHICH DESCENT SONIC BOOM GROUND FOOTPRINTS WERE PREDICTED BUT NO MEASUREMENTS WERE MADE

MSN Number	Date		Descent Footprint		
	Launch	Landing	Approximate Ground Track	Land Area Involved	Landing Site
STS-3	3-22-82	3-30-82	W-E	Arizona-New Mexico	White Sands
STS-6	4-4-83	4-9-83	W-E	Santa Barbara-Edwards AFB	Edwards AFB
STS-8	8-30-83	9-5-83	W-E	Santa Barbara-Edwards AFB	Edwards AFB
STS-9	11-28-83	12-8-83	N-S	Bakersfield-Edwards AFB	Edwards AFB
STS-41-C	4-6-84	4-13-84	W-E	Santa Barbara-Edwards AFB	Edwards AFB
STS-51-B	4-29-85	5-6-85	S-N	Los Angeles-Edwards AFB	Edwards AFB
STS-51-J	10-3-85	10-7-85	W-E	Santa Barbara-Edwards AFB	Edwards AFB
STS-61-B	11-26-85	12-3-85	S-N	Mexico-California	Edwards AFB
STS-61-C	1-12-86	1-18-86	W-E	Ventura-Edwards AFB	Edwards AFB
STS-38	11-15-90	11-20-90	W-E	Orlando-Titusville	Kennedy Space Center
STS-35	12-2-90	12-11-90	W-E	Santa Barbara-Edwards AFB	Edwards AFB
STS-37	4-5-91	4-11-91	W-E	Santa Barbara-Edwards AFB	Edwards AFB
STS-39	4-28-91	5-6-91	NW-SE	Ocala-Titusville	Kennedy Space Center
STS-40	6-5-91	6-14-91	W-E	Rosamond-Edwards AFB	Edwards AFB
STS-43	8-2-91	8-11-91	W-E	Orlando-Titusville	Kennedy Space Center
STS-48	9-12-91	9-18-91	N-S	Rosamond-Edwards AFB	Edwards AFB
STS-44	11-24-91	12-1-91	W-E	Santa Barbara-Edwards AFB	Edwards AFB
STS-42	1-22-92	1-30-92	W-E	Santa Barbara-Edwards AFB	Edwards AFB
STS-45	3-24-92	4-2-92	W-E	Orlando-Titusville	Kennedy Space Center
STS-49	5-7-92	5-16-92	W-E	Ventura-Edwards AFB	Edwards AFB
STS-50	6-25-92	7-9-92	W-E	Orlando-Titusville	Kennedy Space Center
STS-46	7-31-92	8-8-92	W-E	Orlando-Titusville	Kennedy Space Center
STS-47	9-12-92	9-20-92	WSW-ENE	Orlando-Titusville	Kennedy Space Center
STS-52	10-22-92	11-1-92	W-E	Orlando-Titusville	Kennedy Space Center
STS-53	12-2-92	12-9-92	N-S	Washington-California	Edwards AFB
STS-54	1-13-93	1-19-93	W-E	Orlando-Titusville	Kennedy Space Center
STS-56	4-8-93	4-17-93	N-S	Daytona Beach-Titusville	Kennedy Space Center
STS-55	4-26-93	5-6-93	W-E	Ventura-Edwards AFB	Edwards AFB
STS-57	6-21-93	7-1-93	W-E	Orlando-Titusville	Kennedy Space Center
STS-51	9-12-93	9-22-93	W-E	Orlando-Titusville	Kennedy Space Center
STS-58	10-18-93	11-1-93	NW-SE	Rosamond-Edwards AFB	Edwards AFB
STS-61	12-2-93	12-13-93	W-E	Orlando-Titusville	Kennedy Space Center

Table 2. - Concluded.

MSN Number	Date		Descent Footprint		
	Launch	Landing	Approximate Ground Track	Land Area Involved	Landing Site
STS-60	2-3-94	2-11-94	NW-SE	Ocala-Titusville	Kennedy Space Center
STS-65	7-8-94	7-23-94	W-E	Orlando-Titusville	Kennedy Space Center
STS-64	9-9-94	9-20-94	S-N	Mexico-California	Edwards AFB
STS-68	9-30-94	10-11-94	N-S	Oregon-California	Edwards AFB
STS-66	11-3-94	11-14-94	S-N	Mexico-California	Edwards AFB
STS-63	2-3-95	2-11-95	WNW-SE	Ocala-Titusville	Kennedy Space Center

Table 3. - SELECTED PARAMETERS FROM PREFLIGHT LAUNCH TRAJECTORY DATA FOR STS-41D

Time from lift-off, sec.	Down range distance from lift-off, n.mi.	Mach No.	Altitude, ft.	Latitude, deg.	Longitude, deg.	Heading, deg.	Flight path angle, deg.
50	2	1.09	26511	28.609	80.569	89.425	27.13
55	2	1.23	31643	28.609	80.560	89.415	27.86
60	3	1.39	37184	28.610	80.548	89.354	28.69
65	4	1.58	43209	28.610	80.536	89.376	29.66
70	5	1.80	49797	28.610	80.521	89.340	30.66
75	6	2.04	57098	28.610	80.505	89.386	31.74
80	7	2.29	65213	28.610	80.486	89.397	32.42
85	7.8	2.55	74122	28.610	80.463	89.444	32.61
90	9	2.76	83733	28.610	80.437	89.495	32.22
95	10	3.05	93954	28.611	80.407	89.537	31.62
100	13	3.25	104746	28.611	80.373	89.592	30.98
105	15	3.48	116059	28.611	80.335	89.678	30.29
110	17	3.74	127838	28.611	80.292	89.761	29.57
115	20	3.77	139898	28.611	80.246	89.786	28.72
120	22	3.77	151902	28.611	80.198	89.841	27.80
125	25	3.85	163678	28.610	80.148	89.905	26.88
130	27	3.81	175219	28.610	80.097	89.998	25.98
135	30	3.99	186544	28.610	80.045	90.086	25.04
140	33	4.06	197599	28.609	79.991	90.134	23.92
145	36	4.29	208358	28.609	79.935	90.174	22.84
150	37	4.56	218791	28.608	79.877	90.143	21.63
155	43	4.69	228871	28.608	79.755	90.118	20.47
160	45	4.73	238602	28.607	79.755	90.097	19.36
165	48	4.94	247989	28.607	79.691	90.080	18.28
170	52	5.14	257033	28.606	79.625	90.073	17.23
175	56	5.28	265736	28.606	79.557	90.068	16.23
180	60	5.57	274101	28.606	79.487	90.068	15.26
185	63	5.65	282132	28.605	79.414	90.073	14.33
190	67	5.74	289831	28.605	79.339	90.083	13.44
195	72	5.80	297203	28.604	79.262	90.095	12.59
200	75	5.77	304252	28.604	79.182	80.110	11.77

Table 4. - SELECTED PARAMETERS FROM DESCENT TRAJECTORY FOR STS-51D

Mach No.	Time to Mach 1.0 sec.	Altiitude, ft.	Flight Path Angle, deg.	Latitude, deg.	Longitude, deg.	Heading, deg.	Roll angle, deg.	Angle of Attack, deg.
8.95907	420	158314	-1.19524	29.3679	-86.2253	96.3235	50.5614	37.3864
8.68121	410	156314	-1.37885	29.3371	-85.9485	98.178	54.532	36.9173
8.37793	400	154025	-1.63877	29.2998	-85.6845	100.136	53.7088	36.1244
8.11317	390	151539	-1.70467	29.256	-85.428	101.937	42.8385	35.1739
7.82902	380	149190	-1.74665	29.2083	-85.1862	103.696	46.0986	34.8231
7.57303	370	146806	-1.83826	29.155	-84.9513	105.612	44.5092	33.9226
7.30118	360	144437	-194001	29.098	-84.7311	107.521	46.3127	33.2628
7.05923	350	142539	-2.14253	29.0309	-84.5296	109.617	48.5531	32.6924
6.82228	340	140680	-2.31563	28.9638	-84.3295	111.715	44.3806	31.804
6.56869	330	137979	-2.41586	28.8952	-84.1363	113.808	37.0087	31.1232
6.33766	320	135474	-1.94427	28.8196	-83.9561	114.441	-20.8141	30.1694
6.0965	310	133444	-2.10646	28.756	-83.7776	112.546	-51.8941	29.1476
5.8816	300	131546	-2.66413	28.6926	-83.6057	110.156	-50.6593	28.696
5.66925	290	129198	-2.9178	28.6411	-83.4382	107.834	-42.3189	27.8566
5.43471	280	126594	-2.77231	28.5976	-83.2725	105.733	-34.1486	26.8412
5.23339	270	124106	-2.8029	28.5599	-83.1118	103.435	-43.8817	25.0618
5.0196	260	121550	-3.14689	28.5308	-82.958	100.721	-46.4099	24.6128
4.82614	250	118758	-3.42497	28.5096	-82.8065	97.7719	-42.3867	23.5818
4.61526	240	116038	-3.53706	28.4952	-82.6649	94.9221	-40.8225	22.6725
4.4292	230	113208	-3.64243	28.4873	-82.5219	91.8969	-40.9353	21.7753
4.24544	220	110350	-3.67471	28.4864	-82.3889	88.8543	-37.2814	21.8472
4.04062	210	107625	-3.5906	28.4921	-82.2602	85.7006	-41.3053	20.246
3.86455	200	104791	-3.9438	28.5022	-82.1397	82.1986	-42.9558	19.7657
3.67045	190	101866	-4.28751	28.5181	-82.028	78.5342	-416431	19.1127
3.49675	180	98950.9	-4.55099	28.5407	-81.9176	74.6453	-38.9657	18.131
3.32291	170	96325.8	-4.24966	28.5713	-81.8167	71.607	-8.12863	17.3424
3.13319	160	94218.8	-3.65355	28.5992	-81.7227	73.4529	39.0217	16.4273
2.96756	150	92060.2	-4.40504	28.6235	-81.6312	77.8442	41.1733	16.0482
2.79061	140	89573.5	-5.18991	28.637	-81.5443	82.4161	39.3529	15.5771
2.63474	130	86886.9	-5.93276	28.645	-81.4604	87.211	40.0585	14.967
2.60907	120	83956.5	-7.01765	28.6453	-81.3824	92.7018	37.3752	14.2802
2.34545	110	81108.6	-6.13124	28.6403	-81.3082	95.4627	4.57274	14.4884
2.14666	100	78786.9	-4.74173	28.6346	-81.2404	96.0408	1.0723	12.72
2.01968	90	76916.6	-4.52202	28.6289	-81.1765	96.3126	2.16596	11.7702

Table 4. - Concluded.

Mach No.	Time to Mach 1.0 sec.	Altiitude, ft.	Flight Path Angle, deg.	Latitude, deg.	Longitude, deg.	Heading, deg.	Roll angle, deg.	Angle of Attack, deg.
1.93965	80	75234.5	-5.52419	28.6231	-81.118	96.5111	1.03168	10.4137
1.84952	70	73276.6	-7.48386	28.6172	-81.0626	96.6711	0.980289	9.77728
1.71327	60	70747.7	-9.52742	28.612	-81.0119	96.8403	-1.57261	9.74298
1.59184	50	67931.2	-11.0749	28.6069	-80.9639	96.8348	0.373873	9.44871
1.49226	40	65350.3	-12.0958	28.6012	-80.9197	96.8495	-0.420581	8.39484
1.36409	30	62273.6	-13.6316	28.5971	-80.8786	96.7742	-1.69507	7.99518
1.24941	20	59223.9	-14.6473	28.5933	-80.841	96.1534	-4.73904	7.76011
1.16154	10	56155.6	-15.2323	28.5902	-80.8056	96.0995	2.76422	7.36414
1.00752	0	53176.2	-15.2304	28.5871	-80.7738	97.873	-0.612767	7.82596

Table 5. - Summary of STS-41D Atmospheric Profiles.

Height (ft.)	Wind Speed (ft./sec.)	Wind Dir. (DG)	Temp. (DG C)	Pressure (mb)	Dew Pt. (DG C)	Height (ft.)	Wind Speed (ft./sec.)	Wind Dir. (DG)	Temp. (DG C)	Pressure (mb)	Dew Pt. (DGC)	Height (ft.)	Wind Speed (ft./sec.)	Wind Dir. (DG)	Temp. (DG C)	Pressure (mb)	Dew Pt. (DG C)
21	1	110	26.2	1017.	22.3	67000	39	076	-60.0	54.33		134000	91	104	-25.3	2.744	
1000	0	138	23.7	983.3	22.0	68000	41	075	-59.8	51.76		135000	89	104	-23.8	2.633	
2000	0	233	21.8	949.7	20.3	69000	44	079	-59.2	49.32		136000	86	104	-22.4	2.527	
3000	1	256	19.9	917.0	16.7	70000	46	087	-58.6	47.00		137000	84	105	-21.0	2.426	
4000	2	263	18.0	885.2	12.5	71000	47	091	-57.7	44.80		138000	82	104	-19.6	2.330	
5000	2	265	16.3	854.3	10.8	72000	46	091	-57.6	42.70		139000	77	101	-18.3	2.238	
6000	3	267	14.1	824.2	10.3	73000	44	090	-58.1	40.70		140000	76	096	-17.0	2.150	
7000	8	255	11.6	795.0	9.6	74000	44	088	-58.1	38.80		141000	72	087	-15.8	2.065	
8000	3	244	9.0	766.6	6.7	75000	47	088	-56.9	36.98		142000	77	079	-15.4	1.985	
9000	14	285	8.6	739.0	-5.0	76000	50	089	-56.7	35.26		143000	91	070	-15.8	1.907	
10000	15	277	8.3	712.2	-11.9	77000	51	090	-56.0	33.62		144000	113	066	-15.7	1.833	
11000	14	268	7.8	686.5	-14.2	78000	52	093	-54.5	32.07		145000	119	075	-12.3	1.762	
12000	8	257	6.4	661.5	-14.3	79000	53	096	-53.4	30.59		146000	138	087	-8.9	1.694	
13000	9	299	4.2	637.4	-12.1	80000	54	101	-52.8	29.19		147000	165	084	-6.6	1.630	
14000	15	281	2.1	613.9	-10.1	81000	55	106	-50.8	27.86		148000	158	085	-6.6	1.569	
15000	11	280	0.0	591.1	-11.1	82000	55	109	-50.1	26.60		149000	143	090	-6.8	1.509	
16000	8	245	-1.7	569.1	-13.6	83000	55	110	-48.2	25.41		150000	126	101	-6.9	1.453	
17000	8	262	-3.7	547.7	-14.9	84000	54	108	-46.4	24.27		151000	101	106	-7.2	1.398	
18000	12	292	-5.7	526.9	-15.4	85000	52	104	-49.2	23.19		152000	82	106	-8.2	1.345	
19000	13	281	-8.1	506.8	-16.1	86000	53	095	-49.4	22.15		153000	86	116	-9.2	1.294	
20000	12	287	-10.2	487.3	-19.7	87000	56	087	-49.3	21.15		154000	91	120	-10.2	1.244	
21000	15	265	-11.7	468.5	-25.5	88000	60	081	-49.2	20.20		155000	86	114	-11.2	1.197	
22000	15	281	-13.5	450.2	-27.2	89000	64	079	-49.0	19.29		156000	82	102	-12.2	1.151	
23000	21	277	-15.0	432.5	-28.5	90000	67	079	-48.7	18.42		157000	97	099	-11.8	1.107	
24000	16	268	-17.1	415.4	-29.3	91000	70	079	-48.3	17.60		158000	92	094	-10.9	1.064	
25000	16	270	-19.5	398.9	-29.2	92000	75	081	-48.0	16.81		159000	82	078	-10.0	1.023	
26000	29	283	-21.8	382.8	-28.8	93000	80	082	-46.6	16.06		160000	104	074	-9.1	0.9845	
27000	32	285	-23.8	367.3	-29.8	94000	85	085	-45.6	15.35		161000	136	074	-8.3	0.9471	
28000	31	279	-26.1	352.3	-33.9	95000	89	089	-46.0	14.67		162000	157	079	-7.9	0.9113	
29000	29	266	-28.0	337.8	-38.8	96000	91	093	-45.9	14.02		163000	145	086	-8.0	0.8768	
30000	31	287	-30.2	323.7	-41.2	97000	92	095	-45.2	13.40		164000	135	091	-8.4	0.8436	
31000	23	303	-32.3	310.2	-44.5	98000	89	095	-43.9	12.81		165000	124	098	-8.5	0.8116	
32000	28	299	-34.8	297.0	-47.4	99000	92	094	-42.8	12.34		166000	119	105	-8.8	0.7808	

Table 5. - Concluded.

Height (ft.)	Wind Speed (ft./sec.)	Wind Dir. (DG)	Temp. (DG C)	Pressure (mb)	Dew Pt. (DG C)	Height (ft.)	Wind Speed (ft./sec.)	Wind Dir. (DG)	Temp. (DG C)	Pressure (mb)	Dew Pt. (DGC)	Height (ft.)	Wind Speed (ft./sec.)	Wind Dir. (DG)	Temp. (DG C)	Pressure (mb)	Dew Pt. (DG C)
33000	26	290	-37.4	284.3	-46.8	100000	99	097	-41.7	11.80		167000	104	115	-9.0	0.7512	
34000	25	279	-39.8	272.1	-47.6	101000	101	099	-40.6	11.29		168000	109	120	-9.3	0.7226	
35000	28	282	-42.1	260.2	-49.9	102000	99	100	-39.5	10.80		169000	106	129	-9.6	0.6952	
36000	29	281	-44.4	248.7	-52.3	103000	94	101	-38.5	10.33		170000	92	140	-9.7	0.6687	
37000	31	280	-46.9	237.7	-54.4	104000	87	101	-37.5	9.892		171000	79	155	-9.9	0.6432	
38000	30	266	-49.4	227.0	-56.4	105000	81	100	-36.6	9.470		172000	64	169	-10.1	0.6187	
39000	40	261	-52.0	216.6	-58.6	106000	79	098	-36.1	9.068		173000	54	185	-10.3	0.5951	
40000	42	265	-54.6	206.7	-60.8	107000	79	094	-36.2	8.683		174000	38	201	-10.5	0.5724	
41000	40	262	-57.1	197.1	-62.9	108000	81	090	-36.6	8.313		175000	23	216	-11.0	0.5506	
42000	41	262	-59.6	187.8		109000	82	088	-37.0	7.959		176000	18	306	-13.1	0.5294	
43000	39	266	-62.1	178.9		110000	84	087	-37.3	7.620		177000	43	335	-15.1	0.5090	
44000	40	265	-64.4	170.3		111000	86	084	-37.1	7.295		178000	62	343	-17.2	0.4891	
45000	42	268	-65.9	162.0		112000	84	083	-36.1	6.985		179000	59	358	-19.2	0.4699	
46000	37	287	-66.7	154.1		113000	81	080	-35.1	6.689		180000	45	014	-21.4	0.4513	
47000	32	294	-68.4	146.5		114000	79	075	-34.1	6.407		181000	40	052	-23.5	0.4333	
48000	17	303	-68.7	139.3		115000	76	071	-33.1	6.138		182000	54	069	-25.5	0.4159	
49000	17	297	-69.2	132.4		116000	74	064	-32.2	5.881		183000	60	076	-27.8	0.3990	
50000	20	197	-67.2	125.9		117000	76	063	-32.0	5.636		184000	50	058	-27.0	0.3827	
51000	20	181	-66.2	119.8		118000	77	066	-32.9	5.400		185000	59	037	-25.6	0.3672	
52000	14	176	-67.3	113.9		119000	82	072	-33.7	5.173		186000	84	035	-23.1	0.3525	
53000	8	075	-65.6	108.4		120000	87	080	-33.7	4.956		187000	108	030	-20.9	0.3384	
54000	2	076	-65.2	103.1		121000	89	086	-33.6	4.748		188000	143	051	-19.1	0.3251	
55000	10	084	-65.4	98.09		122000	94	090	-33.0	4.549		189000	152	060	-18.6	0.3123	
56000	9	114	-65.9	93.32		123000	96	092	-31.9	4.359		190000	158	070	-18.4	0.3000	
57000	7	119	-65.9	88.78		124000	97	089	-30.6	4.178		191000	168	080	-18.8	0.2882	
58000	19	117	-65.3	84.47		125000	101	087	-29.4	4.005		192000	168	089	-18.4	0.2769	
59000	20	116	-65.2	80.37		126000	101	087	-28.8	3.840		193000	141	097	-18.5	0.2660	
60000	21	098	-64.7	76.48		127000	99	087	-29.3	3.682		194000	135	109	-18.7	0.2556	
61000	28	080	-63.1	72.80		128000	99	089	-30.2	3.530		195000	128	119	-18.7	0.2455	
62000	35	074	-63.5	69.30		129000	99	093	-30.4	3.384		196000	119	129	-18.5	0.2359	
63000	38	076	-62.3	65.98		130000	101	095	-29.9	3.244		197000	111	140	-19.2	0.2266	
64000	39	078	-61.3	62.83		131000	101	096	-29.3	3.110		198000	116	139	-18.3	0.2177	
65000	39	079	-60.1	59.85		132000	97	100	-28.3	2.982		199000	123	144	-18.4	0.2092	
66000	38	078	-59.5	57.02		133000	92	103	-26.8	2.860		200000	116	145	-19.8	0.2009	

Table 6. - Summary of STS Sonic Boom Signature Characteristics

STS MSN Flt. Phase	Meas. System	Meas. Site	Micro-phone	Sigs. Scanned	Signature Characteristics									
					Δp_o, meas.	Δp_o, psf pred.	ΔT, sec.	Δt_o, sec.	I_o, lb/ft^2-sec	Waveform category	$\tau_{1/2}$, msec	$\tau_{3/4}$, msec	$\tau_{,max}$, msec	$\tau_{10\text{-}90}$ msec
1 Reentry	Analog	California (0)		Yes	0.70	0.75	0.680	0.347	0.128	NR	1.60	2.90	21.30	3.60
		(1)			1.23	1.01	0.562	0.264	0.183	N	0.50	2.10	26.90	3.00
		(2)			0.92	1.17	0.518	0.289	0.146	N	1.30	3.00	4.70	3.30
		(3)			1.15	1.14	0.463	0.267	0.163	NR	2.00	9.40	44.90	20.00
		(4)			1.56	1.49	0.443	0.232	0.203	NR	1.70	2.60	6.10	3.20
		(5)			1.60	1.83	0.397	0.215	0.184	N	0.80	1.10	7.40	3.70
		(6)			2.32	1.94	0.388	0.212	0.244	N	1.30	1.60	3.70	2.20
		(7)			1.94	1.94	0.379	0.201	0.192	N	0.80	1.10	14.10	2.60
		(8)			1.78	1.57	0.382	0.207	0.186	N	1.50	1.80	5.00	3.70
		(9)			2.16	1.68	0.372	0.201	0.203	P	1.60	2.00	2.60	1.70
		(10)			1.86	1.83	0.372	0.208	0.186	P	0.80	1.10	3.30	0.90
2 Reentry	Analog	Bakersfield (1)		none available	1.44	2.00	----	----	----	----	----	----	----	----
		(2)			2.28	2.10	----	----	----	----	----	----	----	----
		(3)			1.74	2.10	----	----	----	----	----	----	----	----
		(4)			2.16	2.10	----	----	----	----	----	----	----	----
4 Reentry	Analog	EAFB (1)		none available	0.94	1.22	----	----	----	----	----	----	----	----
		(2)			0.88	1.01	----	----	----	----	----	----	----	----
		(3)			0.28	0.74	----	----	----	----	----	----	----	----
		(4)			0.06	0.62	----	----	----	----	----	----	----	----
5 Ascent	Analog	Atlantic Ocean (2)		Yes	3.63	3.10	5.700	1.568	2.357	post focus	9.00	9.00	23.00	3.00

Table 6. - Continued.

STS MSN Flt. Phase	Meas. System	Meas. Site	Micro-phone	Sigs. Scanned	Signature Characteristics									
					Δp_o, meas.	Δp_o, psf pred.	ΔT, sec.	Δt_o, sec.	I_o, lb/ft^2-sec	Waveform category	$\tau_{1/2}$, msec	$\tau_{3/4}$, msec	$\tau_{,max}$, msec	$\tau_{10\text{-}90}$ msec
7 Ascent	Analog	Atlantic Ocean (2)		Yes	5.17		3.200	0.542	0.878	focus	50.00	56.00	78.00	58.00
		(3)			2.15	--	7.600	1.968	1.372	post-focus	20.00	1796.0	1806.0	1794.0
		(4)			1.85	--	7.400	1.112	0.983	post--focus	10.00	14.00	30.00	18.00
		(5)			6.81	--	4.050	0.496	0.915	focus	176.00	184.00	196.00	178.00
		(7)		----	cut-off re: prior to focus line									
		(8)		Yes	3.02	--	2.620	1.602	1.023	near-focus	22.00	98.00	140.00	98.0
		(9)			0.66	--	8.188	1.850	1.046	post-focus	24.00	48.00	152.00	90.00
41B Reentry	Analog	Florida (1)		Yes	0.94	--	0.550	0.303	0.152	N	0.90	3.90	13.60	5.10
		(2)			0.94	1.10	0.505	0.268	0.143	N	3.40	4.70	31.10	6.50
	Digital	Florida (U4)	U441BLND	No	1.00	--	0.518	0.262	0.144	N	2.30	3.56	7.70	5.63
		(U6)	U641BLND		0.95	--	0.517	0.265	0.135	NR	3.27	4.80	10.14	5.67
	Analog	Florida (3)		Yes	1.19	1.10	0.457	0.257	0.161	R	3.10	12.60	33.70	19.40
	Digital	(3A)			1.30	1.50	0.453	0.246	0.168	N	3.10	5.20	14.30	6.30
		Florida (U3)	U341BLND		1.84	--	0.434	0.226	0.207	N	2.83	4.84	14.99	6.25
		(U9)	U941BLND		1.40	--	0.446	0.231	0.163	N	3.04	5.03	18.84	6.08
	Analog	Florida (4)			0.91	1.10	0.376	0.220	0.120	RP	7.20	15.10	65.00	56.90
	Digital	Florida (U8)	U841BLND	No	1.00	--	0.381	0.199	0.126	RP	6.32	9.83	67.74	16.85
	Analog	Florida (5)		Yes	1.65	2.20	0.383	0.196	0.180	N	1.40	1.60	15.20	2.10
	Digital	(U7)	U741BLND	No	1.86	--	0.394	0.188	0.180	N	0.75	2.00	2.63	2.00
	Analog	(6)		Yes	1.54	1.60	0.403	0.212	0.144	P	1.20	1.60	3.60	1.60
		(7)			1.07	1.50	0.375	0.200	0.120	N	1.20	2.30	6.00	4.40

Table 6. - Continued.

STS MSN Flt. Phase	Meas. System	Meas. Site	Micro-phone	Sigs. Scanned	Signature Characteristics									
					Δp_o, meas.	Δp_o, psf pred.	ΔT, sec.	Δt_o, sec.	I_o, lb/ft^2-sec	Waveform category	$\tau_{1/2}$, msec	$\tau_{3/4}$, msec	$\tau_{,max}$, msec	τ_{10-90} msec
41D Ascent	Analog	Atlantic Ocean (1)		Yes	0.64	--	3.800	2.124	0.484	Pre-focus	200.00	246.00	348.00	272.00
		(2)			1.36	--	4.000	0.500	0.248	Pre-focus	50.00	59.00	79.00	72.00
		(3)			2.05	--	5.700	0.758	0.647	Pre-focus	10.00	10.00	51.00	17.00
	Digital	(U7)	U741DLAU	No	2.30	--	4.600	0.700	0.690	Post-focus	2.67	5.94	23.18	8.92
	Analog	(4)		Yes	1.31	--	4.300	0.586	0.310	Pre-focus	77.00	89.00	143.00	99.00
	Digital	(U1)	U141DLAU	No	1.58	--	3.200	0.600	0.450	Pre-focus	35.17	41.70	76.50	68.53
		(U4)	U441DLAU		1.56		3.100	0.650	0.450	Pre-focus	36.66	42.88	71.36	65.14
	Analog	(5)		Yes	2.23	--	3.501	2.846	1.440	Post-focus	893.00	903.00	912.00	905.00
		(6)			1.14	--	5.302	2.577	1.020	Post-focus	167.00	957.00	962.00	955.00
		(7)			0.38	--	4.700	0.385	0.116	Post-focus	29.00	34.00	41.00	34.00
	Digital	(U5)	Cut-off re: prior to focus line											
		(U8)	U841DLAU	No	1.77	--	1.700	0.600	0.750	Post-focus	1.09	1.13	3.27	1.09
		(U3)	U341DLAU		3.62	--	2.900	0.600	0.900	Near-focus	10.28	11.49	15.72	12.10
		(U2)	U241DLAU		1.67	--	5.400	1.400	1.100	Post-focus	239.67	274.72	284.73	275.34
		(U9)	----	----	Cutoff re: prior to focus line									

Table 6. - Continued.

STS MSN Flt. Phase	Meas. System	Meas. Site	Micro-phone	Sigs. Scanned	Signature Characteristics									
					Δp_o, meas.	Δp_o, psf pred.	ΔT, sec.	Δt_o, sec.	I_o, lb/ft^2-sec	Waveform category	$\tau_{1/2}$, msec	$\tau_{3/4}$, msec	$\tau_{,max}$, msec	τ_{10-90} msec
41G Reentry	Analog	Daytona Beach, FL	22 S	Yes	1.13	––	0.461	0.238	0.157	NR	0.80	0.90	14.30	0.30
	Digital	(U3)			1.24	––	0.491	0.275	0.132	N	2.10	2.90	3.80	3.10
		(U5)			1.08	––	0.492	0.224	0.102	P	0.90	1.10	2.20	1.50
	Analog	MIMS, Fl.	39S		1.69	––	0.393	0.204	0.181	PR	0.70	2.20	15.00	2.00
	Digital	(U4)	U441GLND	No	1.67	––	0.391	0.194	0.156	PP	1.37	5.04	16.61	13.86
		(U6)	U641GLND		1.79	––	0.390	0.210	0.176	PP	1.27	4.87	16.30	13.98
		(U7)	U741GLND		1.80	––	0.392	0.196	0.172	PP	1.25	5.23	16.83	13.98
		(U8)	U841GLND		1.84	––	0.391	0.189	0.174	PP	1.13	4.98	16.86	13.80
51A Reentry	Analog	JSC, Texas		Yes	0.42	––	1.500	0.747	0.143	N	5.80	8.80	35.00	28.00
	Digital	(U6)			0.40		1.523	0.660	0.125	N	7.20	7.80	33.60	8.40
	Analog	Orlanda Fl.	Ch. 2		1.14	––	0.401	0.206	00.127	PP	1.60	3.30	13.60	10.90
	Digital	Orlando,Fl. (U4)	U451ALND	No	1.08	––	0.403	0.206	0.114	PP	1.78	2.96	13.50	5.92
	Analog	Titusville, Fl.		Yes	1.77	––	0.380	0.205	0.186	N	0.80	1.70	7.10	2.40
	Digital	Titusville, Fl (U5)	U551ALND	No	1.92		0.379	0.187	0.174	N	0.80	1.38	5.40	2.18
		(U8)	U851ALND		1.85		0.379	.0176	0.160	N	0.79	1.36	6.79	1.58
51C Reentry	Digital	Titusville Ch. 1		Yes	1.87	––	0.367	0.189	0.177	SP	4.10	6.20	6.80	5.40
		Titusville Ch. 4			1.74	––	0.366	0.188	0.167	SP	3.70	5.90	7.40	6.30
		Titusville Ch. 5			1.75	––	0.366	0.189	0.165	SP	4.10	6.40	7.90	6.60

Table 6. - Continued.

STS MSN Flt. Phase	Meas. System	Meas. Site	Micro-phone	Sigs. Scanned	Signature Characteristics									
					Δp_o, meas.	Δp_o, psf pred.	ΔT, sec.	Δt_o, sec.	I_o, lb/ft^2-sec	Waveform category	$\tau_{1/2}$, msec	$\tau_{3/4}$, msec	$\tau_{,max}$, msec	$\tau_{10\text{-}90}$ msec
51C Reentry (cont.)	Digital	Titusville, Fl. Ch. 6		Yes	1.76	––	0.367	0.189	0.169	SP	3.90	6.40	7.50	6.70
		Orland, Fl. Ch. 2	U551CLND	No	1.75	––	0.399	0.144	0.075	P	2.67	4.23	9.56	5.45
51D Reentry	Digital	Titusville, Fl.	U651DLND	No	2.28	––	0.391	0.213	0.245	PR	2.40	5.22	34.03	12.11
		Sanford, Fl.	U851DLND		1.29	––	0.507	0.252	0.135	PP	9.31	11.39	16.43	12.81
		Weeki Wachee, Fl.	U351DLND		1.00	––	0.608	0.316	0.144	N	2.28	3.87	10.01	5.35
		Bayonet Point, Fl.	U951DLND		0.79		0.664	0.340	0.147	NR	1.30	4.37	52.74	7.79
		Clearwater, Fl.	U451DLND		0.64		0.751	0.330	0.107	NR	3.08	4.90	11.74	5.02
51G Reentry	Digital	Emma Wood State Beach, Ca	Unit 3	Yes	0.92	1.22	0.597	0.315	0.155	NR	2.30	3.20	43.20	11.60
		Channel Island Nat. Park, Ca.	Unit 6		0.87	1.22	0.601	0.317	0.139	NR	1.70	2.50	27.30	17.60
		Channel View Park, Ca.	Unit 4		0.90	1.18	0.631	0.340	0.132	P	1.40	2.60	5.00	3.70

Table 6. - Continued.

STS MSN Flt. Phase	Meas. System	Meas. Site	Micro-phone	Sigs. Scanned	Signature Characteristics									
					Δp_o, meas.	Δp_o, psf pred.	ΔT, sec.	Δt_o, sec.	I_o, lb/ft^2-sec	Waveform category	$\tau_{1/2}$, msec	$\tau_{3/4}$, msec	$\tau_{,max}$, msec	τ_{10-90} msec
51F Reentry	Digital	Cockatoo Inn, Ca	U351FLND	No	0.97	0.74	0.476	0.212	0.099	PR	6.38	8.89	13.00	10.72
		Compton Point,Ca.	U751FLND		0.86	0.84	0.451	0.210	0.102	NR	2.81	4.61	20.01	7.42
		Artesia Blvd.,Ca.	U951FLND		1.27	1.10	0.501	0.234	0.146	N	1.55	10.93	15.93	13.07
51-I Reentry	Digital	U. Calif .Santa Barbara,Ca.	Unit 6	Yes	0.69	0.92	0.653	0.390	0.113	NR	1.90	2.90	21.40	6.20
		Channel Island Nat. Park, Ca.	Unit 9		0.88	1.16	0.597	0.304	0124	NP	1.50	2.40	3.80	2.50
61A Reentry	Digital	Northridge Park, Ca.	Site 1	Yes	1.37	1.10	0.472	0.240	0.162	N	1.50	4.20	23.00	6.20
	Digital	Grenada Hill Park, Ca.	Site 2	Yes	1.11	1.10	0.466	0.246	0.133	N	1.50	2.90	9.30	3.50
		Brand Park, Ca.	Site 3		1.16	1.10	0.453	0.204	0.112	NR	1.40	2.50	16.20	7.10

Table 6. - Continued.

STS MSN Flt. Phase	Meas. System	Meas. Site	Micro-phone	Sigs. Scanned	Signature Characteristics									
					Δp_o, meas.	Δp_o, psf pred.	ΔT, sec.	Δt_o, sec.	I_o, lb/ft^2-sec	Waveform category	$\tau_{1/2}$, msec	$\tau_{3/4}$, msec	$\tau_{,max}$, msec	τ_{10-90} msec
26 Reentry	Analog	Kauai, Hawaii	Site 1	Yes	0.10	0.01	2.454	1.305	0.068	PR	12.00	95.50	124.50	102.00
	Digital	Santa Barbara, Ca.	U1MBO	No	1.07	0.88	0.619	0.314	0.143	N	2.25	3.12	7.87	4.62
		Ventura, Ca.	Site 3	Yes	0.65	0.93	0.661	0.352	0.121	N	2.20	3.00	25.20	10.60
		Oxnard, Ca.	Site 4		0.68	0.82	0.676	0.365	0.123	N	2.40	4.00	24.60	14.90
		Lake Sher-wood, Ca.	Site 5	----	Beyond Lat. C.O.									
		Santa Paula, Ca.	Site 6	Yes	1.04	0.93	0.641	0.313	0.143	PR	4.80	28.10	41.40	30.10
		Oak Flat, Ca.	Site 7		0.61	0.75	0.535	0.260	0.097	N	1.40	2.70	6.00	3.30
		Lions Can-yon, Ca.	Site 8		1.04	1.13	0.572	0.272	0.154	N	1.00	1.90	20.70	3.90
		Gold Hill, Ca.	U10MBO	No	1.19	0.98	0.453	0.231	0.128	N	1.12	1.68	4.14	2.57
		Pine Moun-tain, Ca.	U11MBO		1.16	1.16	0.543	0.261	0.122	N	2.09	3.03	3.87	2.82
		Wheeler Ridge, Ca.	U13MBO		1.28	1.16	0.519	0.244	0.158	N	0.86	1.40	2.59	1.40
		Conner, Ca.	U12MBO		0.82	0.82	0.593	0.284	0.109	SPR	1.14	1.48	2.63	1.60
27 Reentry	Digital	C. Blanco, OR	U4MBI	No	0.39	--	1.311	0.492	0.115	NR	6.06	13.03	32.12	21.54
		Folsom L., Ca..	U2MBOTB		0.75	--	0.911	0.444	0.141	NP	2.60	6.11	13.00	6.63
		Sequoia, Ca.	U1MBOTD		0.71	0.57	0.640	0.309	0.106	N	1.49	3.10	11.41	4.09

Table 6. - Continued.

STS MSN Flt. Phase	Meas. System	Meas. Site	Micro-phone	Sigs. Scanned	Signature Characteristics									
					Δp_o, meas.	Δp_o, psf pred.	ΔT, sec.	Δt_o, sec.	I_o, lb/ft^2-sec	Waveform category	$\tau_{1/2}$, msec	$\tau_{3/4}$, msec	$\tau_{,max}$, msec	$\tau_{10\text{-}90}$ msec
29 Reentry	Digital	Ventura, Ca.	SN04MBO	No.	1.19	1.20	0.582	0.294	0.176	N	0.91	1.30	7.67	1.30
		Santa Barbara, Ca.	SN01MBO		0.66	0.60	0.541	0.302	0.099	NR	2.41	4.57	36.58	11.94
30 Reentry	Digital	Ventura, Ca.	U1MBO	No	0.88	1.20	0.636	0.312	0.142	PR	1.25	4.13	21.38	17.63
		Santa Barbara,Ca.	U4MBO		1.17	0.80	0.564	0.291	0.131	NP	1.52	2.41	4.18	2.91
28 Reentry	Digital	California, F	SN10MBO	No	1.40	1.50	0.507	0.236	0.166	N	1.55	2.41	31.85	10.12
		G	SNO8MBO		1.41	1.50	0.485	0.238	0.170	N	1.27	2.03	15.11	3.30
		H	SN12MB2		1.45	1.20	0.470	0.247	0.144	NP	1.16	3.13	16.82	12.41
		I	SN13MBO		0.83	0.90	0.460	0.233	0.098	NR	1.65	4.51	19.47	6.16
		J	SN11MBO		0.72	0.80	0.457	0.256	0.083	NR	2.63	6.62	19.95	9.56
		K	U5MBO		1.40	1.30	0.542	0.259	0.156	NP	1.91	2.79	8.76	3.68
		L	U4MBO		1.24	1.50	0.508	0.258	0.179	NR	1.42	3.35	23.35	5.80
		M	U6MBO		0.85	1.10	0.486	0.268	0.116	NP	1.28	2.18	4.22	2.82
		N	U7MBO		0.91	0.90	0.481	0.253	0.118	NR	2.18	5.63	30.08	12.29
		R	U3MBO		1.12	1.10	0.500	0.245	0.133	PP	1.62	2.99	7.22	3.86
		S	U9MBO		0.83	0.80	0.479	0.225	0.096	N	1.77	3.16	7.34	4.81
		X	U2MBO		1.02	1.10	0.566	0.275	0.148	NR	1.83	2.62	10.74	7.86
34 Reentry	Digital	Chatsworth, Ca	U5MBO	No	1.18	1.30	0.521	0.253	0.139	NP	1.65	2.28	15.19	1.90
		Hidden Hills, Ca.	U12MBO		1.23	1.30	0.519	0.255	0.147	N	1.38	2.07	5.86	2.76
33 Reentry	Digital	Santa Barbara, Ca.	U5MBO	No	1.13	1.80	0.564	0.264	0.145	NP	2.02	3.41	6.05	4.16
		Ojai, Ca.	U1MBO		1.94	0.80	0.539	0.251	0.126	P	3.89	4.64	5.77	4.01

Table 6. - Concluded.

STS MSN Flt. Phase	Meas. System	Meas. Site	Micro-phone	Sigs. Scanned	Signature Characteristics									
					Δp_o, meas.	Δp_o, psf pred.	ΔT, sec.	Δt_o, sec.	I_o, lb/ft^2-sec	Waveform category	$\tau_{1/2}$, msec	$\tau_{3/4}$, msec	$\tau_{,max}$, msec	τ_{10-90} msec
32 Reentry	Digital	Ventura, Ca.	U1MBO	No	1.15	1.30	0.604	0.338	0.174	NP	2.00	3.63	4.88	2.63
		Thousand Oak, Ca.	U5MBO		0.86	1.10	0.649	0.308	0.138	N	2.64	5.41	15.35	11.95
36 Reentry	Digital	Bakersfield	----	----	Beyond Lat. cut-off									
		Lake Isa-bella	U5MBO	No	1.71	1.40	0.523	0.251	0.130	SP	1.64	3.15	5.29	3.65
31 Reentry	Digital	Ojai, Ca. (1)	U5MBO	No	1.16	1.20	0.555	0.264	0.146	NP	1.65	5.96	8.75	7.10
		(2)	U1MBO		0.81	1.20	0.559	0.299	0.141	NR	1.75	10.40	57.74	17.41
		(3)	U3MBO		1.49	1.20	0.559	0.265	0.167	SP	5.79	10.20	13.48	11.34
41 Reentry	Digital	Goleta, Ca.	U3MBO	No	0.92	0.90	0.610	0.312	0.148	N	2.54	4.95	13.84	7.75
		Santa Barbara, Ca.	U1MBO		0.93	0.97	0.603	0.312	0.139	N	2.52	5.67	25.32	9.32

Table 7. - SUMMARY OF MAXIMUM SONIC BOOM OVERPRESSURES MEASURED ON STS MISSIONS

MSN NO.	Sonic Boom Signature				Flight Phase	Approximate Flight Conditions at Boom Origin		Remarks
	Δp. psf	Waveform	Date	Time, Z		Mach No.	Altitude, ft.	
STS-1	2.32	N	4-14-81	18:16:34	Re-entry	1.8	71.000	
STS-2	2.28	--	11-14-81	21:18:00	Re-entry	2.0	72,000	Signatures unavailable
STS-4	0.94	--	7-4-82	16:04:00	Re-entry	3.3	97,000	Signatures unavailable
STS-5	3.63	post-focus	11-11-82	12:23:41	Ascent	3.6	112,000	Ascent focus region
STS-7	6.81	focus	6-18-83	11:38:27.3	Ascent	3.6	147,000	Ascent focus region
STS-41-B	1.86	N	2-11-84	12:12:03	Re-entry	3.3	95,000	
STS-41-D	3.62	near-focus	8-30-84	12:48:17	Ascent	3.6	163.000	Ascent focus region
STS-41-G	1.84	PP	10-13-84	16:22:39	Re-entry	1.6	66,000	
STS-51-A	1.92	N	11-16-84	11:56:13	Re-entry	1.4	60,000	
STS-51-C	1.87	SP	1-27-85	21:19:36	Re-entry	1.4	60,000	
STS-51-D	2.28	PR	4-19-85	13:50:35	Re-entry	1.5	59,000	
STS-51-G	0.92	NR	6-24-85	13:06:43	Re-entry	4.0	106,000	
STS-51-F	1.27	N	8-06-85	19:40:30	Re-entry	3.6	99,000	
STS-51-I	0.88	NP	9-03-85	13:09:54	Re-entry	4.0	108,000	
STS-61-A	1.37	N	11-06-85	17:39:28	Re-entry	3.0	92,000	
STS-26	1.28	N	10-03-88	16:31:57	Re-entry	3.2	95,448	
STS-27	0.75	NP	12-06-88	23:27:53	Re-entry	6.2	130,000	
STS-29	1.19	N	3-18-89	14-29-58	Re-entry	4.2	108,000	
STS-30	1.17	NP	5-08-89	19:37:23	Re-entry	4.5	113,000	
STS-28	1.45	NP	8-13-89	13:32:59	Re-entry	3.0	91,000	
STS-34	1.23	N	10-23-89	16:27:16	Re-entry	3.6	100,000	
STS-33	1.94	P	11-28-89	00:24:26	Re-entry	3.8	95,000	
STS-32	1.15	NP	1-20-90	9:29:45	Re-entry	4.1	104,000	
STS-36	1.71	SP	3-04-90	18:03:39	Re-entry	3.1	95,000	
STS-31	1.49	SP	4-29-90	13:44:03	Re-entry	3.9	105,000	
STS-41	0.93	N	10-10-90	13:51:05	Re-entry	4.5	114,000	

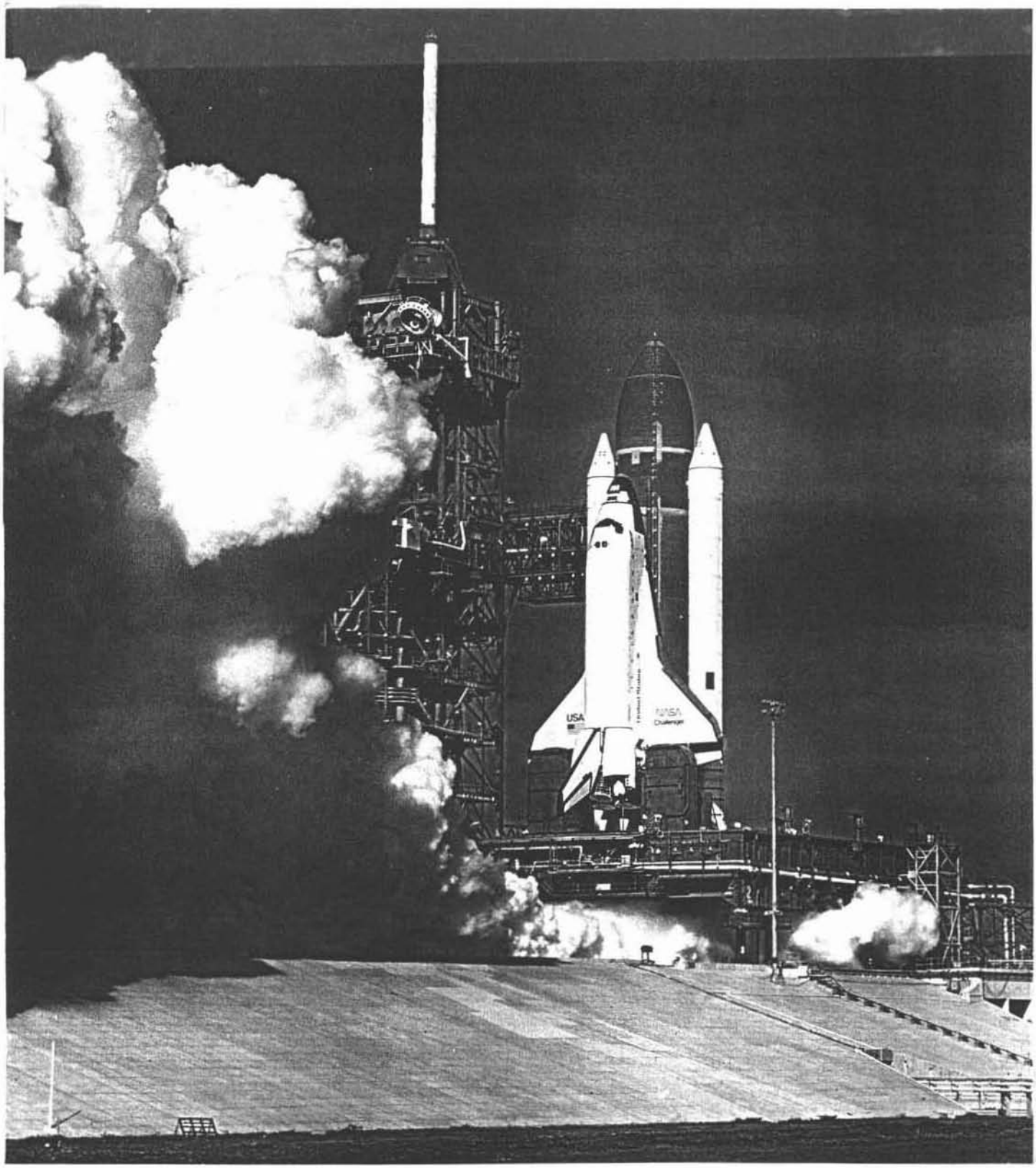

Figure 1. - Photograph of space shuttle launch vehicle at lift-off.

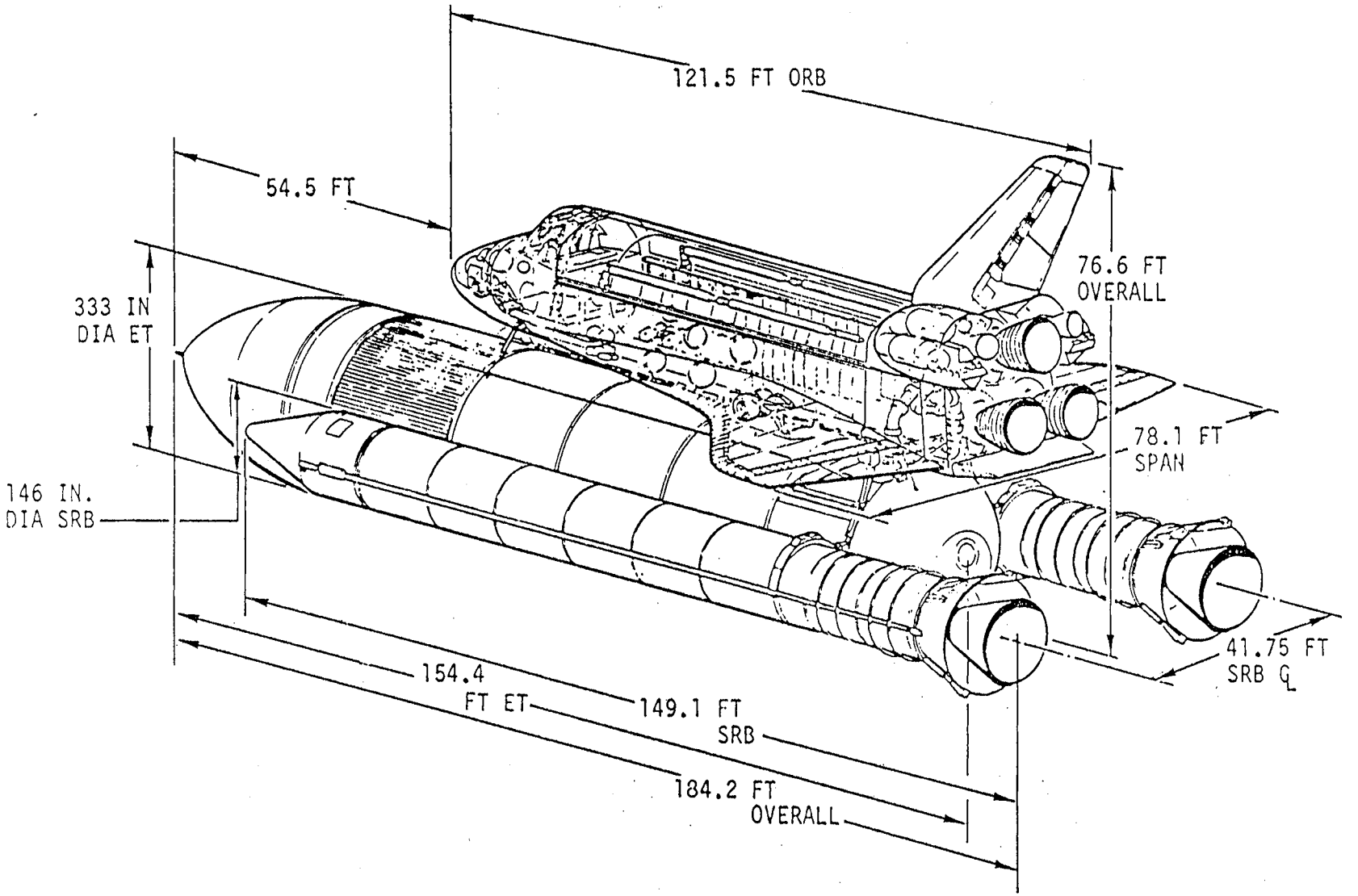

Figure 2. - Schematic of space shuttle launch vehicle

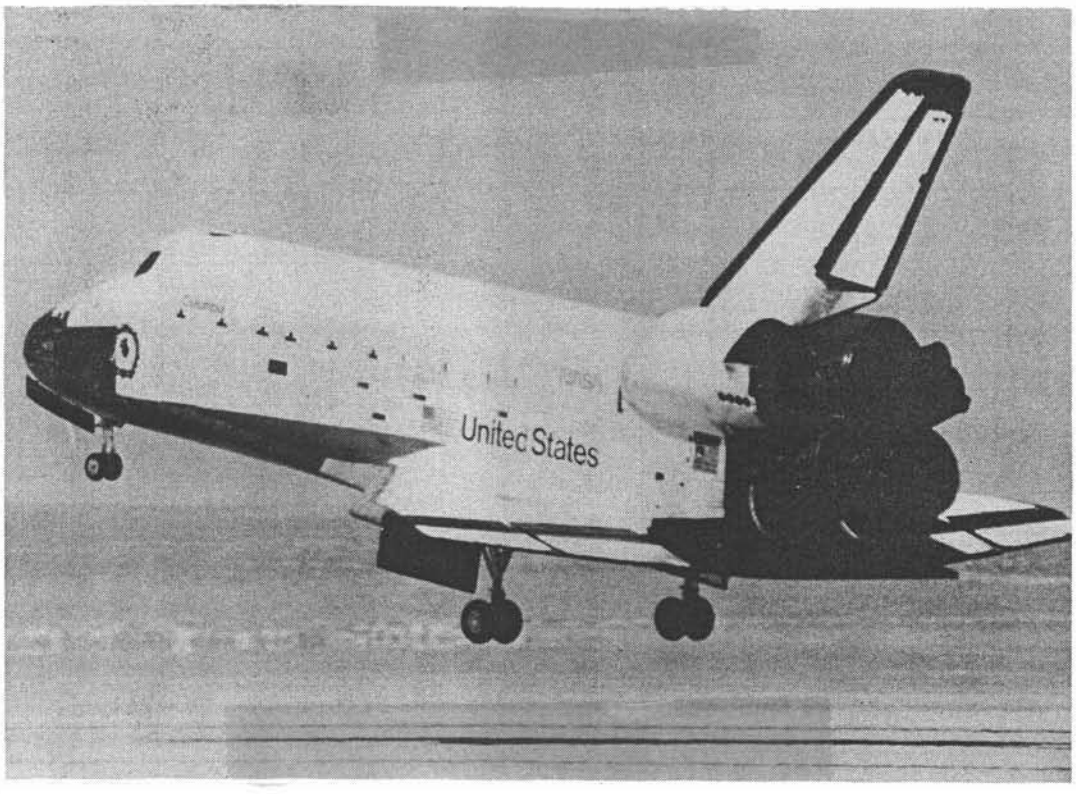

Figure 3. Orbiter Columbia nearing touchdown.

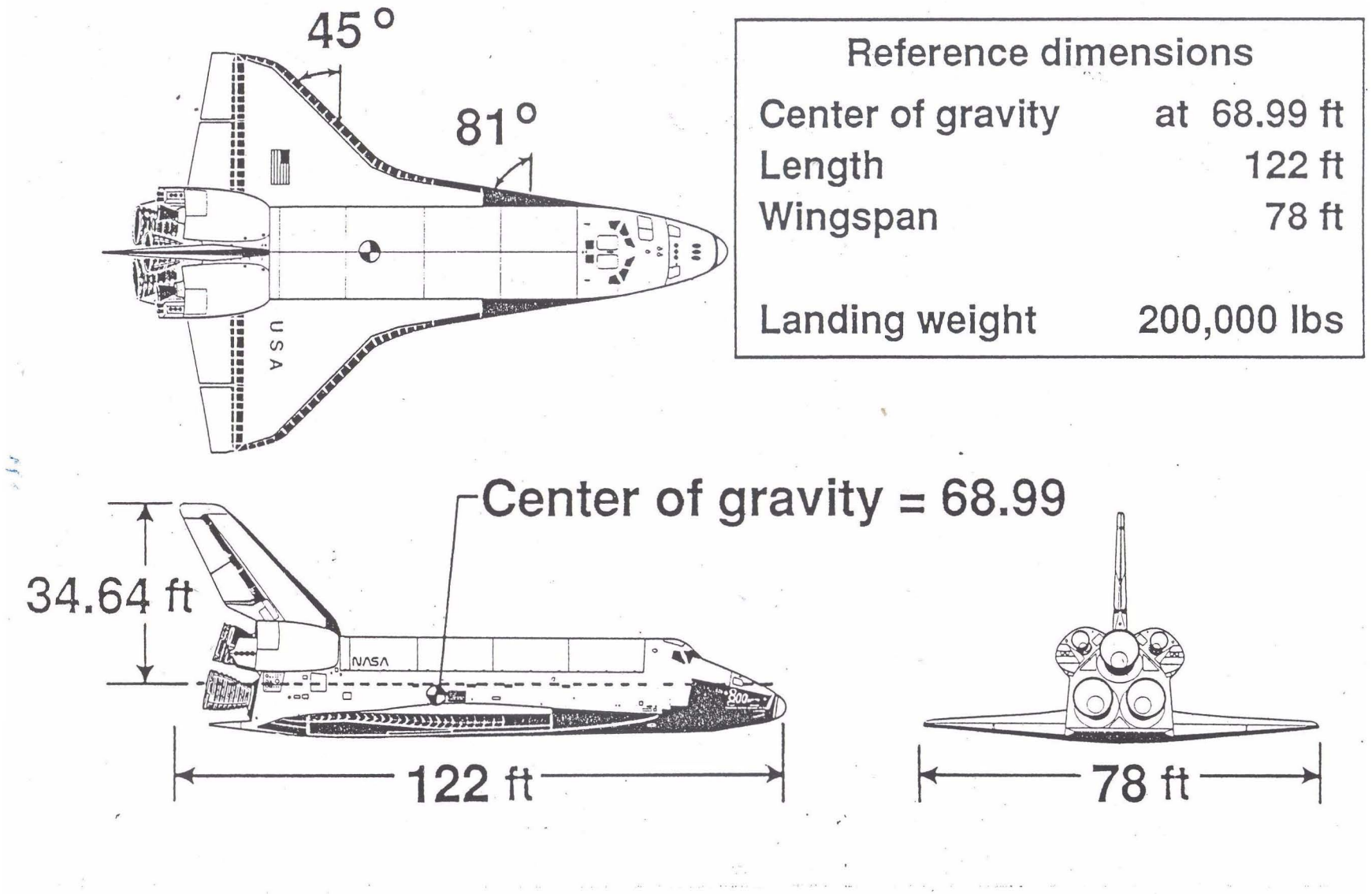

Figure 4. - STS Orbiter characteristics.

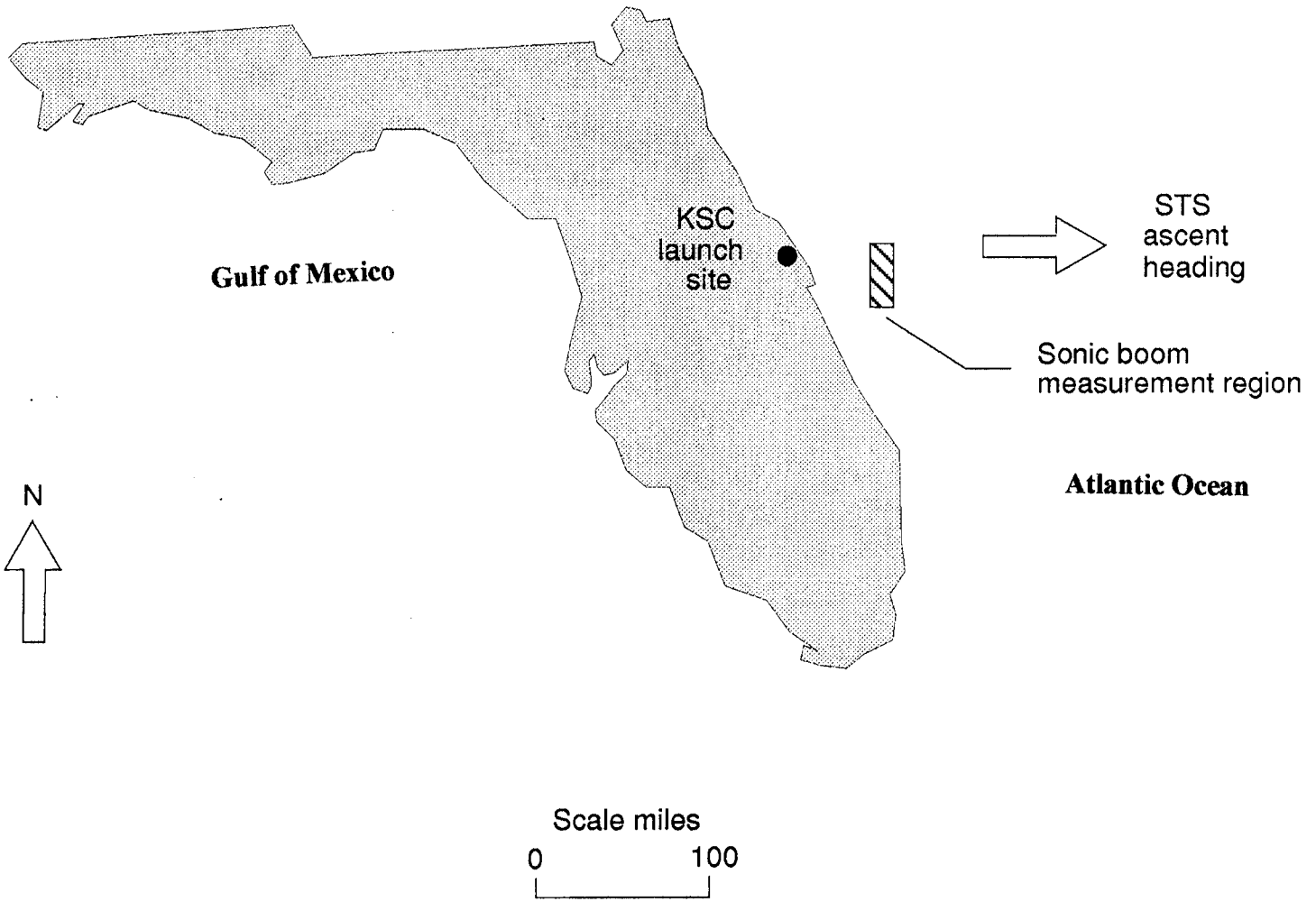

Figure 5.- STS launch site and sonic boom measurement regions.

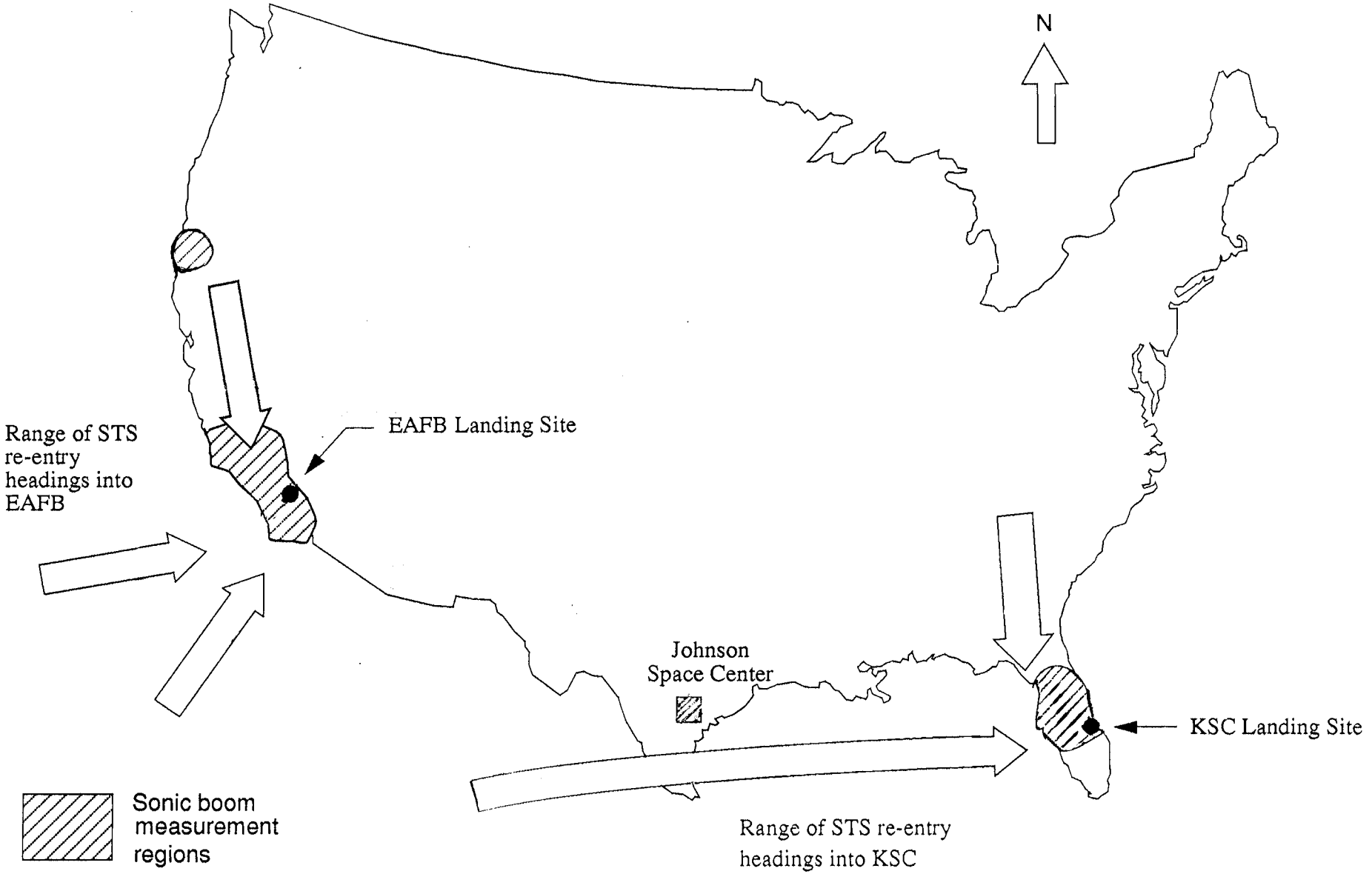

Figure 6.- STS landing sites and sonic boom measurement regions

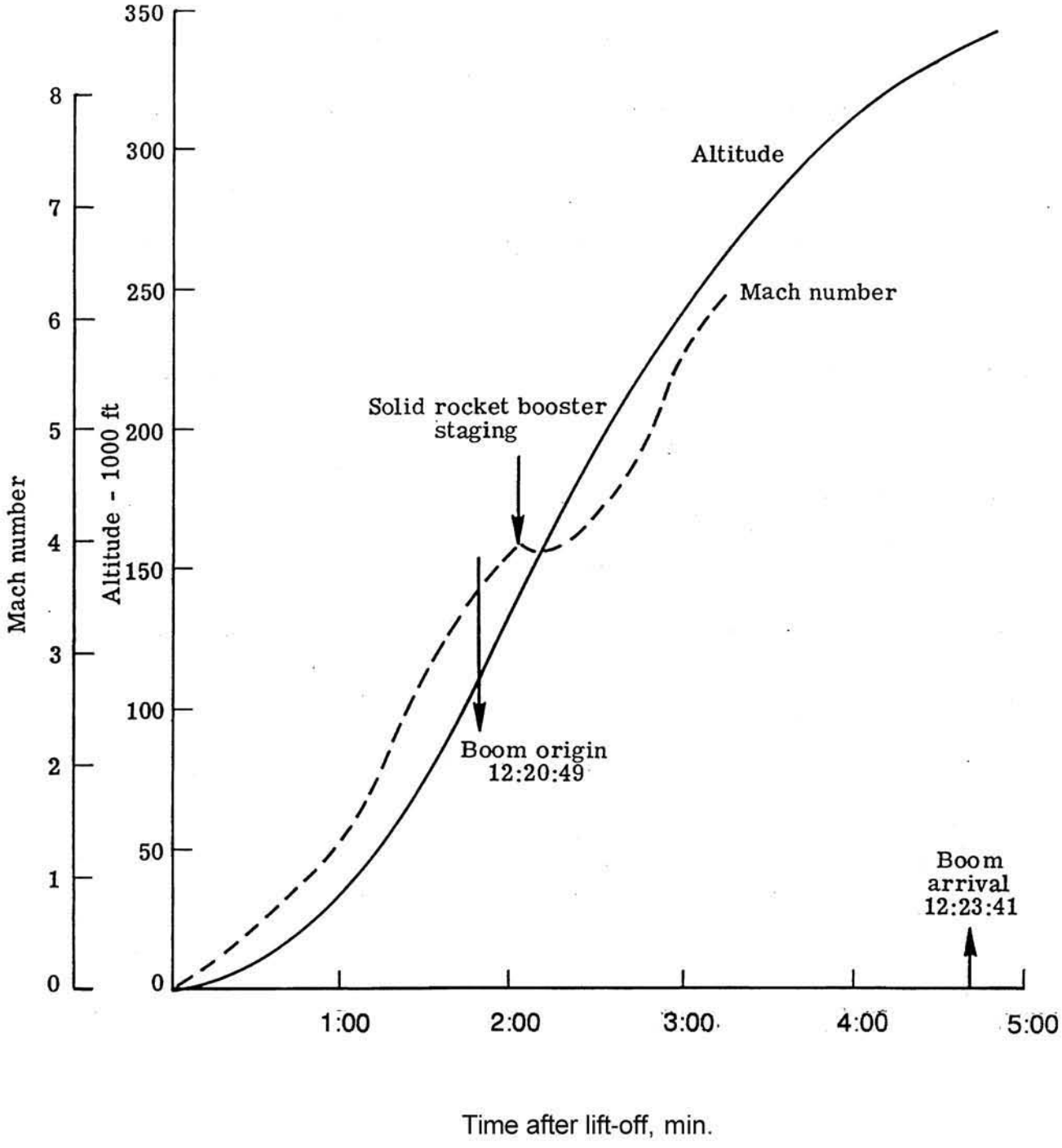

Figure 7. - Representative STS launch-ascent Mach-altitude trajectory (STS-5).

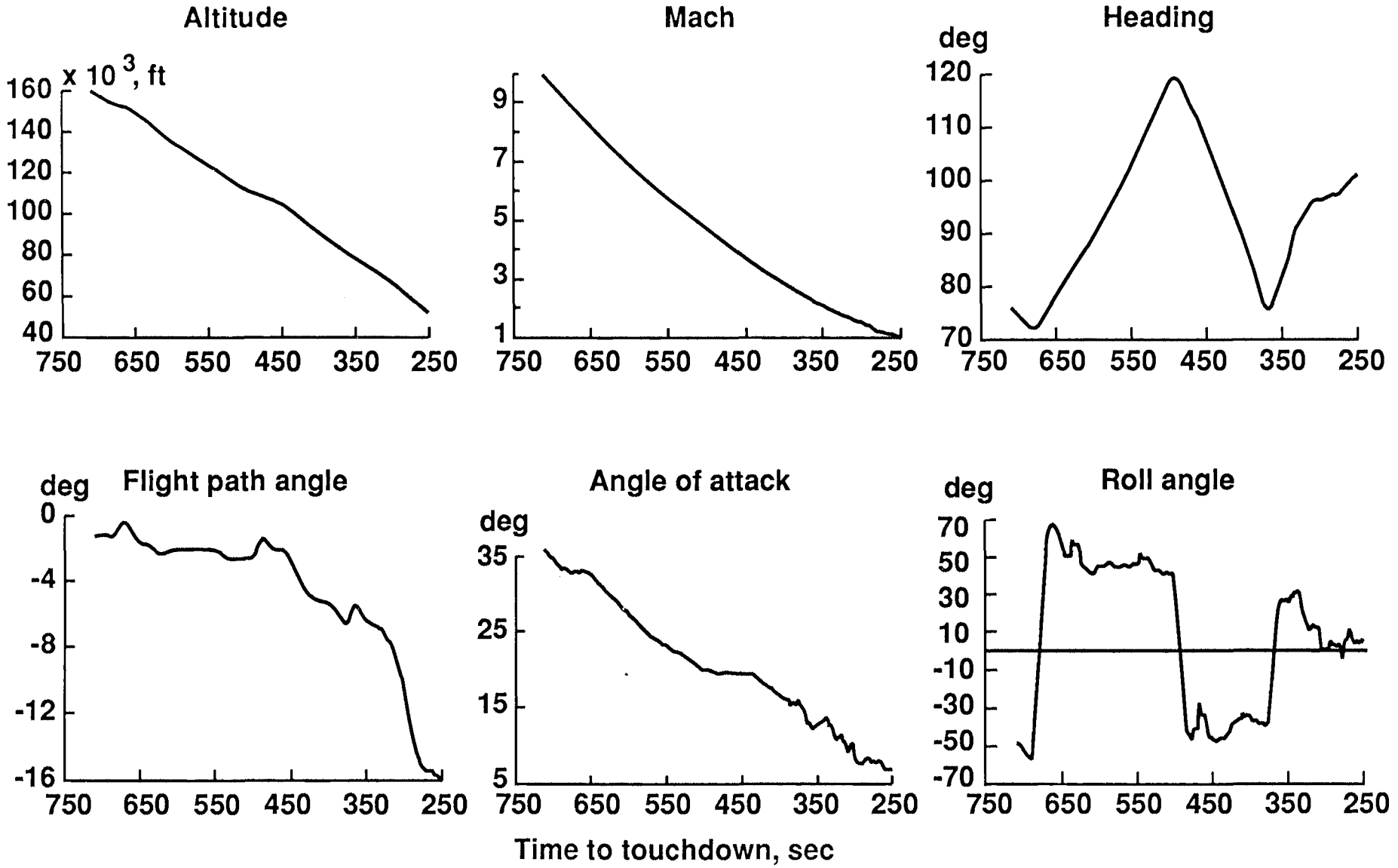

Figure 8. - Time histories of STS orbiter reentry-descent flight parameters (STS-26)

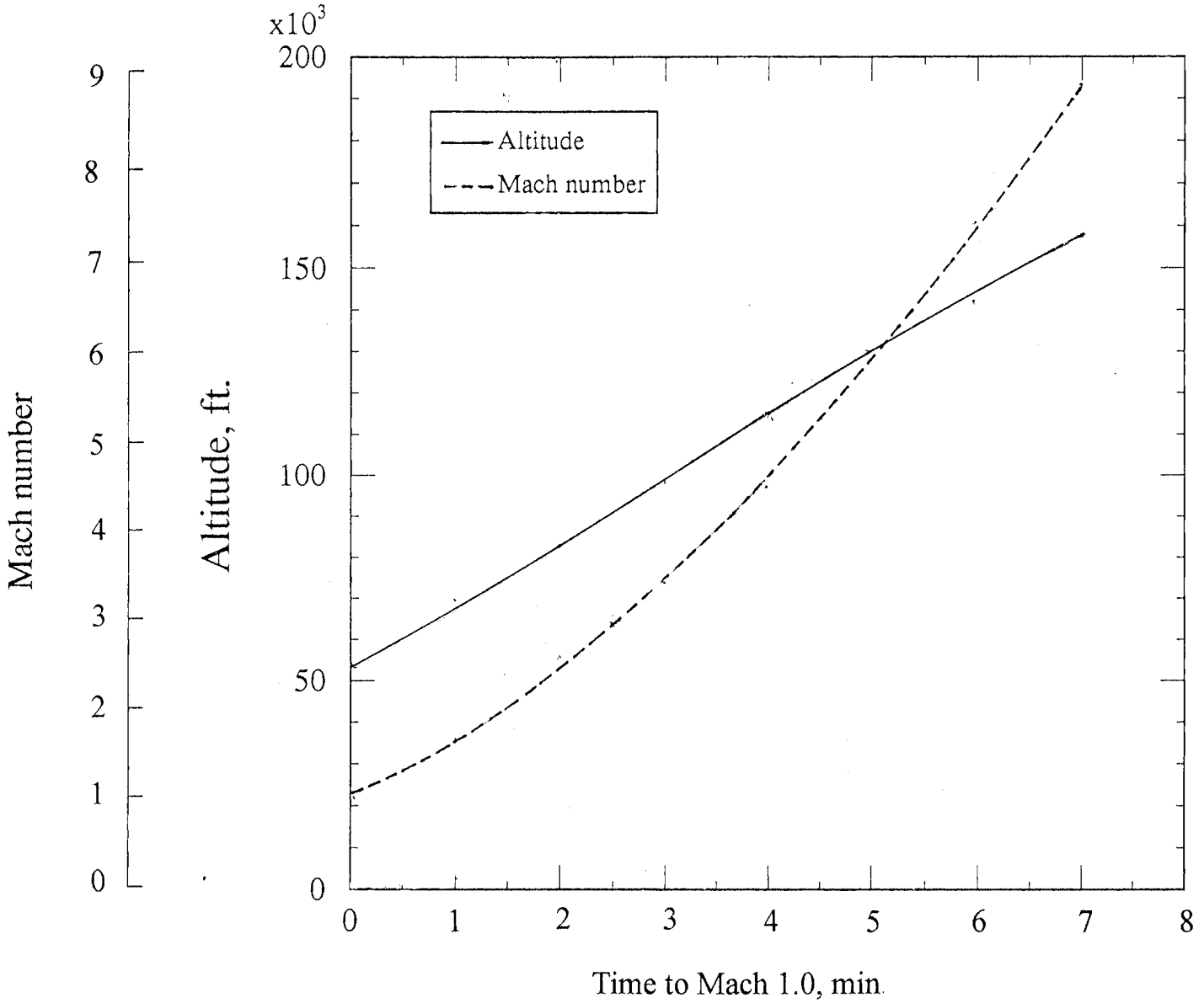

Figure 9. - Representative STS reentry-descent to landing Mach-altitude trajectory. (STS-51D)

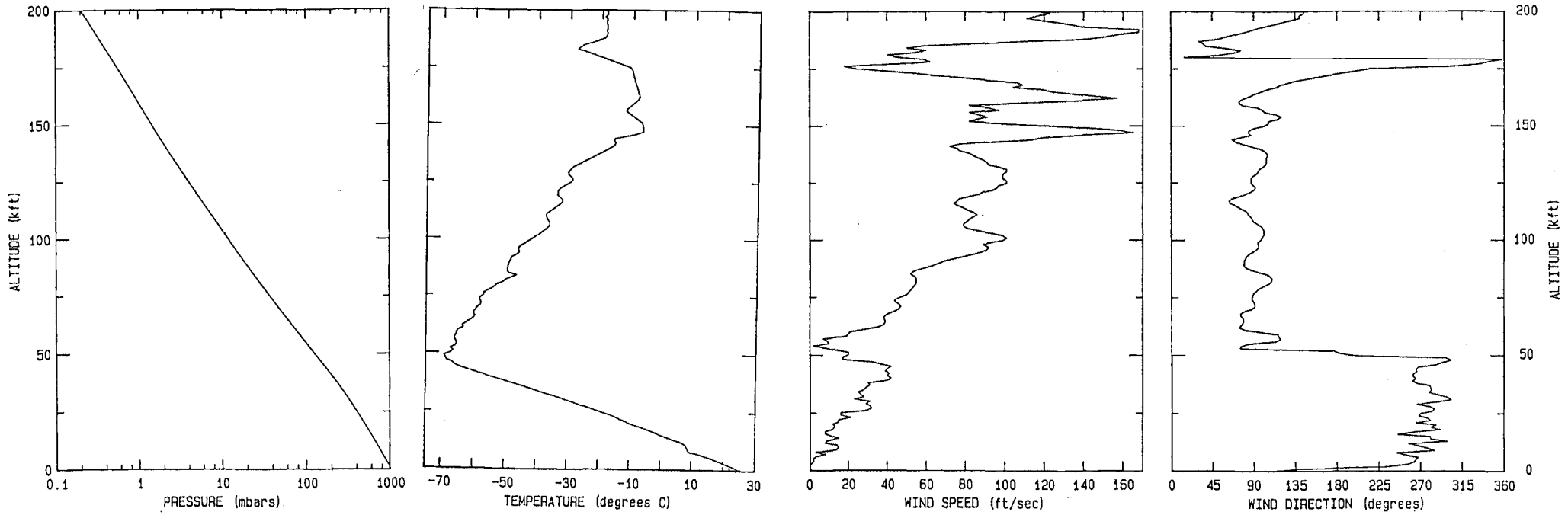

Figure 10 - Type of atmospheric information acquired on STS sonic boom measurements. (STS-41D ascent)

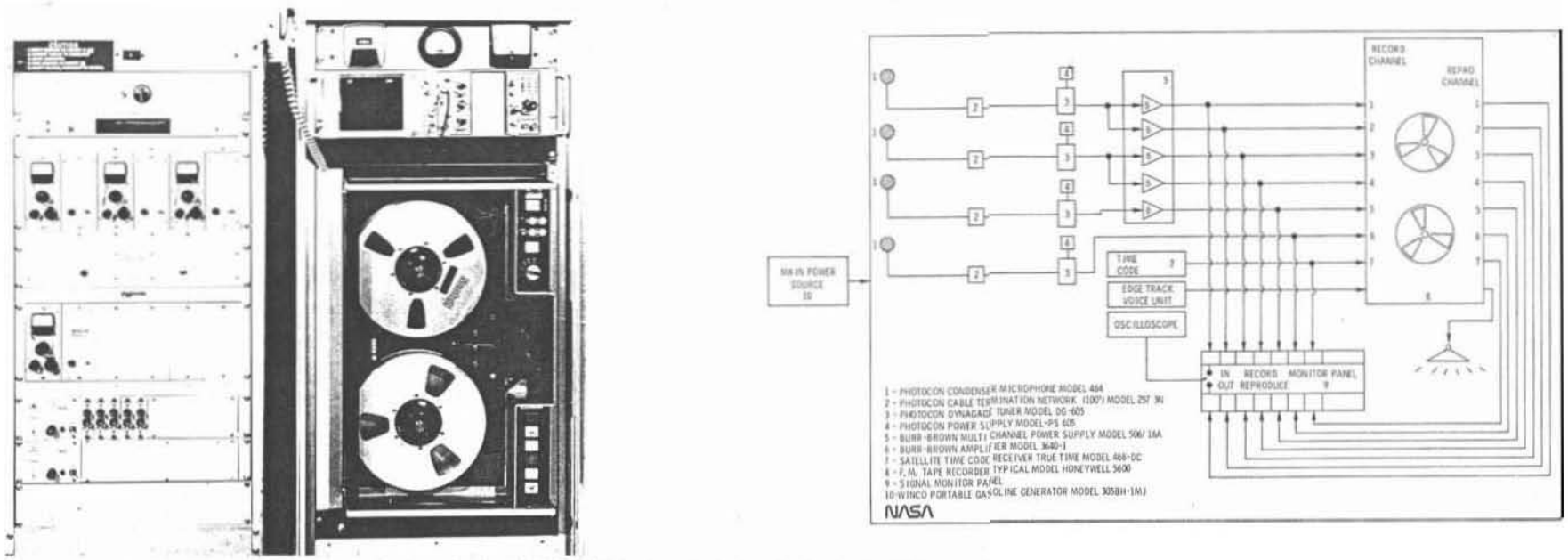

(a) Sonic boom data acquisition system - SBDAS

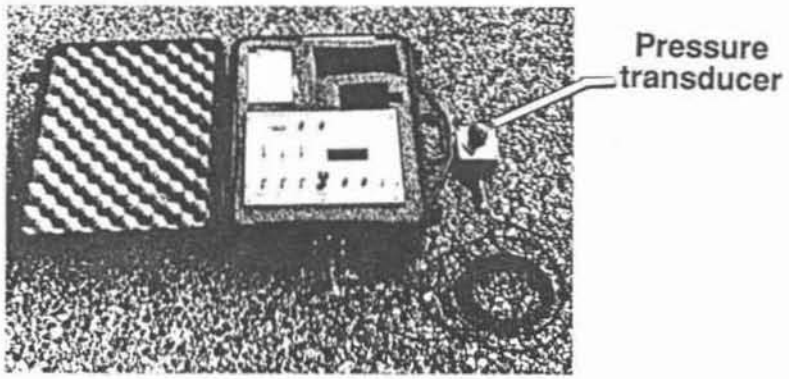

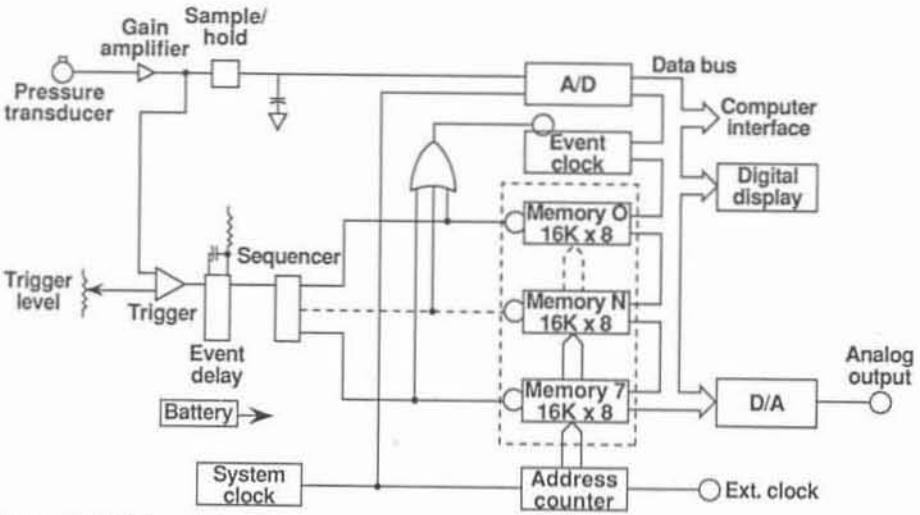

(b) Portable automatic triggering system - PATS

Figure 11. - Photographs and schematics of analog and digital sonic boom measurement systems.

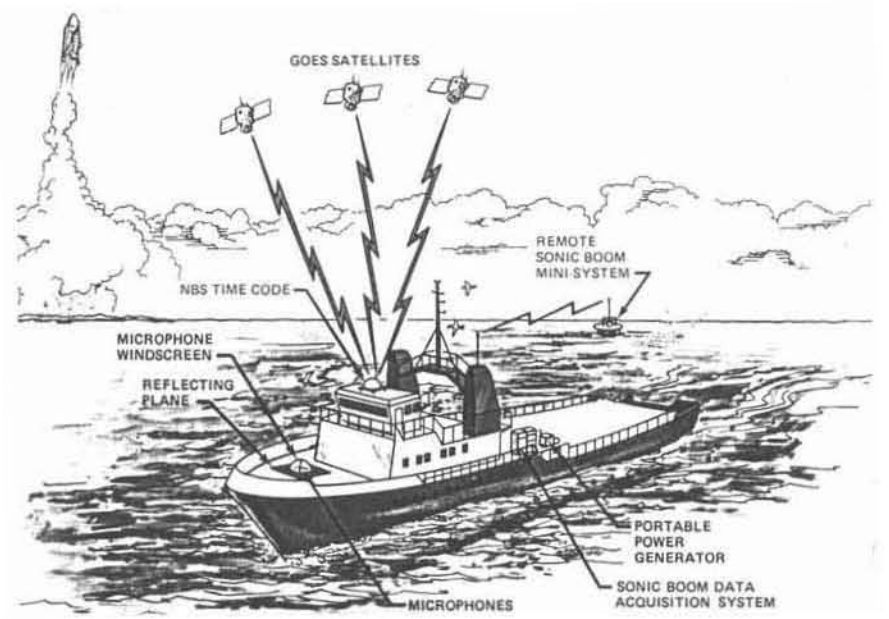

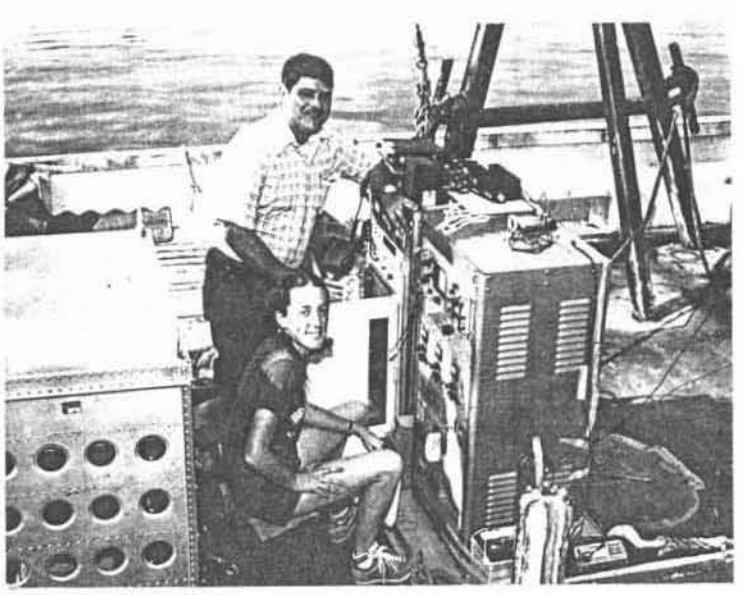

(a) Aboard ship for ascent measurements

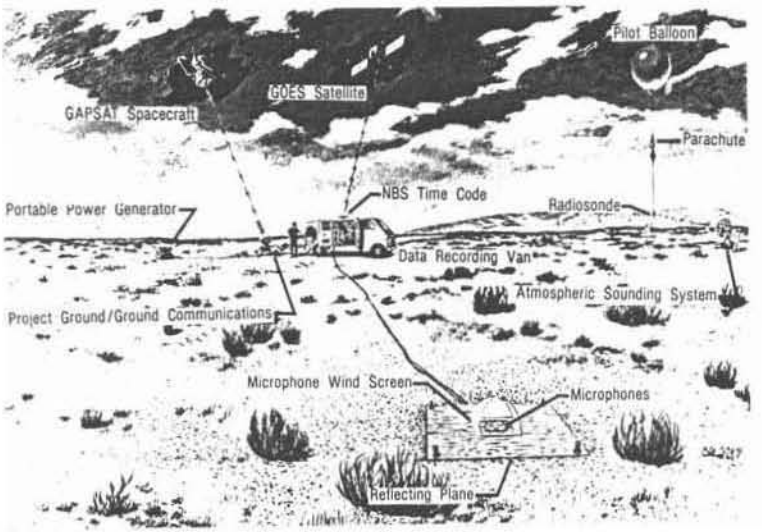

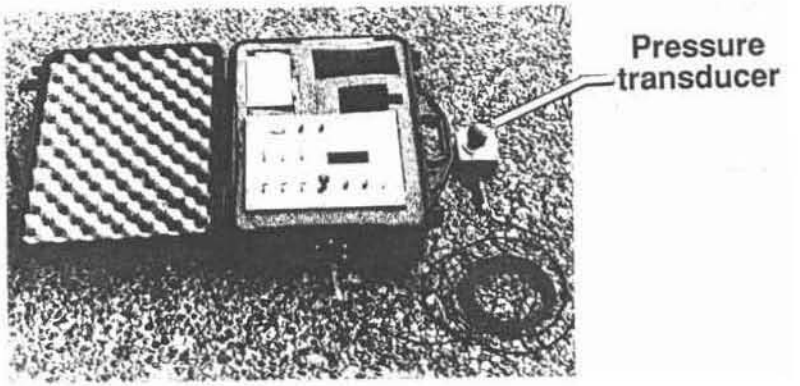

(b) Land based for re-entry measurements

Figure 12. - Typical STS sonic boom measurement station setup.

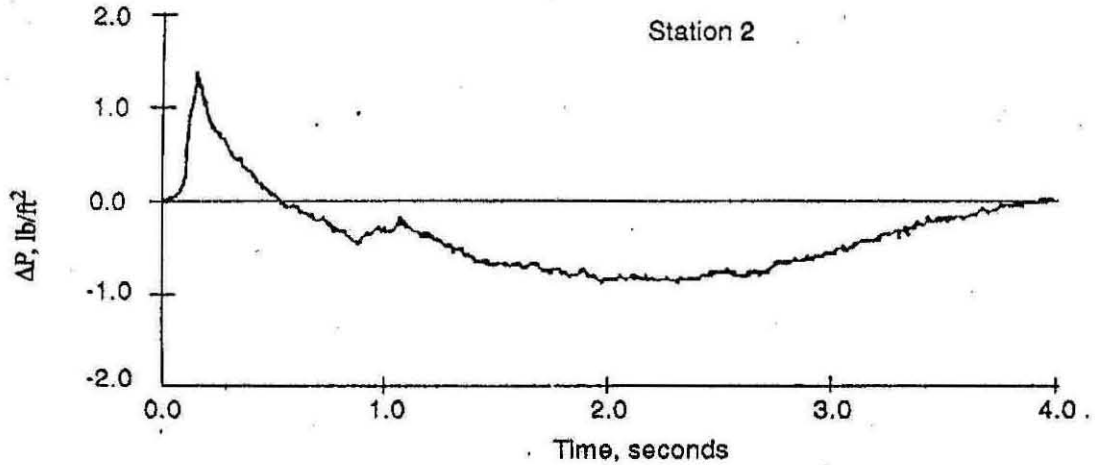

a) STS-41D ascent

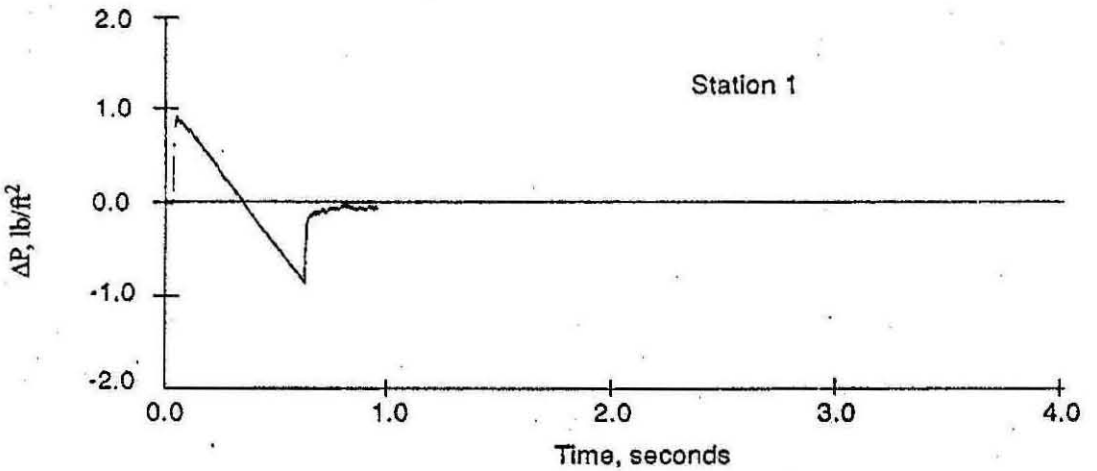

b) STS-41B re-entry

MSN	Approximate Mach and altitude at which booms were generated.	
STS-41D	3.57	163,000 ft.
STS-41B	4.2	108,000 ft.

Figure 13. - Representative measured sonic boom signatures from STS ascent and reentry.

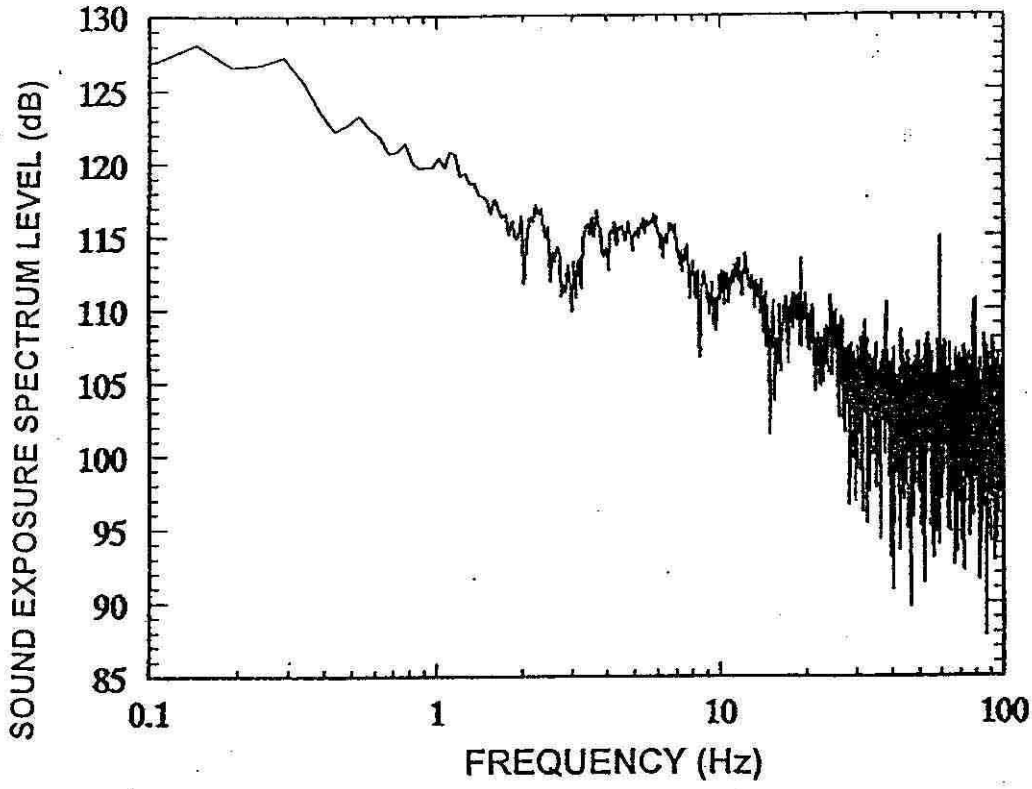

(a) STS-41D, ascent, M = 3.57, h = 163,000 ft.

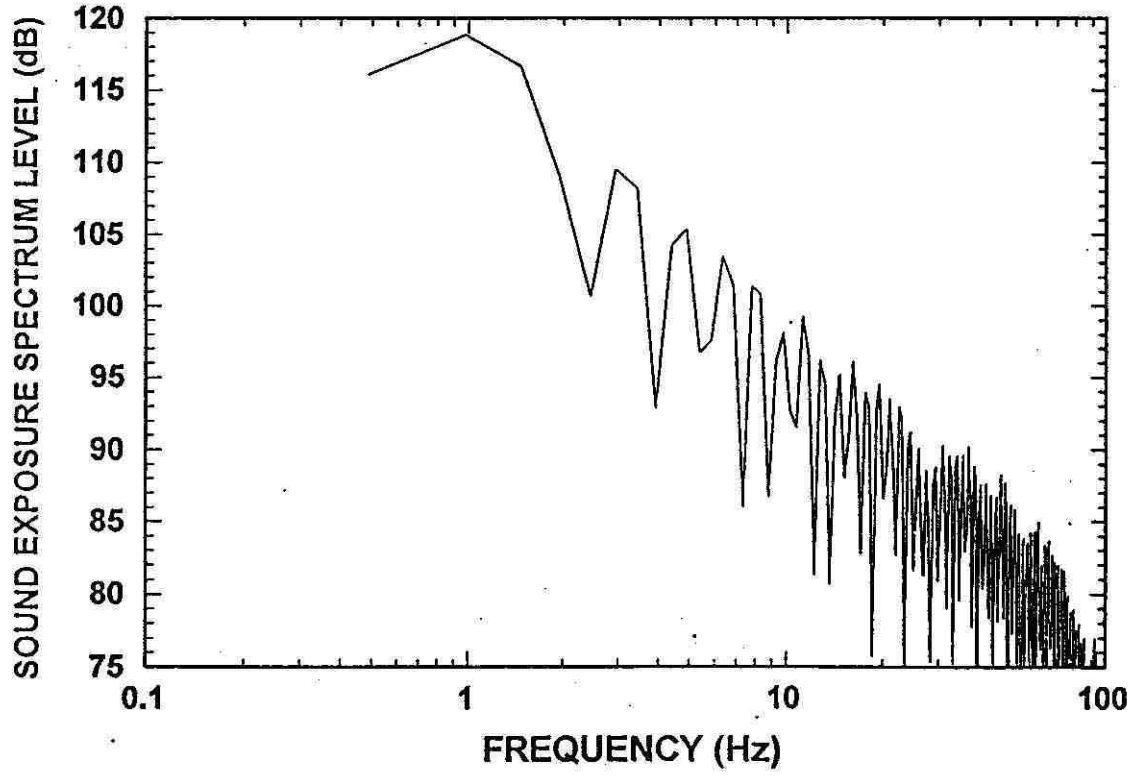

(b) STS-41B, reentry, M = 4.2, h = 108,000 ft.

Figure 14. - Typical noise spectra associated with STS ascent and reentry sonic boom signatures.

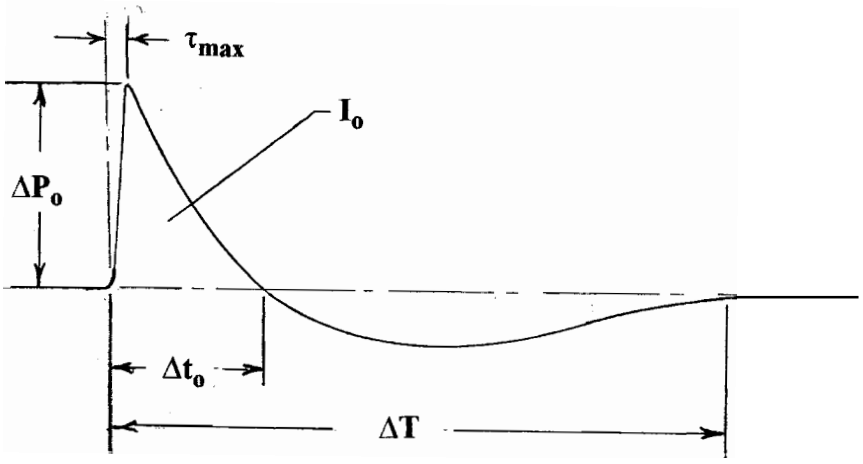

(a) Launch-ascent.

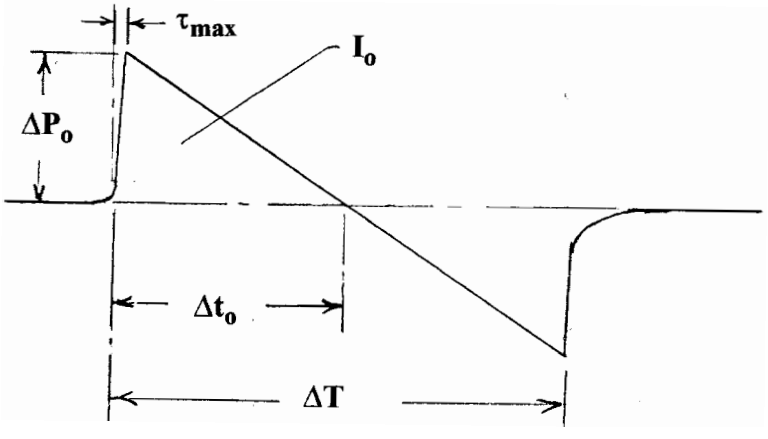

(b) Reentry-descent.

Figure 15. - Sonic boom signature characteristics.

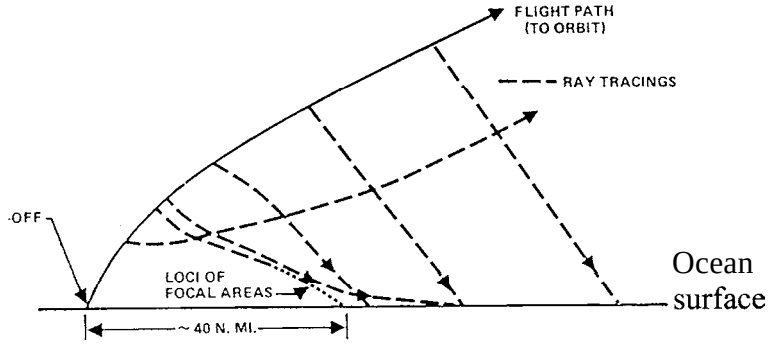

(a) Origin of launch-ascent focus boom.

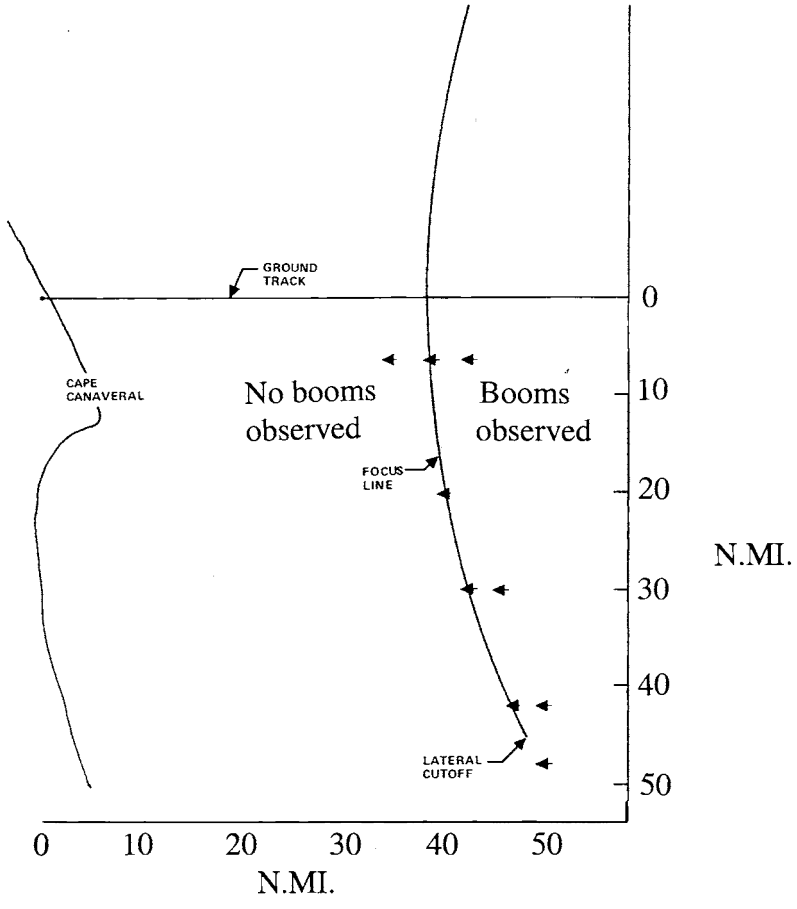

(b) Planview of launch-ascent focus boom region with planned measurement locations.

Figure 16. - Description of launch-ascent focus boom region.

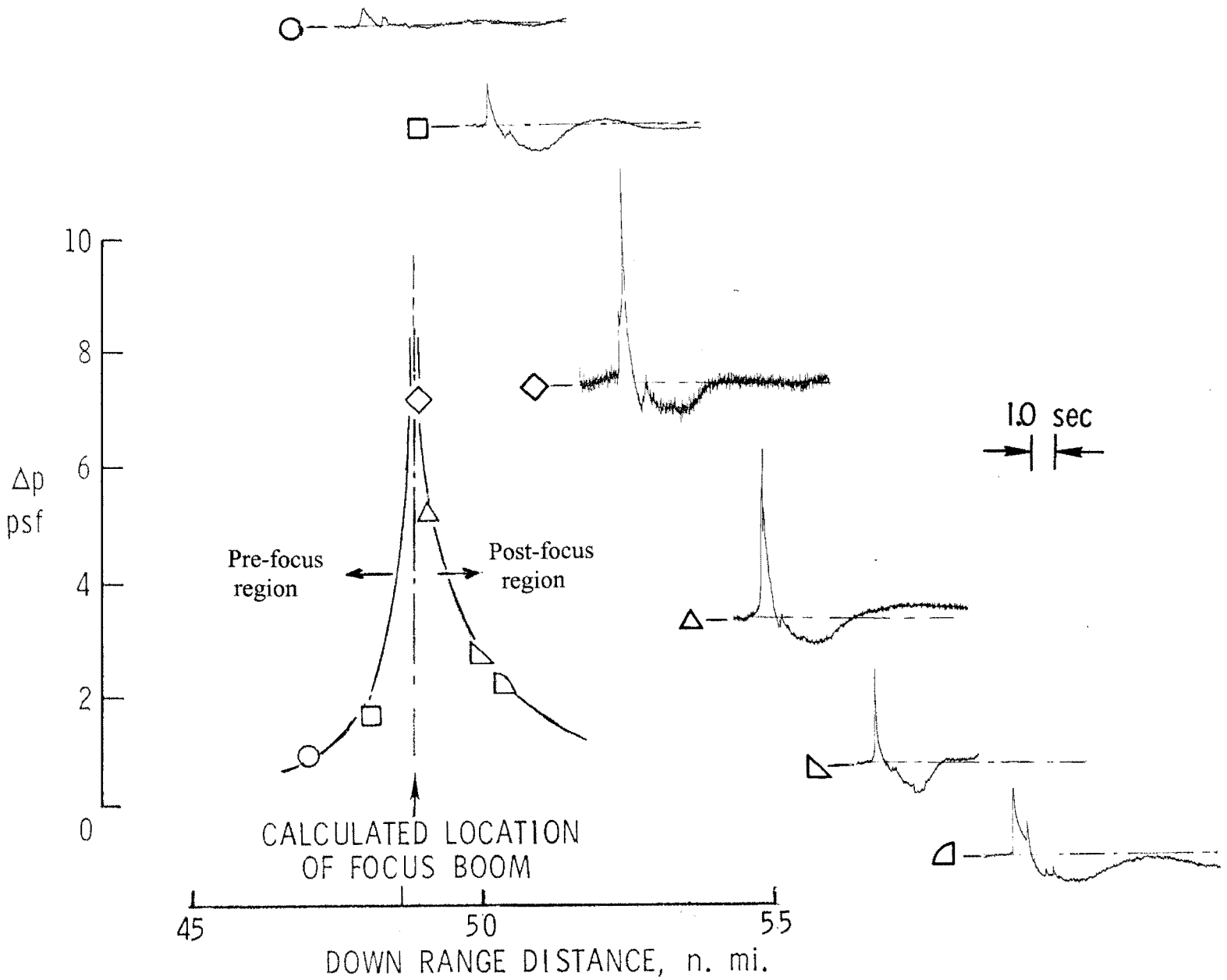

Figure 17. - STS launch-ascent sonic boom signatures within focus region.

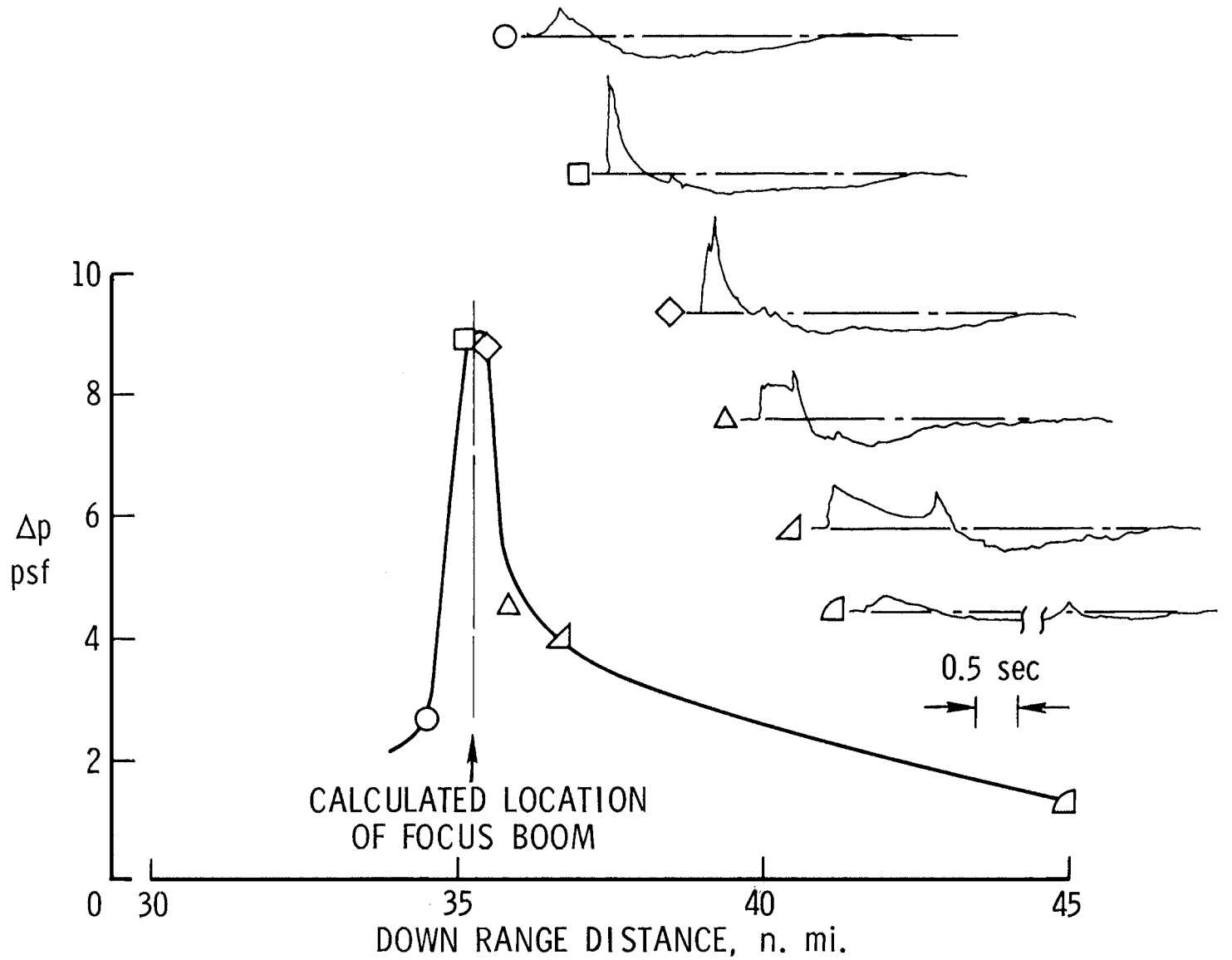

Figure 18. - Saturn-Apollo 17 launch-ascent sonic boom signatures within focus region (ref. 3).

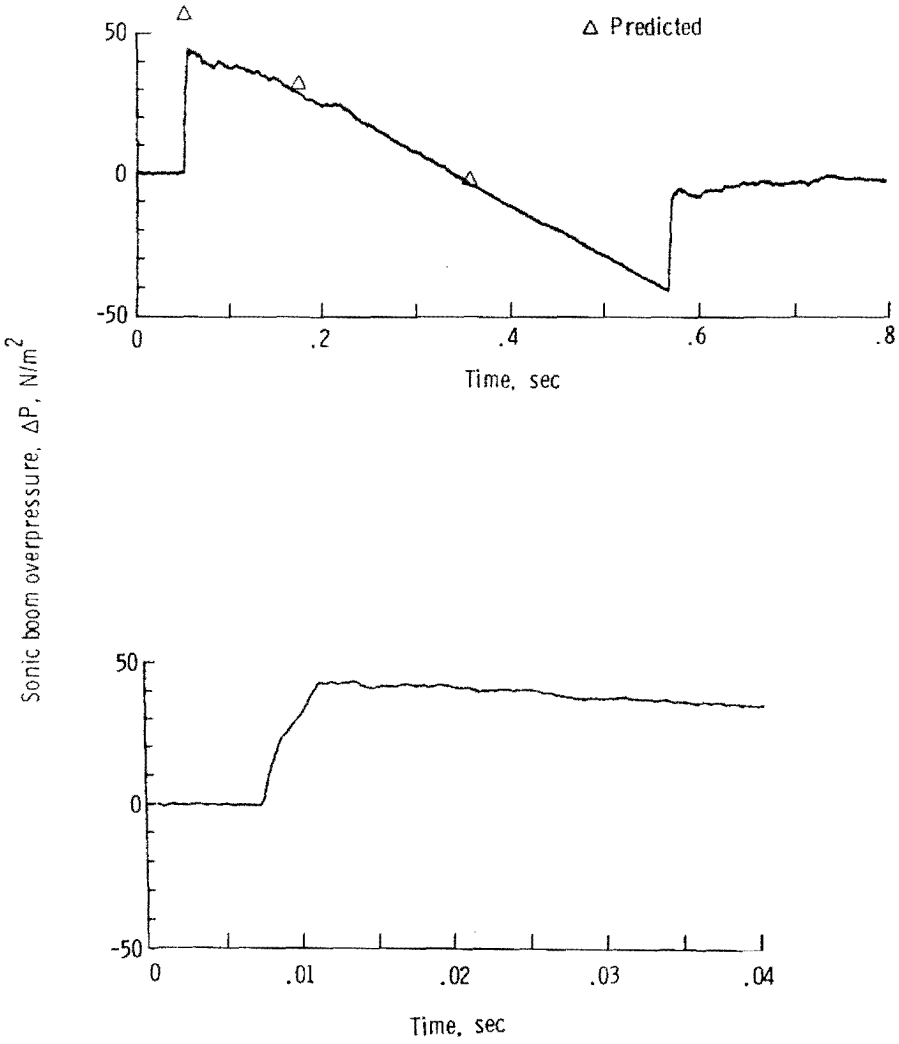

(a) Station 2 (M = 3.41 at 99,715 ft. MSL)

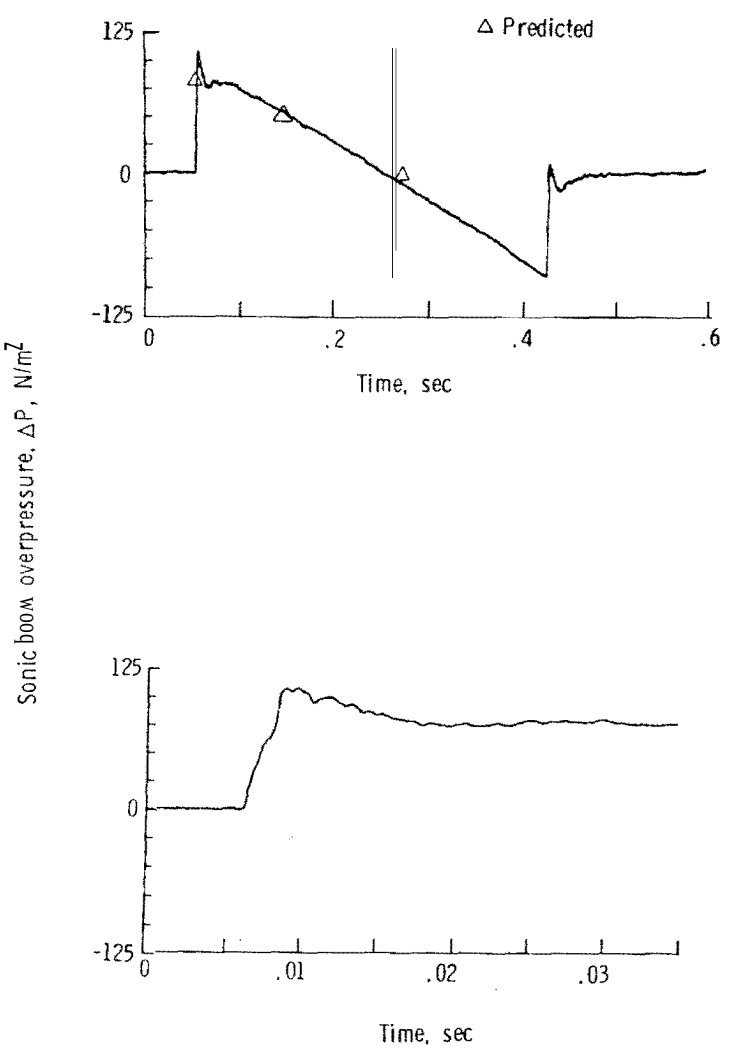

(b) Station 9 (M = 1.40 at 62,658 ft. MS

Figure 19. - Measured sonic boom signatures near the ground track during reentry-descent of STS-1 Orbiter along with details of the bow-shock rise time (from ref. 37).

Measured Signature	Waveform Category	MSN	Boom Time, Z	Boom Time, Local
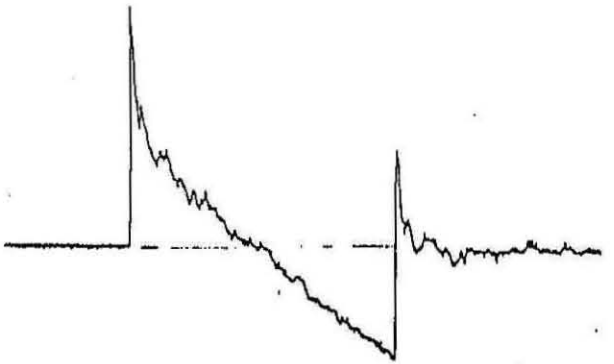	Peaked (P)	STS-33	00:24:26	4:24 pm
	Normal Peaked (NP)	STS-31	13:44:00	6:44 am
	Normal Rounded (NR)	STS-31	13:44:02	6:44 am

Figure 20. - Variation in measured sonic boom signatures from STS descent resulting from the atmosphere. (OJAI, CA, M ~ 3.6, H ~ 100,000 ft).

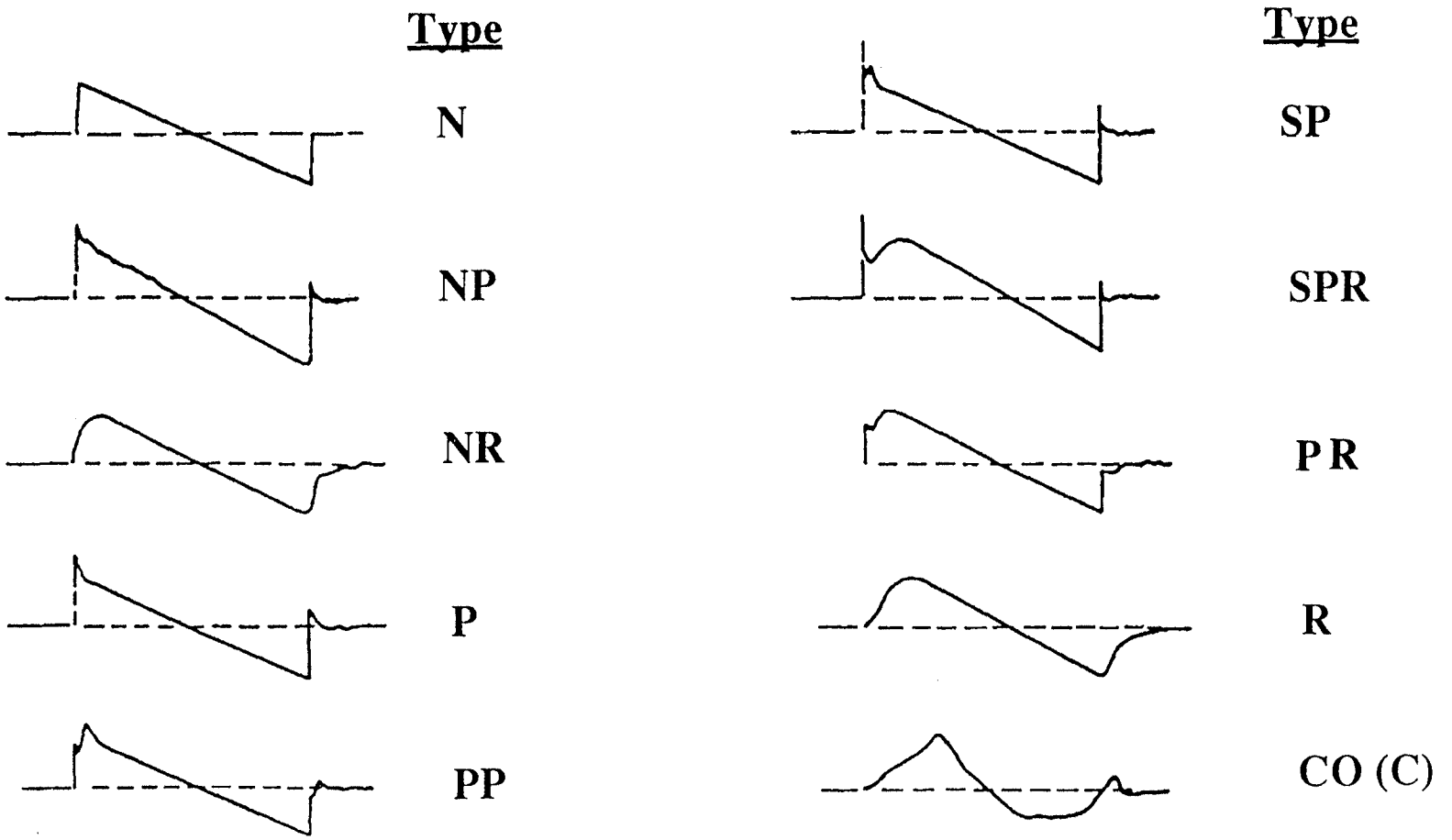

Figure 21 Sonic boom waveform categories.

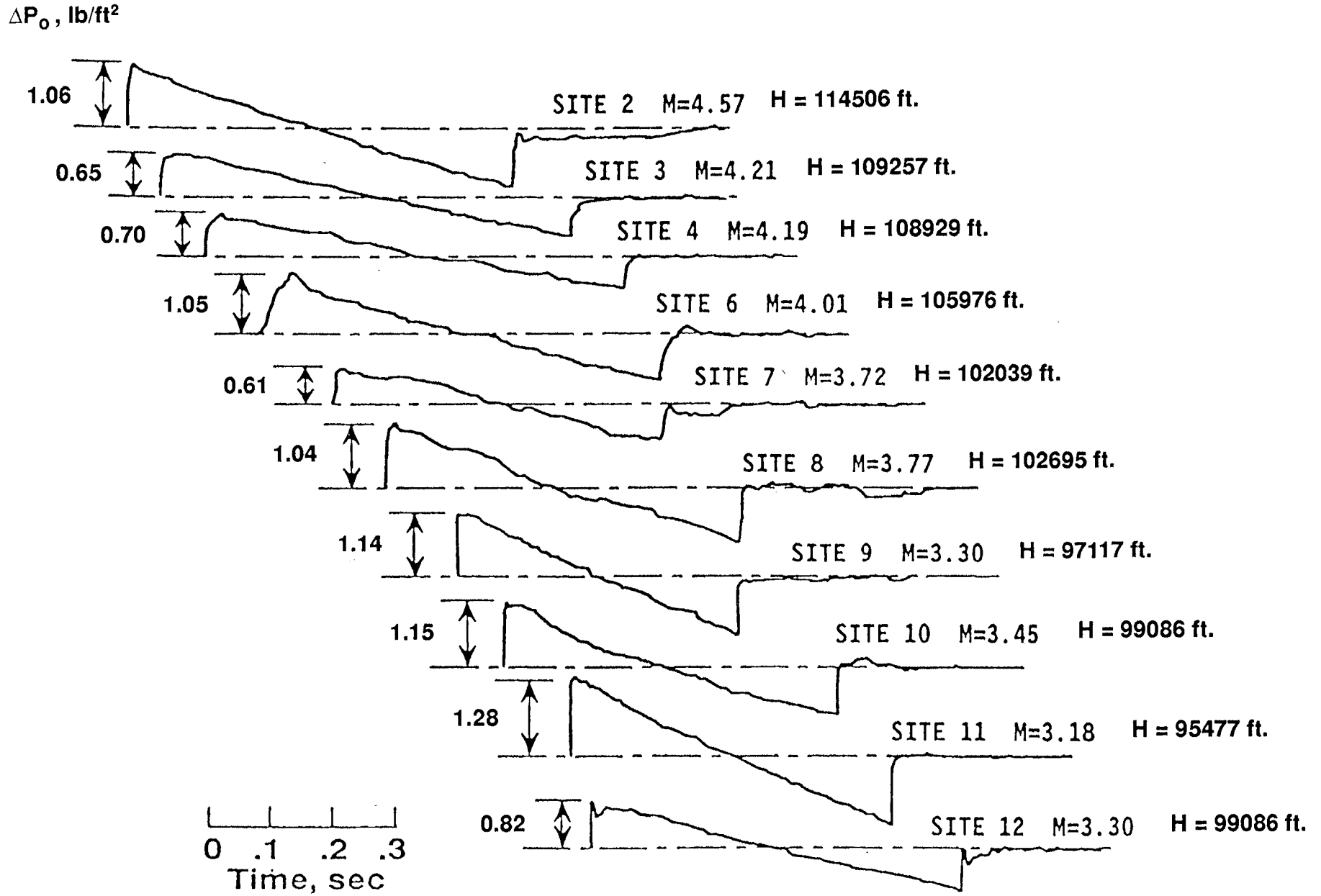

Figure 22. - Comparison of pressure signatures from the 10 measurement sites in California which received sonic booms from STS-26 reentry.(from ref. 38).

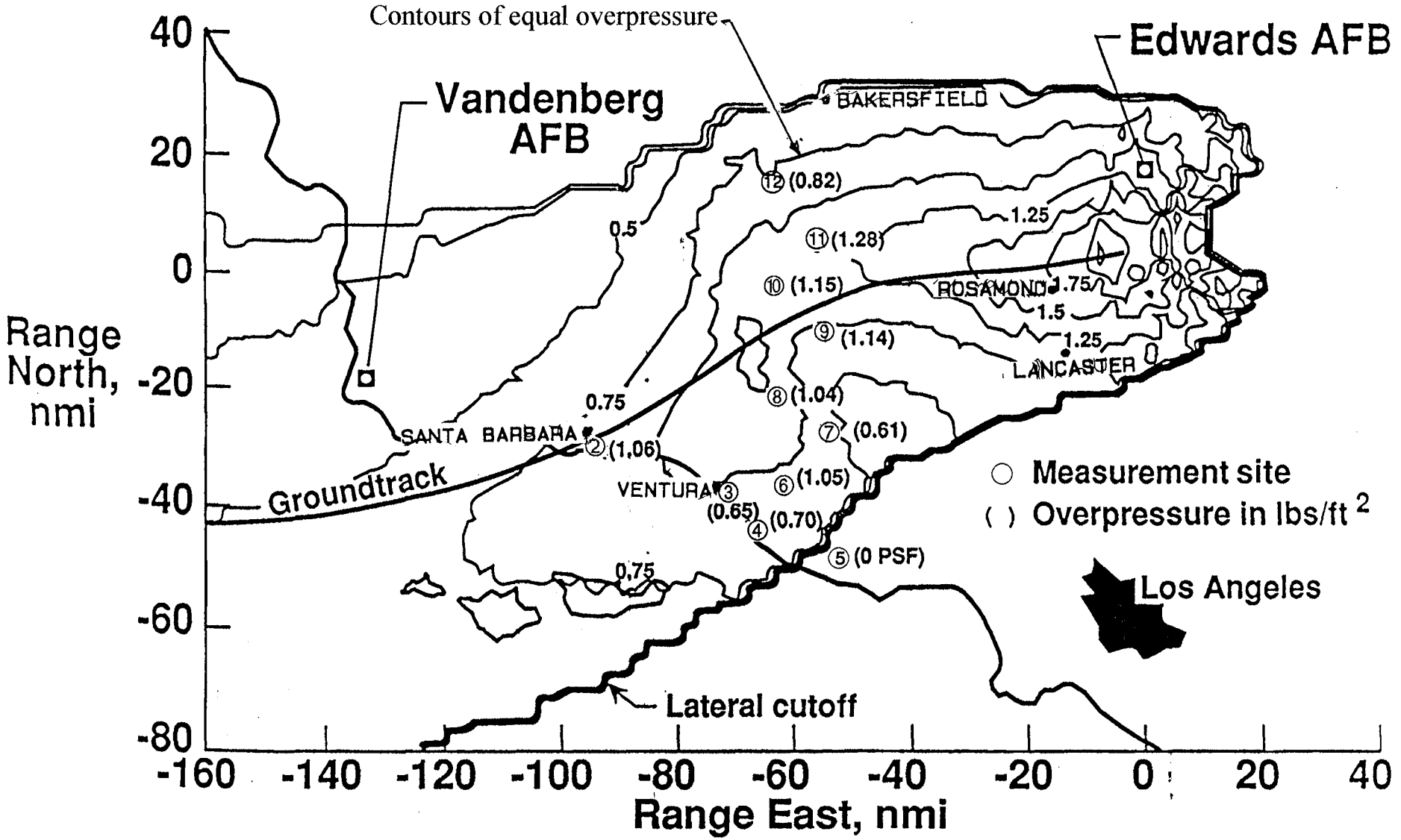

Figure 23 Comparison of measured and predicted sonic boom overpressures observed at the 11 measurement sites in California from STS-26 reentry.(from ref. 38).

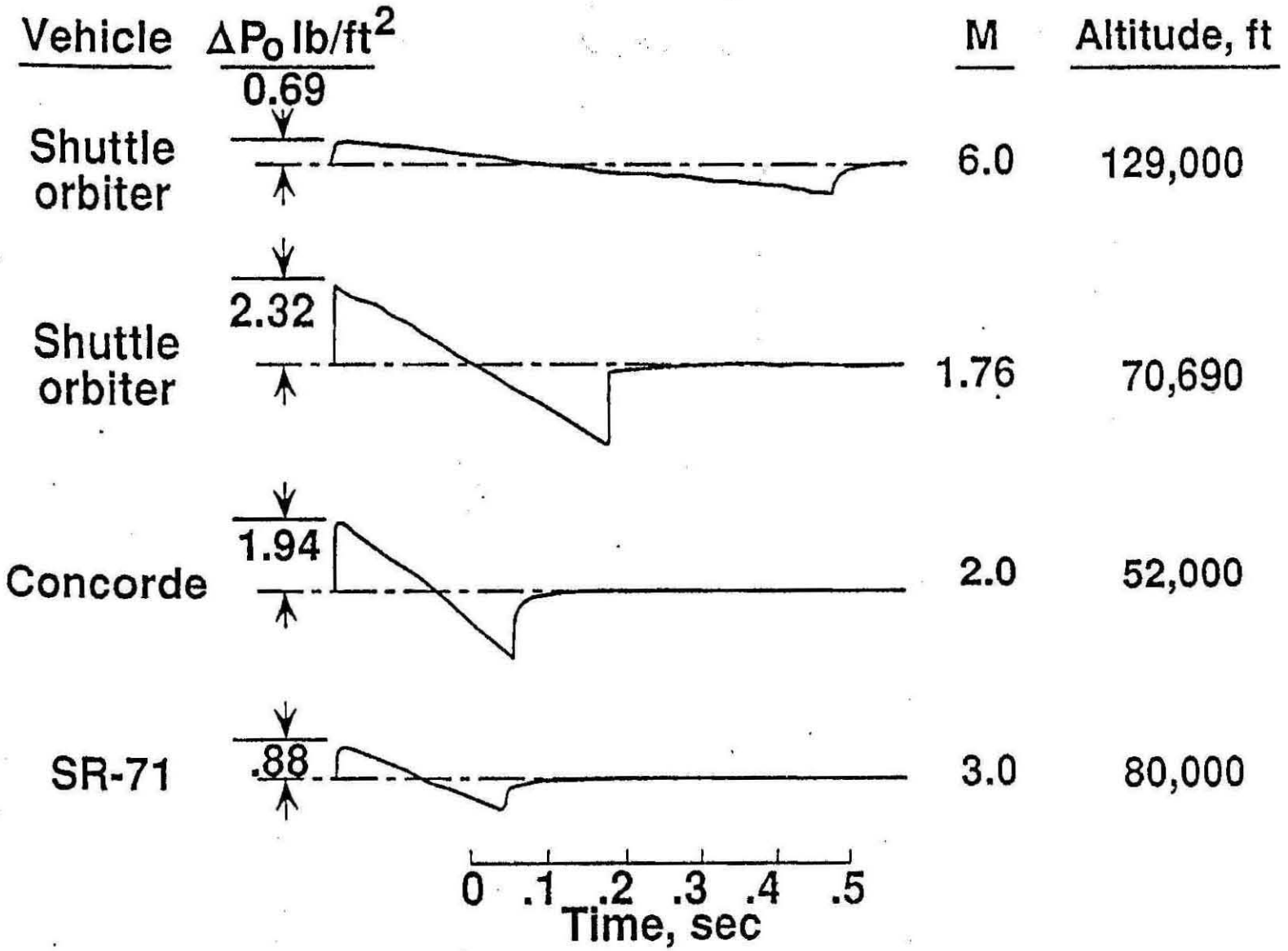

Figure 24. - Comparison of measured on-track sonic boom signatures for reentry-descent of the STS Orbiter and other aircraft.

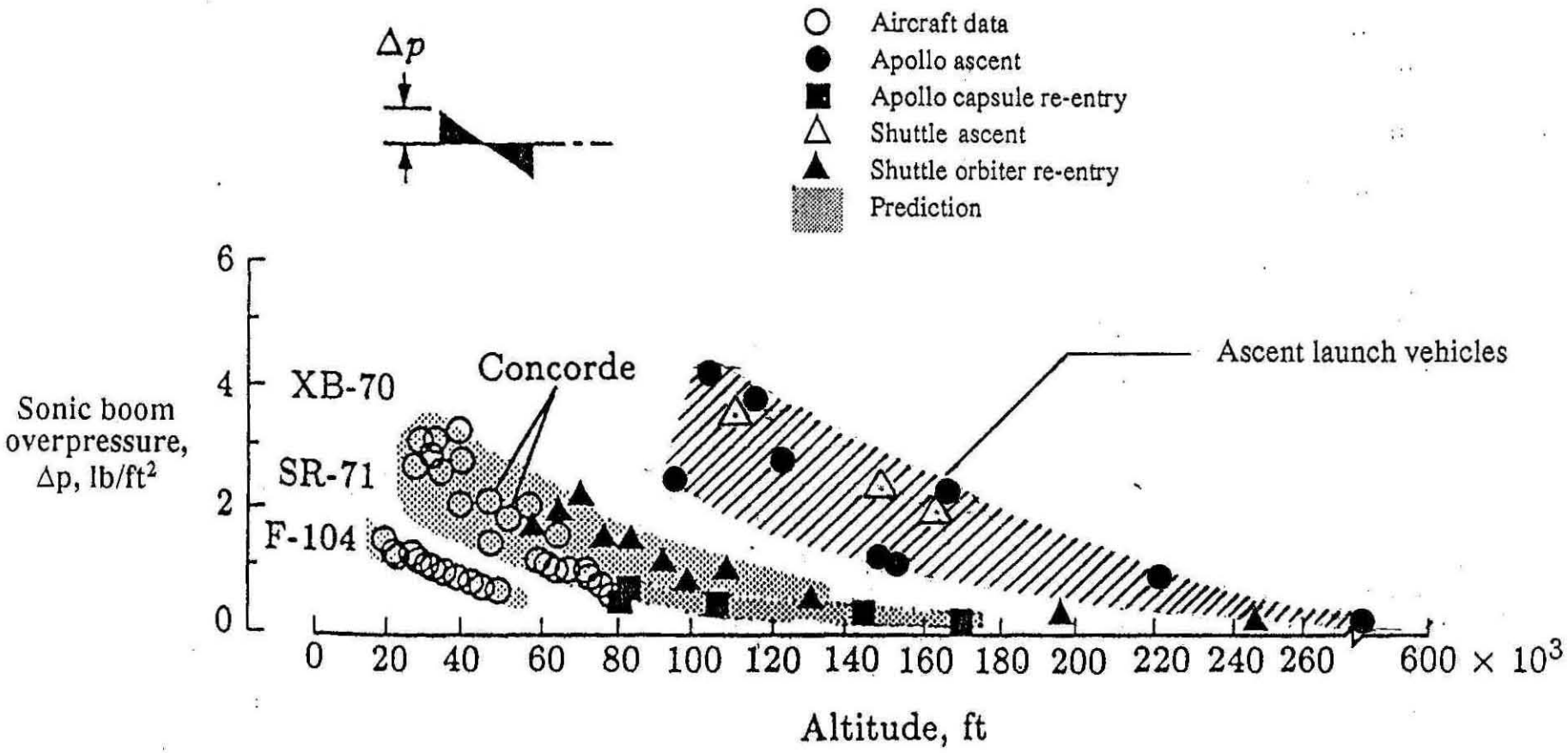

Figure 25. - Measure and predicted sonic boom overpressures near the ground track for several aircraft and spacecraft.

REPORT DOCUMENTATION PAGE

Form Approved
OMB No. 0704-0188

1. REPORT DATE *(DD-MM-YYYY)*	2. REPORT TYPE	3. DATES COVERED *(From - To)*
01- 04 - 2011	Contractor Report	

4. TITLE AND SUBTITLE
A Compilation of Space Shuttle Sonic Boom Measurements

5a. CONTRACT NUMBER
NNL05AB74T

5b. GRANT NUMBER

5c. PROGRAM ELEMENT NUMBER

6. AUTHOR(S)
Maglieri, Domenic J.; Henderson, Herbert R.; Massey, Steven J.; Stansbery, Eugene G.

5d. PROJECT NUMBER

5e. TASK NUMBER

5f. WORK UNIT NUMBER
984754.02.07.07.11.01

7. PERFORMING ORGANIZATION NAME(S) AND ADDRESS(ES)
NASA Langley Research Center
Hampton, VA 23681-2199

Eagle Aeronautics, Inc.
13 West Mercury Boulevard
Hampton, VA 23669-2508

8. PERFORMING ORGANIZATION REPORT NUMBER

9. SPONSORING/MONITORING AGENCY NAME(S) AND ADDRESS(ES)
National Aeronautics and Space Administration
Washington, DC 20546-0001

10. SPONSOR/MONITOR'S ACRONYM(S)
NASA

11. SPONSOR/MONITOR'S REPORT NUMBER(S)
NASA/CR-2011-217080

12. DISTRIBUTION/AVAILABILITY STATEMENT
Unclassified - Unlimited
Subject Category 71
Availability: NASA CASI (443) 757-5802

13. SUPPLEMENTARY NOTES
STS sonic boom database available on CD-ROM as a supplement to this report.
Langley Technical Monitor: Peter G. Coen

14. ABSTRACT

Sonic boom measurements have been obtained on 26 flights of the Space Shuttle system beginning with the launch of STS-1 on April 12, 1981, to the reentry-descent of STS-41 into EAFB on Oct. 10, 1990. A total of 23 boom measurements were acquired within the focus region off the Florida coast during 3 STS launch-ascents and 113 boom measurements were acquired during 23 STS reentry-descent to landing into Florida and California. Sonic boom measurements were made under, and lateral to, the vehicle ground track and cover the Mach-altitude range of about 1.3 to 23 and 54,000 feet to 243,000 feet, respectively. Vehicle operational data, flight profiles and weather data were also gathered during the flights. This STS boom database is contained in 26 documents, some are formal and referenceable but most internal documents. Another 38 documents, also non-referenceable, contain predicted sonic boom footprints for reentry-descent flights on which no measurements were made. The purpose of this report is to provide an overview of the STS sonic boom database and summarize the main findings.

15. SUBJECT TERMS
Sonic boom signatures; Rise times; Spectra; Footprints; Focussing; Atmospheric effects

16. SECURITY CLASSIFICATION OF:			17. LIMITATION OF ABSTRACT	18. NUMBER OF PAGES	19a. NAME OF RESPONSIBLE PERSON
a. REPORT	b. ABSTRACT	c. THIS PAGE			STI Help Desk (email: help@sti.nasa.gov)
					19b. TELEPHONE NUMBER *(Include area code)*
U	U	U	UU	73	(443) 757-5802